

# Spherical Aromaticity of Fullerenes

Michael Bühl\*<sup>†</sup> and Andreas Hirsch\*<sup>‡</sup>

Max-Planck-Institut für Kohlenforschung, Kaiser-Wilhelm-Platz 1, D-45470 Mülheim an der Ruhr, Germany, and Institut für Organische Chemie der Universität Erlangen-Nürnberg, Henkestr. 42, D-91054 Erlangen, Germany

Received August 21, 2000

## Contents

I. Introduction	1153
II. Structural Criteria	1154
III. Energetic Criteria	1158
1. MO Resonance Energies of Fullerenes	1158
2. Topological Resonance Energies of Fullerenes	1159
3. VB Model of C <sub>60</sub>	1159
4. Isodesmic Equations	1159
5. Heat of Hydrogenation	1160
6. Summary	1160
IV. Reactivity Criteria	1160
1. Reactivity Indices	1160
2. Principles of Fullerene Reactivity	1160
A. Retention of the Structural Type	1160
B. Chemical Indication of Cyclic Electron Delocalization within C <sub>60</sub> : <i>cis</i> -1 Reactivity	1162
C. Charge and Spin Localization in Monoadducts with Nucleophiles and Radicals	1162
D. Fullerene Adducts Containing Two-Dimensional Aromatic Substructures	1163
3. Summary	1165
V. Magnetic Criteria	1165
1. Application of Magnetic Criteria to Fullerenes	1166
A. "Exohedral" Probes	1167
B. "Endohedral" Probes	1169
C. "Theoretical" Probes	1171
2. Application of Magnetic Criteria to Fullerene Derivatives	1172
A. Anions	1172
B. Adducts	1173
C. Heterofullerenes	1177
3. Summary	1177
VI. Nature of Aromaticity in Fullerenes and Count Rules	1177
1. Topological Count Rules—"Magic Numbers"	1177
2. Spherical Aromaticity in I <sub>h</sub> Symmetrical Fullerenes: The 2(N+1) <sup>2</sup> Rule	1178
VII. Conclusion	1179
VIII. Acknowledgment	1179
IX. References	1179

## I. Introduction

When buckminsterfullerene was discovered in 1985,<sup>1</sup> Kroto suggested that it could be "the first example

of a spherical aromatic molecule". Later, at about the time when Krätschmer and Huffman reported on the synthesis of fullerenes in bulk quantities,<sup>2</sup> he pointed out the vision that "it could be that we are entering a new age for just as the pre-Columbian assumption that the earth was flat made way for a round world-view, it may be that, post buckminsterfullerene, the traditional assumption that polyaromatic organic chemistry is essentially a flat field may also make for a bright, nonplanar future".<sup>3</sup> The question whether fullerenes have to be considered aromatic or not has been a debate ever since their discovery. This has to do with initial lack of knowledge of fullerene properties, different interpretations of their newly discovered and unprecedented behavior,<sup>4–11</sup> which is difficult to compare with that of planar aromatics, and of course also with the fact that the definition of aromaticity<sup>12–14</sup> itself is controversial and has changed many times over the last 175 years.

The fullerenes form a unique class of spherical molecules containing a conjugated  $\pi$  system. Each fullerene represents a closed network of fused hexagons and pentagons. This building principle is a consequence of the Euler theorem which states that for the closure of each spherical network of  $n$  hexagons, 12 pentagons are required, with the exception of  $n = 1$ . The presence of the pentagons allows for the introduction of the curvature which requires the C atoms to be pyramidalized. The smallest stable and at the same time the most abundant fullerene is the I<sub>h</sub>-symmetrical buckminsterfullerene C<sub>60</sub> (Figure 1). The next stable homologue is C<sub>70</sub> (Figure 1), followed by higher fullerenes<sup>15–17</sup> like C<sub>76</sub>, C<sub>78</sub>, C<sub>80</sub>, C<sub>82</sub>, C<sub>84</sub>, etc. In terms of valence bond (VB) theory, there are 12 500 Kekulé structures for C<sub>60</sub>, suggesting, at a first glance, that it might be very aromatic. The structure of the fullerenes, especially that of the icosahedral representatives such as C<sub>60</sub>, implies that they should be considered as three-dimensional analogues of benzene and other planar aromatics. In contrast to such classical systems, however, the sp<sup>2</sup> networks of the fullerenes have no boundaries which are saturated by hydrogen atoms.<sup>18</sup> As a consequence, the characteristic aromatic substitution reactions retaining the conjugated  $\pi$  system are not possible for fullerenes. This is just one example for the general problem to evaluate the aromaticity of fullerenes. What are suitable aromaticity criteria for fullerenes? Against which standards should the aromatic properties of fullerenes be measured? Are there count rules similar to the Hückel rule for planar monocyclic aromatics which express the occurrence of aromaticity with respect to the number of  $\pi$  electrons?

<sup>†</sup> Max-Planck-Institut für Kohlenforschung. Fax: +49-208-3062996. E-mail: buehl@mpi-muelheim.mpg.de.

<sup>‡</sup> Institut für Organische Chemie der Universität Erlangen-Nürnberg. Fax: +49-9131-8522537. E-mail: hirsch@organik.uni-erlangen.de.



Michael Bühl was born in Würzburg, Germany, in 1962. He studied chemistry at the University of Erlangen, Germany, where he obtained his Ph.D. degree in 1992 under the supervision of Paul Schleyer. After a postdoctoral stay at the University of Georgia in Athens, GA, with Henry F. Schaefer III, he moved to the University of Zurich (Switzerland), where he finished his Habilitation in 1998. Since 1999 he has been Group Leader in the Theoretical Department of the Max-Planck-Institut für Kohlenforschung in Mülheim/Ruhr (Germany). His main research interests are rooted in the application of modern quantum-chemical tools to study structures and reactivities of organic and transition-metal compounds, with emphasis on the computation of NMR properties. His main areas of application are fullerenes, computational support of experimentally determined structures, and homogeneous catalysis with transition-metal complexes.



Andreas Hirsch was born in Esslingen, Germany, in 1960. He studied chemistry at the University of Tübingen, Germany, where he obtained his Ph.D. degree in 1990 under Michael Hanack. He has conducted postdoctoral research at the Institute for Polymers and Organic Solids in Santa Barbara, CA, with Fred Wudl. In 1991 he subsequently returned to Tübingen as Research Associate at the Institute of Organic Chemistry. After his Habilitation in 1994, he joined the faculty of the Department of Chemistry at the University of Karlsruhe as Professor. Since October 1995, he has been Full Professor of Organic Chemistry at the Friedrich-Alexander-Universität Erlangen-Nürnberg. Andreas Hirsch's main research activities have been focused on the development of methodologies of efficient syntheses of exohedral derivatives of fullerenes and the use of such compounds as structural templates and building blocks for supramolecular architectures and nanomaterials. Other research interests are in the area of synthesis of dendrimers, calixarene conjugates, new alkynes, new types of synthetic lipids and amphiphiles, model compounds for photoinduced charge separation, chemical derivatization, and solubilization of carbon nanotubes, including investigation of their synthetic potential and properties as new materials.

Compared to benzene, being the archetype of a two-dimensional aromatic molecule,<sup>19</sup> the discussion of aromaticity in fullerenes must take into account the strain provided by the pyramidalization of the C atoms.<sup>18</sup> The rich exohedral chemistry of fullerenes,<sup>8,20–26</sup> which is basically addition to the conju-

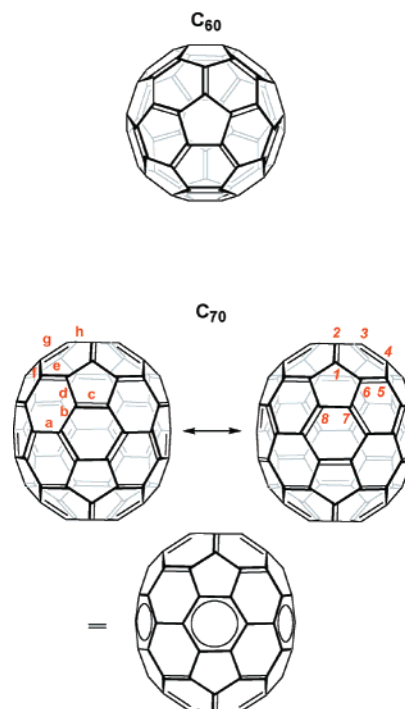


**Figure 1.** Schematic representation of  $C_{60}$  and  $C_{70}$ .

gated  $\pi$  system, is to a large extent driven by the reduction of strain.<sup>18</sup> Analysis of the reactivity and regiochemistry of addition reactions reveals a behavior reminiscent of electron-deficient olefins. However, especially the magnetic properties of fullerenes clearly reflect delocalized character of the conjugated  $\pi$  system, which, depending on the number of  $\pi$  electrons, can cause the occurrence of diamagnetic or paramagnetic ring currents within the loops of the hexagons and pentagons (see section V). Neutral  $C_{60}$ , for example, containing diatropic hexagons and paratropic pentagons was labeled “ambiguously aromatic”.<sup>18</sup> Whereas in the early fullerene days the debate about the presence or absence of aromaticity in fullerenes was controversial, the accumulating amount of experimental and theoretical research within the last years provided a much clearer interpretation of this term with respect to this new class of compounds. It is the aim of this review to summarize the research of fullerene aromaticity. The evaluation of fullerene aromaticity is based on the classical aromaticity criteria, namely, structure, energy, reactivity, and magnetism, which are covered in this sequence in the following sections. Finally, the nature of fullerene aromaticity considering count rules involving the whole  $\pi$ -electron system and the presence of two-dimensional Hückel-aromatic substructures will be discussed.

## II. Structural Criteria

Icosahedral buckminsterfullerene is the only  $C_{60}$  isomer and the smallest possible fullerene that obeys the ‘isolated pentagon rule’ (IPR).<sup>28,29</sup> The IPR predicts that those fullerene isomers with all pentagons isolated by hexagons will be stabilized against struc-

**Table 1. Calculated and Measured Bond Distances in C<sub>60</sub> [Å]**

method	[5,6]-bonds	[6,6]-bonds	ref
HF(STO-3G)	1.465	1.376	51
HF(7s3p/4s2p)	1.453	1.369	52
LDF(11s6p)	1.43	1.39	53
HF	1.448	1.370	54
MP2	1.446	1.406	55
NMR	1.45	1.40	56
neutron diffraction	1.444	1.391	57
electron diffraction	1.458	1.401	58
X-ray	1.467	1.355	59

tures with adjacent pentagons. The destabilization of non-IPR fullerenes is due to an increase of strain energy caused by enforced bond angles accompanied with higher pyramidalization of the C atoms. In addition, it was suggested that the pentalene-type 8  $\pi$ -electron substructures may lead to resonance destabilization.<sup>30,31</sup> The destabilizing effect of abutting pentagons in fullerenes was investigated quantitatively by Fowler and Zerbetto.<sup>32</sup> If, in addition to IPR violating fullerenes, open-shell structures and unfavorable *para* relationships<sup>31</sup> of pentagons are avoided, the huge number of possible isomers reduces considerably. With these constraints, magic numbers<sup>33–38</sup> for stable fullerenes C<sub>n</sub> can be predicted, which are  $n = 60$  (one isomer), 70 (one isomer), 72 (one isomer), 76 (one isomer), 78 (five isomers), etc. Next to C<sub>60</sub> and C<sub>70</sub>, structural assignment based on <sup>13</sup>C NMR, X-ray crystallography, and, in some cases by supporting stability calculations was possible for the IPR fullerenes D<sub>2</sub>-C<sub>76</sub>, C<sub>2v</sub>-C<sub>78</sub>, D<sub>3</sub>-C<sub>78</sub>, C<sub>2v'</sub>-C<sub>78</sub>, D<sub>2</sub>-C<sub>80</sub>, C<sub>2</sub>-C<sub>82</sub>, D<sub>2d</sub>-C<sub>84</sub>, D<sub>2</sub>-C<sub>84</sub>,<sup>17,39–47</sup> and recently also for the endohedral compound Sc<sub>3</sub>N@C<sub>80</sub><sup>48</sup> involving the icosahedral C<sub>80</sub> cage, which is unstable as parent fullerene. IPR satisfying D<sub>5h</sub>-C<sub>70</sub> contains, in addition to the corannulene-type poles, an equatorial belt consisting of a cyclic phenylene.

The fact that the bonds located at the junctions of the hexagons ([6,6]-bonds) are shorter than the bonds in the pentagonal rings ([5,6]-bonds)<sup>49,50</sup> is very important for the analysis of the structure criterion of the aromaticity of C<sub>60</sub>. The bond-length alternation has been shown theoretically and experimentally (Table 1) and implies cyclohexatriene and [5]radialene substructures—a view that is strongly supported by the regioselectivity of addition reactions (see section IV). A related structural trend is observed for C<sub>70</sub>, especially within its polar caps (Table 2), and for derivatives of I<sub>h</sub>-C<sub>80</sub><sup>48</sup> and D<sub>2d</sub>-C<sub>84</sub><sup>44</sup> investigated by X-ray crystallography.

The degree of bond-length alternation in C<sub>60</sub>, however, is lower than that of linear polyenes and reminiscent of those found in aromatic polycyclic hydrocarbons.<sup>18</sup> In higher fullerenes such as C<sub>78</sub> and C<sub>84</sub>, the bond-length alternation can be even more pronounced.<sup>44,63</sup> For example, the most reactive [6,6]-bond in D<sub>2d</sub>-C<sub>84</sub> has a length of only 1.332 (11) Å,<sup>44</sup> thus being much shorter than a [6,6]-bond within C<sub>60</sub> (~1.38 Å). Bond order calculations for C<sub>60</sub>, C<sub>70</sub>, C<sub>76</sub>, the five isomers of C<sub>78</sub>, and D<sub>2</sub>-C<sub>84</sub> as well as D<sub>2d</sub>-C<sub>84</sub> are summarized in ref 64.

To determine the origin of the bond-length alternation within C<sub>60</sub>, the influence of the symmetry and

**Table 2. Calculated and Experimental Structure of C<sub>70</sub>**

bond type	bond length (Å)		
	experiment		theory
	<i>a</i>	<i>b</i>	(dzp/SCF) <sup>60</sup>
a	1.462	1.462	1.475
b	1.423	1.414	1.407
c	1.441	1.426	1.415
d	1.432	1.447	1.457
e	1.372	1.378	1.361
f	1.453	1.445	1.446
g	1.381	1.387	1.375
h	1.463	1.453	1.451

<sup>a</sup> Data were taken from the crystal structure of the complex ( $\eta^2$ -C<sub>70</sub>)Ir(CO)Cl(PPh<sub>3</sub>)<sub>2</sub>.<sup>61</sup> <sup>b</sup> Data were taken from the crystal structure of C<sub>70</sub>·6(S<sub>8</sub>).<sup>62</sup>

**Table 3. Electron Ground-State Configurations of the Fully (Bold) and Partially Filled  $\pi$  Shells of Icosahedral Fullerenes**

<i>l</i> <sup>a</sup>	shell	electrons/shell	$n_c$ <sup>b</sup>	HOMO ( <i>I<sub>h</sub></i> symmetry) <sup>c</sup>
0	s	2	<b>2</b>	<b>a<sub>g</sub><sup>2</sup></b>
1	p	6	<b>8</b>	<b>t<sub>1u</sub><sup>6</sup></b>
2	d	10	<b>18</b>	<b>h<sub>g</sub><sup>10</sup></b>
			24	t <sub>2u</sub> <sup>6</sup>
3	f	14	26	g <sub>u</sub> <sup>8</sup>
			<b>32</b>	<b>t<sub>2u</sub><sup>6</sup>g<sub>u</sub><sup>8</sup></b>
			40	g <sub>g</sub> <sup>8</sup>
4	g	18	42	h <sub>g</sub> <sup>10</sup>
			<b>50</b>	<b>g<sub>g</sub><sup>8</sup>h<sub>g</sub><sup>10</sup></b>
			56	t <sub>1u</sub> <sup>6</sup> or t <sub>2u</sub> <sup>6</sup>
			60	h <sub>u</sub> <sup>10</sup>
5	h	22	62	t <sub>1u</sub> <sup>6</sup> t <sub>2u</sub> <sup>6</sup>
			66	t <sub>1u</sub> <sup>6</sup> h <sub>u</sub> <sup>10</sup> or t <sub>2u</sub> <sup>6</sup> h <sub>u</sub> <sup>10</sup>
			<b>72</b>	<b>t<sub>1u</sub><sup>6</sup>t<sub>2u</sub><sup>6</sup>h<sub>u</sub><sup>10</sup></b>

<sup>a</sup> Angular momentum quantum number for a spherical shell of  $\pi$  electrons. <sup>b</sup> Number of  $\pi$  electrons for closed-shell ground-state configurations in icosahedral symmetry. <sup>c</sup> HOMO symmetries for all levels of given *l*; the superscripted digit shows the number of electrons for complete occupation of the shell.

occupation of the  $\pi$  orbitals has been evaluated.<sup>23,65–67</sup> In a first approximation, the  $\pi$ -electron system of an icosahedral fullerene like C<sub>20</sub>, C<sub>60</sub>, or C<sub>80</sub> can be described with a spherical electron gas incasing the  $\sigma$  framework in a double skin. The wave functions of this electron gas are characterized by the angular momentum quantum numbers  $l = 0, 1, 2, 3, \dots$  corresponding to s, p, d, and f  $\pi$  shells. These shells are analogues of atomic orbitals. The most significant difference is that the sphere defined by the  $\sigma$  framework represents a nodal plane and the electron density in the center of the sphere approaches zero. The irreducible representations of the icosahedral group can be found using group theory by lowering the symmetry from full rotational symmetry to icosahedral symmetry treated as a perturbation (Table 3).<sup>10,23,49,65,66,68</sup>

Considering the Pauli principle, it can be seen that upon occupation with  $2(N+1)^2$  electrons, all  $\pi$  shells are completely filled. The shape of the molecular s, p, d, and g orbitals is still very reminiscent of that of the corresponding atomic H-like orbitals (Figure 2). The charged fullerene C<sub>60</sub><sup>10+</sup>,<sup>67,69</sup> for example, represents a closed-shell system with  $n = 50$   $\pi$  electrons where all  $\pi$  orbitals up to  $l = 4$  (g shell) are completely occupied. Since the angular momenta are

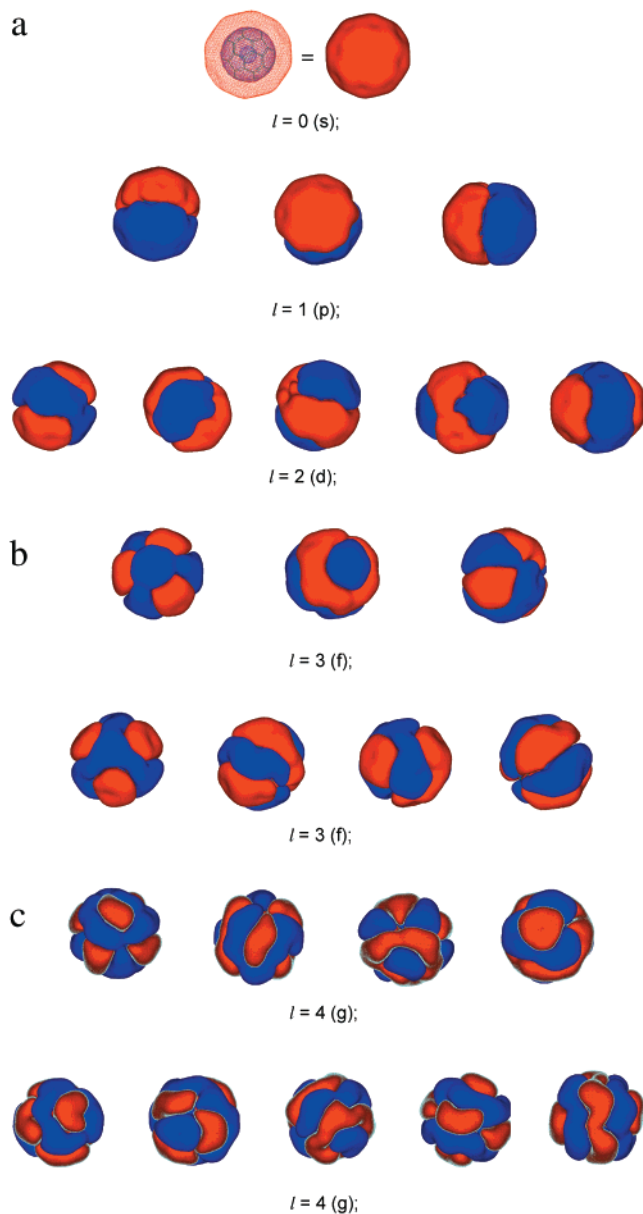


**Figure 2.** PM3/MNDO-calculated  $\pi$  orbitals of  $C_{60}^{10+}$ . The position of the  $C_{60}$  skeleton is the same in all orbital presentations. The s orbital is also shown in *wire mesh* presentation. This makes the nodal plane visible, which is hidden in the other presentations. (Reprinted with permission from ref 67. Copyright 2000 Wiley-VCH.)

symmetrically distributed, no distortion from spherical or icosahedral symmetry is expected in cases where all states are completely filled. Hence, no significant bond-length alternation is expected for  $C_{60}^{10+}$ . The B3LYP/6-31G\*<sup>-</sup>-calculated lengths of the [6,6]- and [5,6]-bonds of  $C_{60}^{10+}$  ( $I_h$  symmetry) are 1.48 and 1.44 Å.<sup>67,69</sup> Therefore, the bond-length alternation is lower than that of neutral  $C_{60}$  and comparable with that in  $T_h$ -symmetrical hexakisadducts<sup>70</sup> containing benzenoid substructures (see section IV).

What are the consequences of filling the  $l=5$  (h) shell on the geometry of  $C_{60}$ ? The complete filling of the  $l=5$  state would lead to an accumulation of 72  $\pi$  electrons, assuming that all the  $l=5$  states are filled, before any  $l=6$  level is being occupied. In icosahedral symmetry, the  $l=5$  states are split into the  $h_u + t_{1u} + t_{2u}$  irreducible representations (Table

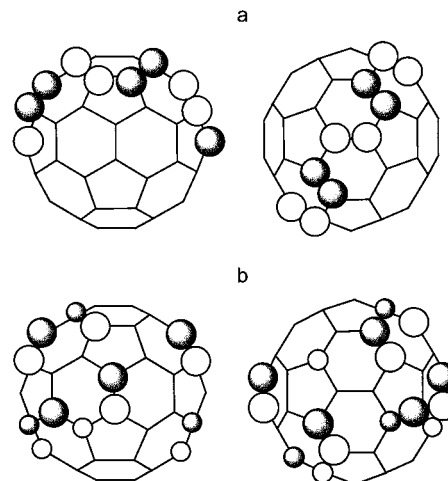


**Figure 3.** Schematic representation of one of the five degenerate HOMOs (a) and one of the three degenerate LUMOs (b) of  $C_{60}$ . Each orbital is represented by a front and side view. Only the exohedral part of the orbitals projected to the corresponding C atoms is shown for clarity.<sup>23</sup>

3).<sup>10,23,49,65,66,68,71</sup> The lowest energy level is the  $h_u$  level, which in neutral  $C_{60}$  is completely filled with the 10 available electrons. The resulting  $h_u^{10}$  ground state is nondegenerate (Hund's rule) and has the angular momentum quantum numbers  $L=0$ ,  $S=0$ ,  $J=0$ , and the many-electron  $h_u^{10}$  configuration has  $A_g$  symmetry within the point group  $I_h$ . A comparison of the representations of the sets of  $\sigma^*$  orbitals along the [6,6]-bonds with that of the  $\pi$  electrons shows that when filling the  $h_u$  shell, the occupied  $\pi$  orbitals form a set which is completely equivalent to the set of localized  $\sigma$  orbitals along the [6,6]-bonds.<sup>65,66</sup> Therefore, the molecular orbitals can be weakly localized at these sites by a unitary transformation. This distortion exactly corresponds to the internal structural degree of freedom that the  $C_{60}$  molecule has without breaking the  $I_h$  symmetry.<sup>65,66</sup> Looking at the symmetries of the  $h_u$  orbitals reveals bonding interactions with the [6,6]-bonds and antibonding interactions in the [5,6]-bonds (Figure 3).<sup>23,72</sup> As a consequence, filling the  $h_u$  orbitals causes a shortening of the [6,6]-bonds, which leads to an increase in bond energy and at the same time favors longer [5,6]-bonds by reducing antibonding interactions.<sup>73</sup> More pronounced distortions were calculated for the partially filled systems  $C_{60}^{2+}$ ,  $C_{60}^{4+}$ ,  $C_{60}^{6+}$ , and  $C_{60}^{8+}$ . Here, even a symmetry lowering was predicted to  $D_{5d}$  or  $C_{5v}$ , respectively.<sup>69</sup>

Adding 12 electrons into the  $t_{1u}$  and  $t_{2u}$  orbitals would lead to a closed-shell situation again. In contrast to icosahedral  $C_{80}$ , however, an anomaly is observed for  $C_{60}$ , since the  $t_{1g}$  orbitals derived from the  $l=6$  shell are lower in energy than the  $t_{2u}$  orbitals from the  $l=5$  shell. As a consequence, the  $t_{1g}$  orbitals are filled before the  $t_{2u}$  orbitals. In contrast to the  $h_u$  orbitals, the nodes of the  $t_{1u}$  and  $t_{1g}$  orbitals are located at the [6,6]-sites and the bonding interactions at the [5,6]-sites. As a consequence, filling the  $t_{1u}$  and  $t_{1g}$  is expected to favor bond length equalization. Indeed, calculations<sup>74</sup> on  $K_6C_{60}$  showed that the bond lengths become more equalized with the [6,6]-bonds being 1.42 Å and the [5,6]-bonds 1.45 Å. The same

calculations on  $C_{60}^{12-}$  ( $Li_{12}C_{60}$ ) predict a further elongation of the [6,6]-bonds (1.45 Å) and already a shortening of the [5,6]-bonds (1.44 Å).<sup>74</sup> In the crystal structure of  $K_6C_{60}$ , the lengths of the [6,6]- and [5,6]-bonds were found to be 1.445(3) and 1.432(10) Å, respectively.<sup>75</sup>

The bond-length alternation in  $C_{60}$  is obviously not only caused by the nature of the  $\sigma$  framework. The difference in bond lengths between [6,6]- and [5,6]-bonds is directly connected with the symmetry and the occupation of its molecular  $\pi$  orbitals. The shortening of one of the types of bonds is equivalent to a partial localization of the  $\pi$  orbitals into localized bonds. It is the filling of the  $h_u$ ,  $t_{1u}$ , and  $t_{1g}$  orbitals which is responsible for the degree of bond-length alternation. This is closely related to the situation in the annulenes where depending on the filling of the molecular orbitals with either  $4N$  or  $4N + 2$   $\pi$  electrons a distortion from the ideal  $D_{nh}$  takes place or not. Calculations on the icosahedral homologues  $C_{20}$  and  $C_{80}$  revealed the same behavior.<sup>67</sup> Only the closed-shell species  $C_{20}^{2+}$  (closed  $l = 2$  shell,  $n_c = 18$ ) and  $C_{80}^{8+}$  (closed  $l = 5$  shell,  $n_c = 72$ ) exhibit ideal  $I_h$  symmetry, whereas symmetry lowering is predicted to  $C_2$  for  $C_{20}$  and to  $D_{5d}$  for  $C_{80}$ .

The distortion of neutral  $C_{60}$  caused by the filling of the  $h_u$  orbitals and the resulting increase in bond-length alternation has a direct consequence for the evaluation of the VB structures. The shorter [6,6]-bonds have more double-bond character than the longer [5,6]-bonds.<sup>73</sup> Hence, the VB structure depicted in Figure 1 consisting of [6,6]-double bonds and a [5,6]-single bond represents a good description of the electronic and chemical properties (see section IV) of neutral  $C_{60}$ . Moreover, a clear distinction between the archetypal aromatic benzene can be drawn.<sup>76</sup> In benzene, the fully symmetric charge density requires a VB description where at least two  $D_{3h}$ -symmetric VB structures are mixed leading to the equivalence of all six bonds. The VB structure of  $C_{60}$ , however (Figure 1), already exhibits the full  $I_h$  symmetry of the carbon framework. This VB structure is the only one of the 12 500 to satisfy the symmetry criterion. There are 20  $C_{60}$  isomers that surpass the count of 12 500 Kekulé structures, although they are less stable (non-IPR isomers).<sup>76</sup> Some mixing in of other VB structures in  $I_h C_{60}$  certainly improves the energy but in contrast to benzene is not forced by symmetry. The principal Kekulé structure depicted in Figure 1 is at the same time the most important VB structure according to the Fries rule.<sup>77,78</sup> The Fries rule is an empirical rule which states that the Kekulé structures with the largest number of Kekulé benzene rings are dominant. On the basis of the aromaticity criterion of the maximum number of equivalent resonance structures,  $C_{60}$ , where VB structures containing double bonds in pentagons are unimportant, has to be considered to be not very aromatic. Resonant VB structures have also been considered to explain electronic properties such as hyperpolarizabilities  $\beta$  of push-pull fullerene derivatives.<sup>79</sup> It was found that two types of resonant structures in terms of single-double bond alternation are of importance. The first resonant structure starts and finishes with

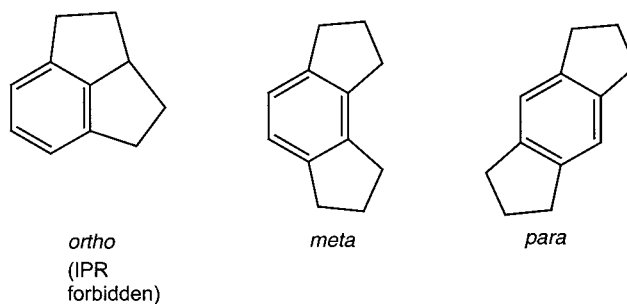


**Figure 4.** *Ortho*-, *meta*- and *para*-relationships of pentagons within fullerenes.

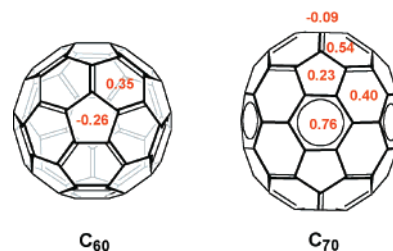


**Figure 5.** HOMA values<sup>81</sup> for the pentagons and hexagons in  $C_{60}$  (electron diffraction structure in the gas phase) and  $C_{70} \cdot 6S_8$ .

[6,6]-double bonds and contributes positively to  $\beta$ ; the second starts and finishes with [5,6]-single bonds and contributes negatively. The ratio of their contribution is roughly 2:1.<sup>79</sup> To represent  $C_{70}$  properly, in contrast to  $C_{60}$ , two VB structures are required. Therefore, in a first approximation  $C_{70}$  can be represented by two corannulene caps connected by an equatorial belt consisting of five benzene-like rings. These benzene-like rings form a cyclic phenylene (Figure 1).<sup>80</sup>

The minimization of double bonds in five-membered rings is considered to be a general principle that governs the preferred formation of fullerene isomers containing the highest number of Kekulé benzene rings.<sup>31</sup> If the pentagons are located in a *meta* relationship, an "ideal" bond distribution is provided (Figure 4). In contrast, a *para* relationship does not allow for the formation of Kekulé benzene rings. The latter arrangement is found throughout icosahedral  $C_{80}$ .<sup>31</sup>

Application of the structural aromaticity index HOMA (harmonic oscillator model of aromaticity), which employs experimental bond lengths and describes the degree of alternation of bond lengths in question as well as their deviations from the optimal lengths attributed to the typical aromatic state, leads to the conclusion that the pentagons in fullerenes and their derivatives exhibit very weak aromatic or antiaromatic character, with HOMA values ranging from  $-0.26$  to  $0.25$ .<sup>14,81</sup> In contrast, the hexagons exhibit a much larger variation in aromatic character, with values ranging from  $0.1$  ( $C_{60}^-$ ) to  $0.76$  in  $C_{70} \cdot 6S_8$ . For the systems under consideration, the pentagons were found to be less aromatic than the hexagons, except for the case of  $C_{60}^-$ . On the basis of this criterion,  $C_{60}$  was found to be less aromatic than  $C_{70}$  (Figure 5). The results are in good agreement with magnetic susceptibility studies.

**Table 4. Resonances Energies (RE) for C<sub>60</sub> and Benzene<sup>12</sup>**

scheme of resonance energy calculation	C <sub>60</sub> RE	RE/e uncorrected	RE/e uncorrected <sup>a</sup>	benzene	
				RE	RE/e
HRE, $\beta^{82,83}$	33.16	0.553	0.365	2	0.333
HSRE, $\beta^{84}$	1.87	0.031	0.027	0.39	0.065
CCMRE, <sup>b</sup> eV <sup>89–91</sup>	7.20	0.120	0.101	0.841	0.140
LM, eV <sup>89</sup>	11.18	0.186	0.157	0.821	0.137
AS, $\beta^{89}$	1.96	0.033	0.029	0.44	0.073
TRE, $\beta^{85–88}$	1.643	0.027	0.024	0.276	0.046

<sup>a</sup> According to 3D-HMO model,  $\rho = 0.879$ ;<sup>94</sup> the correction for nonplanarity in CCMRE and LN calculations is 0.84. <sup>b</sup> Herdon's parameters:  $R_1 = 0.841$  eV,  $R_2 = 0.336$  eV,  $Q_1 = -0.65$  eV.

In conclusion, the evaluation of the structural criteria of aromaticity shows that C<sub>60</sub> exhibits a pronounced bond-length alternation between [6,6]- and [5,6]-bonds. This is a consequence of the incomplete filling of the  $l = 5$  shell. Charged C<sub>60</sub> systems with completely filled shells, especially C<sub>60</sub><sup>10+</sup>, are much more aromatic and exhibit a less pronounced bond-length alternation. The same holds true for the icosahedral fullerenes C<sub>20</sub> and C<sub>80</sub>. The applications of structural aromaticity indices reveal ambiguous aromatic character, namely, aromatic hexagons and antiaromatic pentagons within neutral C<sub>60</sub>. The geometry of the polar caps of C<sub>70</sub> are comparable to C<sub>60</sub>. The geometry of the cyclic phenylene-type belt with C<sub>70</sub> suggests a much more pronounced aromatic character of this substructure. Also, here, the pentagons are less aromatic than the hexagons. Bond-length alternation between [6,6]- and [5,6]-bonds is also a typical phenomenon of the isolated higher fullerenes.

### III. Energetic Criteria

The aromatic stabilization of a molecule is the energy contribution which is due to the cyclic bond delocalization. This contribution is defined as the resonance energy (RE).<sup>12</sup> Several schemes for calculating resonance energies, such as Hückel resonance energies,<sup>82,83</sup> Hess–Schaad resonance energies,<sup>84</sup> topological resonance energies,<sup>85–88</sup> conjugated circuits model resonance energies (CCMRE),<sup>89–91</sup> the aromatic stabilization index (AS),<sup>89</sup> and the logarithmic model (LM),<sup>89</sup> have been applied to fullerenes (Table 4).

The problem in determining resonance energies is to single out the contribution from the cyclic bond delocalization from the total energy of the molecule. In other words, model reference structures have to be defined whose energy would differ from that of the molecule under consideration precisely by the component corresponding to the delocalization in question.<sup>12</sup> Further approaches to evaluate the amount of aromatic stabilization in C<sub>60</sub> were based on isodesmic calculations<sup>76</sup> and on estimations of the heat of hydrogenation.<sup>8,76</sup>

#### 1. MO Resonance Energies of Fullerenes

The results of a simple Hückel calculation of C<sub>60</sub> are represented Table 4 and Figure 6. The lowest eigenvalue is equal to  $-3$ . This is characteristic for regular graphs, for which the lowest eigenvalue is equal in magnitude to the valency of their vertexes.

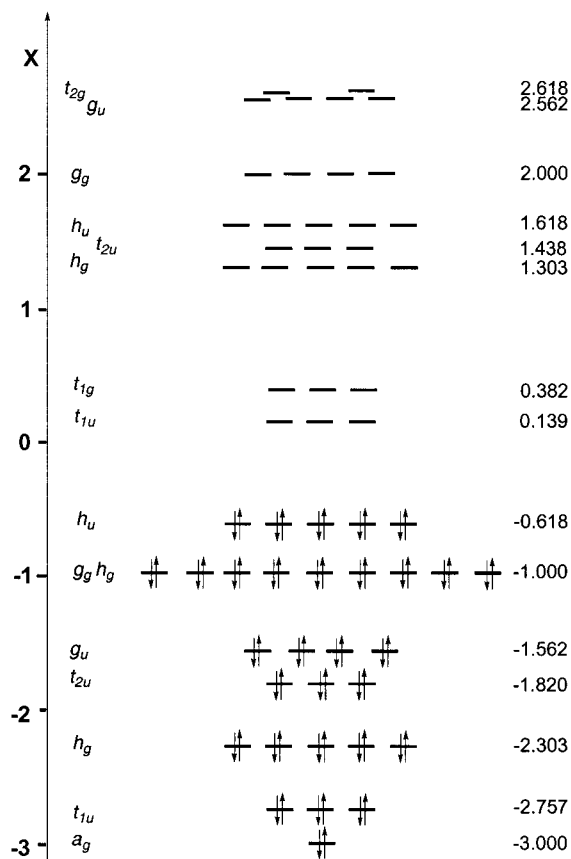


**Figure 6.** Hückel energy levels in units of the parameter  $\beta$  of buckminsterfullerene.

The Hückel  $\pi$ -electron energy  $E_\pi$  (HMO) is equal to twice the sum of the occupied orbital energy levels, that is  $93.168\beta$ . A simple type of HRE for C<sub>60</sub> is given by eq 1<sup>91</sup>

$$\text{HRE}(\text{C}_{60}) = E_\pi(\text{HMO}) - 2n_{\text{C}=\text{C}} = 33.17\beta \quad (1)$$

where  $n_{\text{C}=\text{C}}$  is the number of C–C double bonds in the molecule. The HRE per  $\pi$  electron (HRE/e) is equal to  $0.55\beta$ . This value is higher than the corresponding value for benzene ( $0.33\beta$ ). However, these values cannot be compared directly since C<sub>60</sub> is nonplanar.

To extend the notions of  $\pi$ -electron delocalization to nonplanar systems, concepts of the  $\pi$  orbital and  $\sigma$ - $\pi$  separability had to be defined for the three-dimensional case. Such a scheme, the so-called  $\pi$ -orbital axis vector (POAV), was introduced by Haddon.<sup>18,92–97</sup> The POAV analysis extends  $\sigma$ - $\pi$  separability into three dimensions with the use of the

orbital orthogonality which is the basis of standard hybridization theory. The POAV2 analysis defines a  $\pi$  orbital to be the hybrid orbital that is locally orthogonal to the  $\sigma$  orbitals. The POAV1 analysis is a particular case of it when the  $\sigma$ - $\sigma$  bond angles are equal. It allows the fractional hybridization ( $m/m+1$ ) of the atomic  $\pi$  orbitals ( $s^m p$ ) obtained from the orthogonality relations to be defined. The C atoms of fullerenes are further characterized by their pyramidalization angle ( $\theta_{\sigma\pi} - 90$ ), where  $\theta_{\sigma\pi}$  is the common angle made by the  $\pi$ -orbital axis vector and the three  $\sigma$  bonds. For  $C_{60}$ , an average  $\sigma$ -bond hybridization and a fractional  $s$  character of 0.085 was found. As a consequence, the  $\pi$  orbitals extend further beyond the outer surface than into the interior of  $C_{60}$ . The POAV also explains why  $C_{60}$  is a fairly electronegative molecule, since due to the rehybridization, low-lying  $\pi^*$  orbitals also exhibit considerable  $s$  character. Associated with the non-planarity of fullerenes is the introduction of strain energy. The strain energy in fullerenes was also estimated based on the POAV analysis. The strain in  $C_{60}$ , for example, was deduced to be about 8 kcal/mol per C atom.<sup>18</sup> Calculations of total energies of  $C_{60}$  and higher fullerenes have been performed using various levels of empirical, semiempirical, and ab initio theory. The heats of formation of  $C_{60}$  and  $C_{70}$  have been determined experimentally by calorimetry to be 10.16 kcal/mol per C atom for  $C_{60}$  and 9.65 kcal/mol per C atom for  $C_{70}$ .<sup>8,98</sup> Upon increasing the cluster to giant fullerenes, the RE approaches the value for graphite.<sup>98-101</sup> Since fullerenes are among the most strained organic molecules,<sup>18</sup> it is obvious that the magnitude of aromatic stabilization or antiaromatic destabilization (energetic criterion of aromaticity) caused by the conjugated  $\pi$ -electron system represents an even smaller contribution to the overall energy than in strain-free systems. Therefore, compared to planar aromatics, it is even more important for the classification of the degree of aromaticity to single out the stabilization (destabilization) caused by the cyclic or spherical bond delocalization. The POAV scheme was used to extend the HMO theory to fullerenes.<sup>95,102</sup> The corresponding resonance energies per  $\pi$  electron are comparable to the values for benzene (Table 4). However, it has to be considered that the HRE is used to evaluate the energy of the electron delocalization rather than the cyclic bond delocalization,<sup>12</sup> and therefore, the HRE scheme is, in principle, inadequate to evaluate the degree of aromaticity.

If other models of aromaticity are taken, which are also based on Hückel  $\pi$  energies but use more elaborate reference structures, opposite results were obtained, with benzene being more aromatic than  $C_{60}$ . The Hess-Schaad scheme,<sup>84</sup> in which the reference structure is given in terms of six independent parameters, gives a HSRE/e which is about one-half that of benzene (Table 4). A scheme developed by the Zagreb group affords values comparable to those obtained with the Hess-Schaad model.<sup>91</sup>

## 2. Topological Resonance Energies of Fullerenes

The topological resonance energy (TRE)<sup>85-88</sup> is considered to be a useful measure of aromatic stabil-

ity.<sup>12</sup> It is defined as

$$\text{TRE} = \sum_i g_i (x_i - x_i^{ac}) \quad (2)$$

where  $g_i$  is the number of  $\pi$  electrons populating each bonding energy level of a molecule, the  $x_i$ 's are solutions of the Hückel determinant corresponding to the energy levels represented in Figure 5, and  $x_i^{ac}$ 's are the solutions of the matching polynomial. Like the HSRE, the TRE represent the sole contributions arising from cyclic bond delocalizations. The TRE/e value for  $C_{60}$  is about 0.6 that of benzene (Table 4). Also, these results confirm that uncharged  $C_{60}$  is inferior to benzene in aromatic stability and that it cannot be considered a superaromatic system.  $C_{60}$  has a lower % TRE than the unstable hexacene and heptacene.<sup>85</sup> The % TRE is an aromatic stabilization energy normalized to the total  $\pi$ -binding energy of the polyene reference, which is roughly proportional to the size of the  $\pi$ -electron system. As a consequence, it was found that larger fullerenes have a higher % TRE and that positively charged fullerenes exhibit considerably smaller % TREs than anionic systems.<sup>86</sup> The % TREs were correlated with the amount of aromaticity of the fullerene under consideration. However, this interpretation is not in line with other criteria like structures (section II) and magnetic properties (section V), according to which, for example,  $C_{60}^{10+}$  was found to be much more aromatic than  $C_{60}$ . Further examples are  $C_{70}^{6-}$  and higher neutral fullerenes, which experimentally have been found to be less aromatic than  $C_{70}$ . TREs were also determined for some fullerene derivatives.<sup>88</sup>

## 3. VB Model of $C_{60}$

Kekulé structures were used to calculate the resonance energy of  $C_{60}$  with a VB model, namely, the conjugated-circuit model (CCM).<sup>89-91</sup> The concept of conjugated circuits is based on a graph-theoretical analysis of Kekulé structures. Conjugated circuits contain a regular alternation of C-C single and double bonds. The conjugated circuits were used to determine resonance energies according to

$$\text{CCMRE} = \sum_i (r_n R_n - q_n Q_n) / K \quad (3)$$

with  $K$  being the Kekulé-structure count,  $R_n$  and  $Q_n$  oppositely signed parameters corresponding to  $4N+2$  and  $4N$  conjugated circuits, and  $r_n$  and  $q_n$  the total counts of  $R_n$  and  $Q_n$  circuits. The parameters  $R_n$  and  $Q_n$  are a measure for the aromatic and antiaromatic destabilization, respectively. In this way, the resonance energy for  $C_{60}$  was calculated to be  $\text{CCMRE} = 7.20$  eV or  $\text{CCMRE}/60 = 0.12$  eV (Table 4). The CCM also predicts benzene ( $\text{CCMRE}/6 = 0.14$  eV) to be more aromatic than  $C_{60}$ .

## 4. Isodesmic Equations

A related quantity obtained from ab initio calculations is the bond separation energy, which was

defined for  $C_{60}$  by eq 4<sup>76</sup>



This is an isodesmic equation (i.e., it preserves the number of formal single and double bonds between heavy atoms). The cost of separating the bonds was predicted to be  $0.855E_h$  (2245 kJ/mol). Bond for bond, it is significantly easier to cleave the  $C_{60}$  framework than an aromatic model would suggest. The separation of 90 benzenoid bonds would cost twice as much energy.

## 5. Heat of Hydrogenation

The heat of hydrogenation of  $C_{60}$  has not been measured yet, since the completely hydrogenated fullerene  $C_{60}H_{60}$  is synthetically not available. Theoretical estimates based on the reaction  $C_{60} + 30H_2 \rightarrow C_{60}H_{60}$  indicated a stabilization per double bond in  $C_{60}$  about one-half that in benzene.<sup>76</sup> The heat of hydrogenation of the reaction  $C_{60} + H_2 \rightarrow C_{60}H_2$  leading to the most stable 1,2-isomer was semi-empirically calculated to be 36 kcal/mol.<sup>103</sup> Quite apart from the effect of strain relief, the interpretation of these results is not straightforward because eclipsing interactions between the two H atoms have to be taken into account. Similar calculations with comparable results were carried out for  $C_{70}$ .<sup>104,105</sup>

## 6. Summary

Evaluation of the energy criterium does not reveal any superior aromaticity of  $C_{60}$ . Aromaticity is not an important factor determining the remarkable stability of  $C_{60}$ . The stability of  $C_{60}$  is mainly governed by kinetic factors and by the fact that no substitution reactions are possible without cage rupture (see section IV). The fact that buckminsterfullerene is the most stable  $C_{60}$  isomer is mainly due to strain arguments, since it is the only IPR isomer. However, the RE stabilizations by means of several schemes are also the highest among a number of other isomers.<sup>26,35,106</sup> In conclusion, based on the energetic criteria of aromaticity, such as resonance energies, isodesmic equations, and heats of formation, it can be stated that  $C_{60}$  clearly exhibits an aromatic stability which is significantly inferior to that of benzene. Upon increasing the cluster size to giant fullerenes, the resonance energies approach the value for graphite.

## IV. Reactivity Criteria

### 1. Reactivity Indices

The HOMO–LUMO gap, a qualitative reactivity index,<sup>107</sup> was obtained from Hückel calculations of  $C_{60}$ .<sup>108</sup> The HOMO–LUMO gap of  $C_{60}$  ( $0.757\beta$ ) is much smaller than that of benzene (HOMO–LUMO =  $2\beta$ ). A related index is the absolute chemical hardness  $\eta$ ,<sup>109–111</sup> which is defined by the expression<sup>112,113</sup>

$$\eta = (\text{HOMO} - \text{LUMO})/2 \quad (5)$$

Since  $\eta$  is defined in terms of frontier orbitals, the absolute hardness is considered to be a good reactivity criterion. The harder a molecule (large  $\eta$  value),

the more unreactive it is. The values of hardness for  $C_{60}$  and benzene are  $0.378 (-\beta)$  and  $1.000 (-\beta)$ , respectively. Hence, both molecules can be considered to be hard, with benzene being much less reactive than  $C_{60}$ . Related to absolute chemical hardness  $\eta$  is the  $T$  value.<sup>114–116</sup> This general index for kinetic stability was determined for a whole series of fullerenes.<sup>117</sup> As another reactivity index, bond resonance energies (BRE) were defined as the contribution of a given  $\pi$  bond in fullerenes to the TRE.<sup>118</sup>

These evaluations suggest that  $C_{60}$  and related fullerenes should be more reactive than benzene. However, it is difficult to directly compare the reactivities of these typical representatives of two- and three-dimensional aromatics. In contrast to benzene and other planar aromatics, the  $\pi$  systems of the fullerenes have no boundaries.<sup>18</sup> In other words, the fullerenes contain no hydrogens that can be replaced via substitution reactions. As a consequence, a chemical transformation of fullerenes is always accompanied with a change of the structure, whereas retention of the structural type is characteristic for reactions of benzene-like aromatics. Two main types of primary chemical transformations are possible: addition reactions and redox reactions.

## 2. Principles of Fullerene Reactivity

The chemistry of  $C_{60}$  and that of a series of higher fullerenes has been intensively investigated in the last 10 years. Various areas of fullerene chemistry as well as principles of fullerene reactivity were summarized in a variety of reviews.<sup>4–11,20–26</sup> Here we will focus on those chemical properties which are relevant to aromaticity.

### A. Retention of the Structural Type

Since any exohedral modification of a fullerene is necessarily accompanied with an addition reaction to the carbon framework, the criterion of retention of the structural type can only be considered with respect to (a) reversibility of addition reactions, (b) rearrangements of the addends on the surface, and (c) preferred formation of addition patterns involving the highest possible degree of structural retention. Due to release of strain energy, addition reactions leading to  $sp^3$  C atoms within the fullerene framework are thermodynamically favorable. It was estimated that the advantage of the complexation of a transition-metal fragment to a [6,6]-double bond for the pyramidalization of the two C atoms is about 26 kcal/mol.<sup>18</sup> Similarly, the difference between the MNDO heats of formations of  $C_{60}$  and the most stable isomer of  $C_{60}H_2$  (1,2-adduct) is 35.6 kcal/mol.<sup>103</sup> Hence,  $C_{60}$  and higher fullerenes exhibit a pronounced tendency to undergo addition reactions. However, a variety of additions to  $C_{60}$  are reversible. For example, the [4+2]-cycloadditions of  $C_{60}$  with anthracenes or cyclopentadiene are reversible, in some cases already at room temperature.<sup>119–124</sup> Also, azides bind reversibly and, as a consequence, can be used as protecting groups for [6,6]-double bonds of the fullerene core.<sup>125</sup> Hydrogenated fullerenes such as  $C_{60}H_{18}$  or  $C_{60}H_{36}$  can easily be converted into parent  $C_{60}$  by the action of 2,3-dichloro-5,6-dicy-



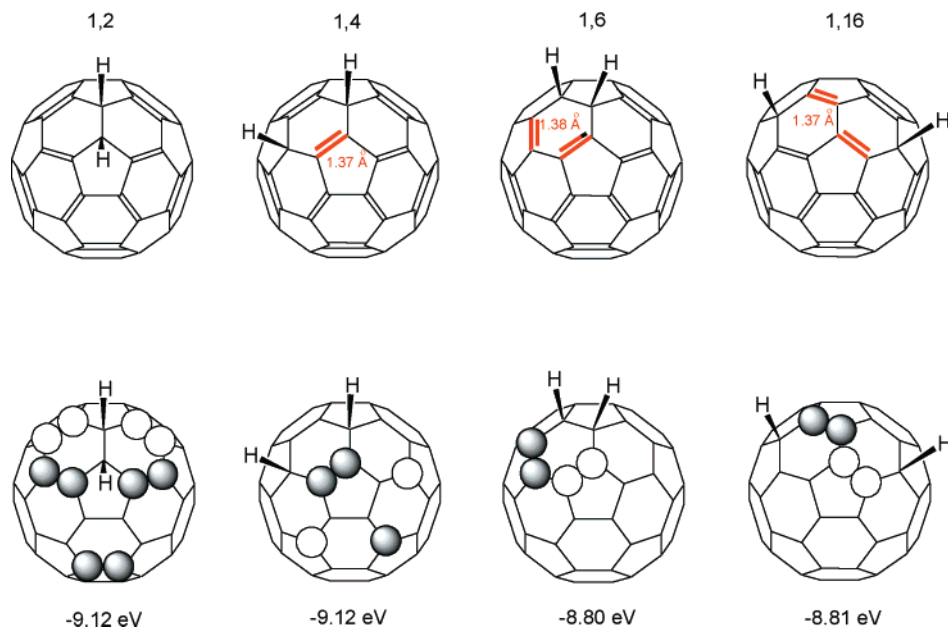
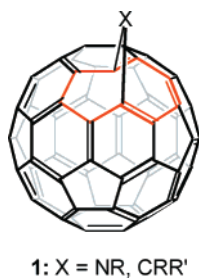


**Figure 7.** Lowest energy VB structures, PM3-calculated lengths of [5,6]-double bonds, HOMO coefficients, and HOMO energies of different dihydro[60]fullerenes<sup>23</sup>.

anobenzoquinone (DDQ) in refluxing toluene.<sup>126</sup> Another reversible reaction of preparative importance is the *retro*-Bingel reaction, where malonate addends can selectively be removed in high yields.<sup>127–129</sup> This retro-reaction is promoted by exhaustive electrolytic reduction at constant potential. The Bingel–*retro*-Bingel strategy was used, e.g., for the preparation of pure constitutional isomers of higher fullerenes, such as  $C_{2v}$ - $C_{78}$ <sup>130</sup> and a new  $C_{84}$  isomer<sup>131</sup> as well as of enantiomerically pure chiral higher fullerenes such as  $^iC$ - $C_{76}$  and  $^iA$ - $C_{76}$ <sup>128</sup> and  $^iC$ - $C_{84}$  and  $^iA$ - $C_{84}$ .<sup>131</sup> Further protocols for reversible addition reactions to fullerenes are the removal of cyclohexene rings fused to the carbon cage by Diels–Alder addition with buta-1,3-dienes<sup>132,133</sup> and the fusion of isoxazoline rings to the fullerene by dipolar cycloaddition with nitrile oxides and removal of the addend with  $Mo(CO)_6$  or diisobutylaluminum hydride (DIBAL-H).<sup>134</sup>

Rearrangements of addends can easily be determined if they are accompanied by a change of the addition pattern.<sup>135,136</sup> Rearrangements within multiple cycloaddition adducts leading to different regioisomers were observed, for example, upon heating of bismalonates<sup>137</sup> or upon two-electron controlled potential electrolysis (CPE) of bis- and trismalonates.<sup>138</sup> Very remarkable rearrangements are the thermolytical conversions of fulleropyrazolines or fullerotrizolines leading to cluster-opened [5,6]-bridged methano- or imino[60]fullerenes **1** accompa-

**Chart 1**



nied by the extrusion of  $N_2$ .<sup>139–154</sup> In these adducts the entire 60  $\pi$ -electron system remains intact. The presence of a structurally largely retained fullerene chromophore within adducts **1** (Chart 1) was demonstrated, for example, by electronic absorption spectroscopy (see also the magnetic properties in section V.1).<sup>139–154</sup>

The regiochemistry of addition to  $C_{60}$  and similarly to higher fullerenes is driven by the maintenance of the orbital symmetry, characterized by bonding  $\pi$  interactions within the [6,6]-bonds and antibonding  $\pi$  interactions within the [5,6]-bonds.<sup>23</sup> In other words, those fullerene adducts are preferably formed in which the number of [5,6]-double bonds within the predominant VB structure is minimized. This behavior is in line with the Fries rule (see section II), which claims the maximum amount of Kekulé benzene units for the predominant VB structure of a polycyclic aromatic system. The introduction of one [5,6]-double bond costs about 8.5 kcal/mol.<sup>23</sup> Adducts formed regioselectively by one or several successive 1,2-additions to [6,6]-double bonds have MO structures which are closely correlated with that of  $C_{60}$ .<sup>23</sup> The lowest energy VB structures of these adducts contain only [6,6]-double bonds. 1,2-Additions take place at [6,6]-double bonds. 1,4-Additions (introduction of one unfavorable [5,6]-double bond) or 1,6-addition to position 1 and 16 (introduction of two [5,6]-double bonds) take place only with sterically demanding addends.<sup>23</sup> The introduction of double bonds within five-membered rings depicted in the corresponding VB structure is caused by strong bonding interactions at these sites (Figure 7). As a consequence, the corresponding [5,6]-bonds are becoming considerably shorter than 'normal' ones.

All these observations indicate that there is a certain but hardly quantifiable propensity of  $C_{60}$  to preserve its structural type and therefore a certain degree of aromaticity. The same is true to some extent for  $C_{70}$ .<sup>15</sup> Additions preferably take place at

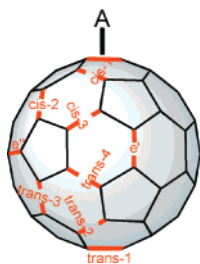


**Figure 8.** Relative positional relationships in a 1,2-adduct of  $C_{60}$ .

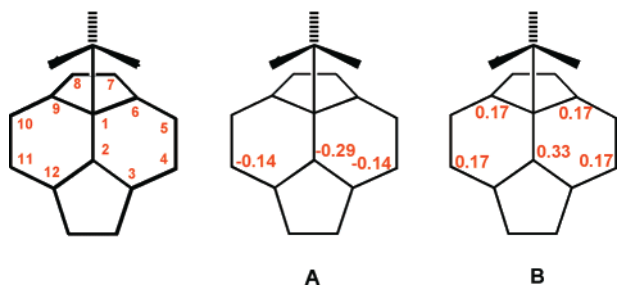


**Figure 9.** Charge distribution (A) (Mulliken charges) and spin distribution (B) in the intermediates  $t\text{-Bu}C_{60}^-$  and  $t\text{-Bu}C_{60}^\bullet$ .<sup>23</sup>

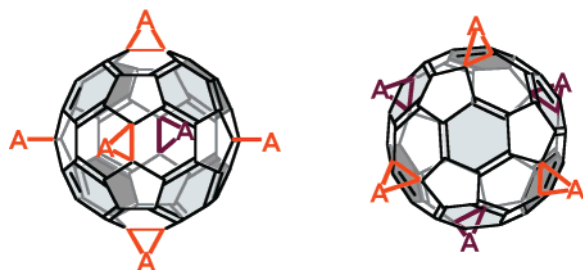


**Figure 10.** Two different views of the schematic representation of a hexakisadduct of  $C_{60}$  with a  $T_h$  symmetrical addition pattern.

the  $C_{60}$ -like [6,6]-double bonds between C1 and C2 or C5 and C7 at the poles. Only recently, the first

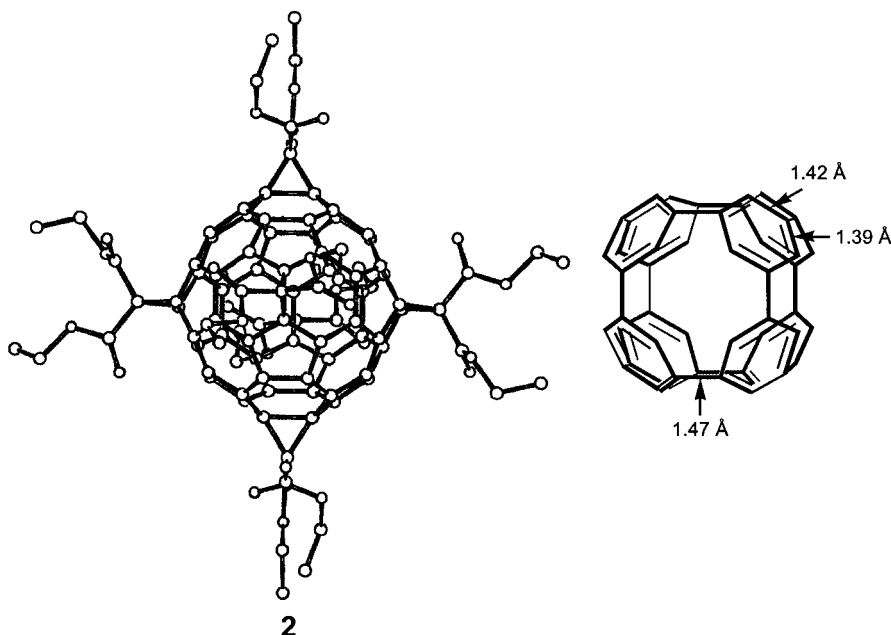


**Figure 11.** Single-crystal X-ray analysis of  $T_h$  symmetrical  $C_{66}(\text{COOEt})_{12}$  (**2**) and cyclophane substructure of the remaining  $\pi$  system, consisting of eight benzenoid rings. (Reprinted with permission from ref 70. Copyright 1995 Wiley-VCH.)

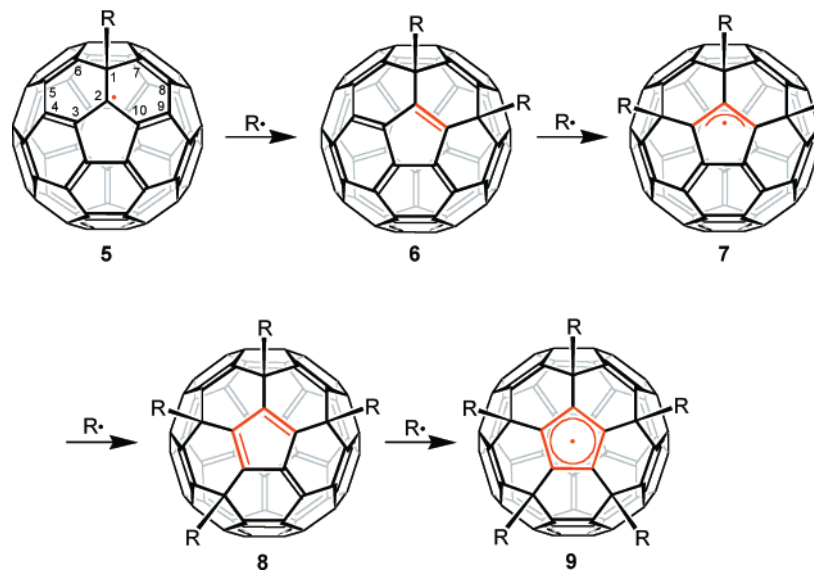
example for an addition to the [5,6]-bond of  $C_{70}$  located between C7 and C8 was discovered.<sup>80</sup> In this case, the [5,6]-bond did not open. An attack to positions 7 and 8 is probably possible due to the fact that this [5,6]-bond has considerable double-bond character (Figure 1).

### B. Chemical Indication of Cyclic Electron Delocalization within $C_{60}$ :cis-1 Reactivity

Analysis of subsequent addition reactions to [6,6]-bonds of  $C_{60}$  revealed that sterically demanding addends preferably bind at  $e$  positions, whereas sterically nondemanding addends prefer  $cis$ -1 positions followed by  $e$  positions (Figure 8).<sup>23,155</sup> The  $e$  regioselectivity<sup>70,135,137,155</sup> and to some extent the  $cis$ -1 selectivity<sup>155</sup> can be explained with the coefficients of frontier orbitals. Due to the complete orthogonality of the three LUMOs and a pronounced orthogonality of the five HOMOs, the energetically favorable frontier orbitals of monoadducts exhibit high coefficients in  $e$  and  $cis$ -1 positions.<sup>23</sup> However, this aspect alone cannot explain the very pronounced  $cis$ -1 selectivity for additions of sterically nondemanding addends. The fact that the  $cis$ -1 bonds in a [6,6]-monoadduct of  $C_{60}$  are shorter than the  $e'$  bonds,<sup>155</sup> although the coefficients in the HOMO are comparable, is due to the disruption of cyclic bond delocalization within the six-membered rings involving the  $cis$ -1 bonds. Hence, the  $cis$ -1 bonds are more reactive than those of intact Kekulé rings within the carbon cage.

### C. Charge and Spin Localization in Monoadducts with Nucleophiles and Radicals

The charge or spin density of primary adducts  $RC_{60}^-$  or  $RC_{60}^\bullet$  formed by nucleophilic or radical additions is highest at position 2 and followed by 4 (11) for nucleophilic additions and at position 2 followed by 4 (11) and 6 (9) for radical additions (Figure 9).<sup>23,156–158</sup> This is also a result of avoiding

**Scheme 1. Successive Additions of Sterically Demanding Radicals to C<sub>60</sub><sup>23</sup>**

formal [5,6]-double bonds. The fact that trapping of such intermediates with electrophiles or radicals occurs preferably at C2 demonstrates again that a pronounced charge or spin delocalization can be ruled out. From this point of view, an electrophilic attack or a radical recombination process at the position 2 is also favored, neglecting eclipsing interactions.

**D. Fullerene Adducts Containing Two-Dimensional Aromatic Substructures**

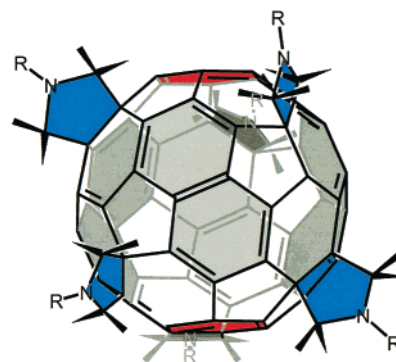
Successive 6-fold additions of transition-metal fragments,<sup>159</sup> malonates,<sup>24,125,137,160–166</sup> dienes,<sup>167</sup> or azomethine ylids<sup>168</sup> were used to synthesize *T<sub>h</sub>*-symmetrical hexakisadducts whose general structure is represented in Figure 10. The inherent aesthetically pleasing structural motif is unique in organic chemistry. A remarkable aspect of this arrangement is the establishment of a supercyclophane substructure within the remaining conjugated  $\pi$  systems (Figure 11). It consists of eight benzenoid rings placed at the vertexes of a cube.

Recently, a variety of methods including template and tether techniques<sup>23,24,27,160</sup> have been developed to make such hexakisadducts available in decagram quantities. Significantly, not only one but different types of addends can be introduced systematically. The driving force for the very regioselective formation of such hexakisadducts is not only the orbital symmetry controlled preference of *e* additions (kinetic control), but also the thermodynamic stability of this addition pattern itself.<sup>23,160</sup> For example, hexakisadduct C<sub>66</sub>(COOEt)<sub>12</sub> (**2**) is stabilized by at least 5 kcal/mol compared to all of the other 43 regioisomeric hexakisadducts that can be formed from successive addition of diethyl malonate to *e,e,e* C<sub>63</sub>(COOEt)<sub>6</sub> (**3**) without introducing unfavorable *cis*-1 additions.<sup>137</sup> As confirmed by X-ray single-crystal analysis,<sup>70</sup> the aromatic character of the remaining  $\pi$  system is enhanced compared to parent C<sub>60</sub>, as deduced, for example, from the less pronounced alternation of [6,6]- and [5,6]-bond lengths (Figure 11). Relative to solutions of C<sub>60</sub> (purple), the light yellow solution of adducts such as **2** exhibit only weak absorptions in

the visible region.<sup>160</sup> During the 6-fold addition of azomethine ylids next to the corresponding *T<sub>h</sub>*-symmetrical hexakisadduct **4** (Chart 2), another isomer with a *D<sub>3h</sub>*-symmetrical addition pattern was formed.<sup>168</sup> This hexakis adduct also contains eight planar aromatic substructures, namely, four naphthalenoid and two benzenoid rings.

Upon reaction of C<sub>60</sub> with a given excess of free radicals,<sup>169,170</sup> amines,<sup>171</sup> iodine chloride,<sup>172</sup> or bromine,<sup>173</sup> and specific organocopper<sup>174</sup> and organolithium reagents,<sup>175</sup> the formation of 1,4,11,14,15,30-hexahydro[60]fullerenes is the predominant if not almost exclusive process. In these hexa- or penta-adducts of C<sub>60</sub>, the addends are bound in five successive 1,4-positions and one 1,2-position. The corresponding corannulene substructure of the fullerene core contains an integral cyclopentadiene moiety whose two [5,6]-double bonds are decoupled from the remaining conjugated  $\pi$ -electron system of the C<sub>60</sub> core (Figure 12)

Mechanistic investigations of the corresponding reaction sequence<sup>169,170</sup> revealed the presence of an intermediate **9** containing an aromatic cyclopentadienyl radical as a characteristic substructure (Scheme 1). The formation of species **7** and **9** from C<sub>60</sub> proceeds by initial addition of one radical leading to the

**Chart 2**

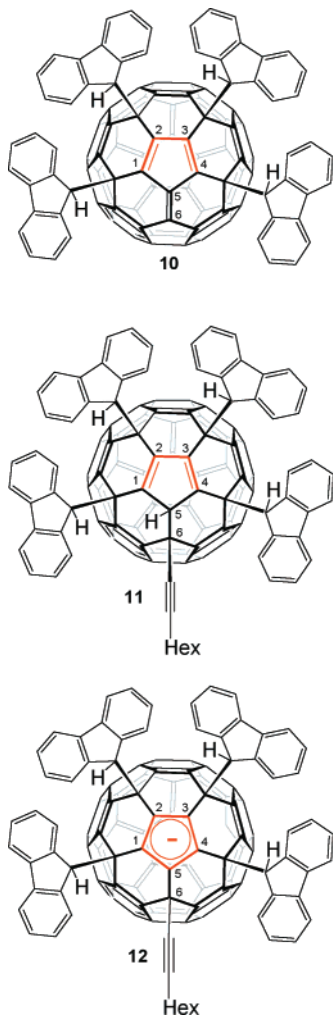


**Figure 12.** Schematic representation of the VB structure of a 1,4,11,14,15,30-hexahydro[60]fullerene.

monoadduct **5**. The unpaired spin in this radical is mostly localized on carbon 2, and, to a lesser extent, on carbons 4, 11, 6, and 9 (Figure 9). This electronic localization as well as the steric requirement of the benzyl group will direct a second attack accompanied with a radical recombination to position 4 or 11. A third attack to the diamagnetic **6** can occur anywhere on the fullerene surface. However, upon formation of **7**, the unfavorable [5,6]-double bond in **6** disappears and a resonance-stabilized allyl radical is formed. Significantly, the formation of the intermediate is also an orbital-controlled process, since high HOMO coefficients are located in the  $\gamma$  positions whose attack leads to adducts such as **7** and **8**, respectively.

A stable representative **10** of an intermediate **8** was obtained upon reaction of  $C_{60}$  with potassium fluorene in the presence of neutral fluorene without

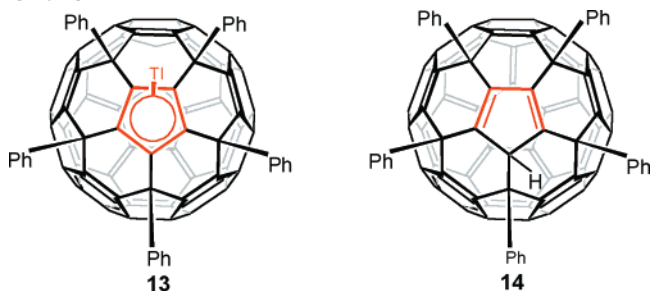
### Chart 3



rigorous exclusion of air in 40% yield (Chart 3).<sup>175</sup> Treatment of **10** and with 1-octynyllithium and subsequent quenching with acid afforded the hexaadduct **11** involving a cyclopentadiene moiety. The reaction intermediate is the cyclopentadienide **12**.<sup>174</sup>

A pentahaptofullerene metal complex **13** was obtained upon reaction of the hexaadduct **14** with TlOEt demonstrating the acidity of the cyclopentadiene (Chart 4).<sup>174</sup> A single-crystal investigation

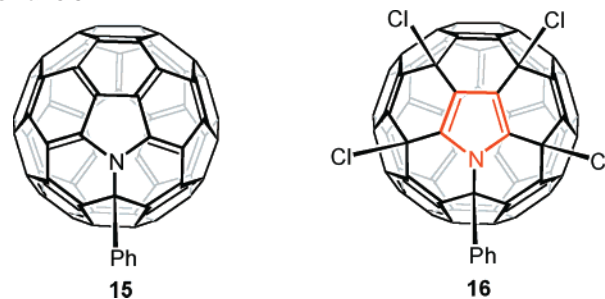
### Chart 4



confirmed the cyclopentadienide character of the complexed five-membered ring. The synthesis of a  $\pi$ -indenyl-type fullerene ligand and its metal complexes was recently accomplished by quantitative trisarylation of  $C_{70}$ .<sup>176</sup> These investigations also demonstrate the double-bond character of the C7–C8 [5,6]-bond within  $C_{70}$  (Figure 1).

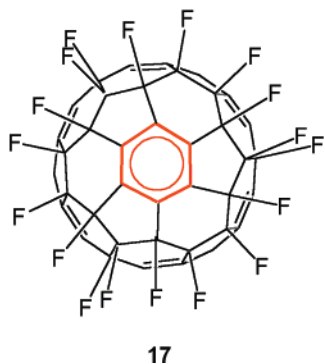
A heterocyclopentadiene addition pattern was obtained by reaction of heterofullerene monoadducts such as **15** with ICl.<sup>177</sup> In this case, a pyrrole substructure within the adduct **16** is decoupled from the remaining 50  $\pi$ -electron system (Chart 5).

### Chart 5



The *cis*-1 selectivity of subsequent additions of sterically nondemanding addends caused inter alia by bond localization of [6,6]-double bonds within the six-membered ring containing the first addend(s) was also observed during hydrogenation<sup>8,178–180</sup> and fluorination<sup>181–184</sup> sequences. A few structurally characterized polyhydro- and polyfluorofullerenes such as  $C_{3v}$ - $C_{60}H_{18}$ ,<sup>178</sup>  $D_{3d}$ - $C_{60}H_{36}$ ,<sup>180</sup>  $C_{3v}$ - $C_{60}F_{18}$  and  $C_{3v}$ - $C_{60}F_{36}$  (both *T* and *C*<sub>3</sub> isomers), and  $D_3$ - $C_{60}F_{48}$  are known.<sup>181,182,184</sup> The high stability especially of the fluorinated representatives was attributed to the presence of benzenoid rings, involving pronounced bond delocalization. Recently, the X-ray crystal structure of  $C_{60}F_{18}$  (**17**, Chart 6) was reported.<sup>181</sup> One hexagonal face at the center of the fluorinated crown within the fullerene cage is flat. The corresponding central hexagon has equal bond lengths, indicating a pronounced Hückel aromatic character. The lower hemisphere of  $C_{60}F_{18}$  does not show any significant

## Chart 6



change of bond lengths compared to parent  $C_{60}$ . The experimental results were reproduced by quantum-chemistry calculations.<sup>181</sup>

### 3. Summary

In general, the chemistry of higher fullerenes is very similar to that of  $C_{60}$ .<sup>15–17</sup> This is particularly true for highly pyramidalized regions, like the pole caps of  $C_{70}$ . Here the  $g$  bonds (Figure 1) are the most reactive ones. The pyramidalization of the  $g$  bonds within  $C_{70}$  as well as the bond lengths are almost the same as that of the [6,6]-bonds within  $C_{60}$  (Tables 1 and 2). The equatorial belt of  $C_{70}$  consisting of the  $a$ ,  $b$ , and  $c$  bonds is much less reactive.

In conclusion, the lack of substitution reactions, which are characteristic of planar aromatics, cannot be taken as a reactivity criterion of fullerenes, since they contain no hydrogen atoms that could be substituted. Therefore, only addition reactions can take place as primary steps on the fullerene surface. The reversibility of several addition reactions could be an indication of the propensity of the retention of the structural type which is considered to be a reactivity criterion of aromaticity. The regioselectivity of two-step additions, such as addition of a nucleophile followed by the trapping of the fullerene intermediate with an electrophile, on the other hand, shows that the negative charge is not delocalized over the whole fullerene. This speaks against a pronounced aromatic character. Also, other reactions, such as the additions of transition-metal fragments, are reminiscent of olefins rather than of aromatics. In many cases an important driving force for the regioselectivity of multiple addition reactions is the formation of substructures that are more aromatic than the substructures of the parent fullerene.

### V. Magnetic Criteria

Cyclic delocalization of  $\pi$  electrons is at the heart of aromaticity. Besides the structural and energetic aspects discussed so far, this delocalization has direct consequences on the magnetic properties and is reflected in characteristic changes of the diamagnetic susceptibility and NMR chemical shifts. Both effects can be rationalized in terms of electric currents induced by the external field, which extend over closed cycles comprising several atoms within the molecule. Ring-current<sup>185</sup> effects have long been recognized as important indicators for aromaticity of mono- and polycyclic compounds.<sup>186,187</sup>

Even before the advent of NMR spectroscopy, their magnetic properties made benzene and its derivatives special because their diamagnetic susceptibilities were found to be larger than expected from the data for other unsaturated compounds. For more quantitative purposes, a refined increment system has been established for the estimation of the molar susceptibilities  $\chi_M$  of unsaturated hydrocarbons. A noticeable excess of the actual, measured value  $\chi_M$  of a given compound, compared to this estimate, has been taken as a measure of the aromatic character of this compound.<sup>188</sup> This so-called diamagnetic susceptibility exaltation  $\Lambda$  has proven to be a valuable diagnostic for aromaticity and antiaromaticity, as indicated by  $\Lambda > 0$  and  $\Lambda < 0$ , respectively. A disadvantage of this approach, however, is that it cannot be easily generalized to heterosubstituted derivatives because in many cases the derivation of the necessary increment system is not straightforward or not possible at all due to the lack of suitable acyclic reference compounds.

The enhancement of the diamagnetic susceptibility caused by a ring current is not an isotropic effect but occurs only when the plane of the ring is oriented perpendicular to the external magnetic field. Consequently, the presence or absence of a pronounced anisotropy  $\Delta\chi$  can, in principle, be taken as evidence for or against a ring current and can thus be employed as an aromaticity probe. The need to correct for local anisotropy effects of single and multiple bonds, however, and limitations in the experimental determination of  $\Delta\chi$  have impeded widespread applications of this property. Moreover, for spherical molecules such as fullerenes, this criterion cannot be sensibly applied at all.

Another indirect effect of a ring current is that the magnetic field it creates modulates the field applied externally and thus causes characteristic changes of the NMR chemical shifts of nearby nuclei. The characteristic deshielding of protons attached to the outside of an aromatic ring or the shielding of protons pointing to the inside (both relative to olefinic  $^1H$  resonances) are textbook examples of such ring-current effects, as is the shielding of nuclei placed above the ring plane. The interpretation of proton NMR spectra in terms of ring-current effects has been described in detail.<sup>189</sup> As with  $\chi$  and  $\Delta\chi$ , chemical shifts  $\delta$  depend on other local factors besides ring currents and it is difficult to deduce, from the raw  $\delta$  values, ring-current strengths which could be used to quantify the degree of aromaticity. Since ring-current-induced chemical shifts are on the order of a few parts per million and have the same magnitude irrespective of the nucleus, ring-current effects on nuclei other than H (or nuclei with similarly small chemical-shift ranges such as  $^6Li$ <sup>190</sup>) are usually obscured altogether by such local factors.

Even though originally conceived by theoreticians, the ring-current concept has not been uncontested in the theoretical community. It has been pointed out that "ring currents themselves are not physically observable" and that "the fact that predictions of ring-current theory may compare favorably with experiment is no proof that ring currents exist".<sup>189</sup> With the

advent of reliable quantum-chemical methods for the computation of magnetic susceptibilities and chemical shifts, additional evidence in favor of the ring-current model has been accumulated. In particular, the special magnetic properties of benzene can be traced back to contributions from the  $\pi$ -electron system and are fully consistent with a near-free circular current.<sup>191</sup> On a more pictorial level, induced current densities have been computed and plotted for several mono- and polycyclic aromatic systems.<sup>192–195</sup> When, in the planar hydrocarbons, the  $\pi$  electrons can be treated separately from the  $\sigma$ -framework, the expected current flows are indeed apparent: diatropic  $\pi$ -electron ring currents are found in Hückel-aromatic systems and currents in the opposite direction (termed paratropic) in Hückel-antiaromatic compounds.

In annelated ring systems, one can note a certain locality of the currents: In biphenylene, for instance, diatropic current flows are found in the benzene moieties, much like in the parent benzene itself, whereas the central cyclobutadienyl-like four-membered ring is characterized by a distinct paratropic ring current.<sup>193a</sup> In general, the overall picture expected from the Hückel rule is seen in these current-density plots, but in most cases only when the  $\pi$  system is regarded separately (which, strictly speaking, is only possible for planar molecules). The total current density is usually dominated by local diatropic currents around the individual nuclei.

Schleyer and co-workers proposed to employ the chemical shift at the very center of a ring system<sup>196</sup> as a probe for ring currents and, thus, for aromaticity and antiaromaticity. These shifts, termed nucleus-independent chemical shifts (NICSs), are usually not accessible experimentally but can be computed reliably with modern quantum-chemical methods and afford a simple and efficient aromaticity probe: For monocyclic rings, NICS values correlate with aromatic stabilization energies, and for polycyclic compounds, they reflect the abovementioned locality by furnishing an aromaticity index for each individual ring. Furthermore, this concept can also be used to probe for three-dimensional aromaticity in spherical molecules by calculating the chemical shift at the center of the cage.

A comprehensive review of these criteria for ring currents has recently been published by Lazzeretti.<sup>197</sup> In the following, applications to fullerenes and fullerene derivatives will be reviewed.

## 1. Application of Magnetic Criteria to Fullerenes

In their 1985 paper, Smalley and co-workers speculated that icosahedral  $C_{60}$  should have unusual magnetic properties.<sup>1</sup> Shortly thereafter, the magnetic response of  $C_{60}$  has been computed with the Hückel-MO-based London method, and a vanishingly small contribution from the  $\pi$  system to the magnetic susceptibility has been predicted.<sup>198</sup> Subsequent determination of  $\chi_M$  has indeed afforded a remarkably small value for  $C_{60}$ ,  $-260 \pm 20$  ppm cgs.<sup>199,200</sup> According to estimates for the so-called local contributions to  $\chi_M$  (i.e., those of the  $\sigma$ -bonds), the latter can almost solely account for the measured value.<sup>199</sup> In other words, the diamagnetic susceptibility exaltation  $\Lambda$  of  $C_{60}$  is essentially zero.

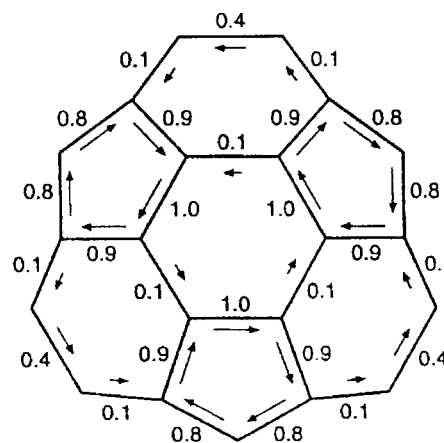


**Figure 13.**  $\pi$ -Electron ring currents in  $C_{60}$ , calculated with the HMO-based London method.<sup>201a</sup> A section along a 3-fold axis is shown with the magnetic field parallel to the latter, and the current strengths are given with respect to that in benzene. (Reprinted with permission from ref 201a. Copyright 1992 American Association for the Advancement of Science.)

Detailed analysis of the theoretical London results has shown that the lack of a  $\pi$ -electron contribution to the susceptibility of  $C_{60}$  is not due to the absence of ring currents. Rather, there are fairly large diatropic ring currents in the hexagons, but the expected diamagnetism is quenched by paratropic ring currents in the pentagons, and the magnitude of the current strengths appeared to be comparable to that in benzene<sup>201</sup> (see Figure 13). The same general picture has been obtained for current densities obtained at the Hartree–Fock ab initio level.<sup>202</sup> In view of these anomalous magnetic properties and the reactivity, which has been described as that of a continuous aromatic molecule, it has been suggested that  $C_{60}$  is of ambiguous aromatic character.<sup>18</sup>

The diamagnetic susceptibility of  $C_{70}$ ,  $-550 \pm 50$  ppm cgs, is substantially larger than that of  $C_{60}$ .<sup>199,200</sup> The major part of this increase has been ascribed to  $\pi$ -electron ring currents.<sup>199</sup> The theoretical London results have afforded a similar picture for  $C_{70}$  as for  $C_{60}$ , namely, dia- and paratropic currents in the six- and five-membered rings, respectively.<sup>201b</sup> For  $C_{70}$ , the cancellation of these two contributions is incomplete and a substantial net diamagnetism remains. This result has also been reproduced in subsequent Hartree–Fock ab initio calculations of  $\chi$ , which afforded a much larger (by ca. 300 ppm cgs) susceptibility exaltation  $\Lambda$  for  $C_{70}$  than for  $C_{60}$ .<sup>203</sup>

If the larger diamagnetism of  $C_{70}$  compared to  $C_{60}$  were due to the fact that the former has more six-membered rings than the latter (the number of five-membered rings being 12 in all fullerenes), then the diamagnetic susceptibility (or rather its exaltation  $\Lambda$  stemming from the  $\pi$  electrons) should increase successively with fullerene size. To our knowledge, no measurements of  $\chi_M$  have been reported for the higher fullerenes (see, however, the endohedral chemical shifts below). According to London calculations for selected isomers of  $C_{76}$ ,  $C_{78}$ ,  $C_{82}$ , and  $C_{84}$ , the total  $\pi$ -electron ring-current contributions to  $\chi$  (denoted  $\chi_{RC}$ ) are actually smaller than that of  $C_{70}$  and only for giant icosahedral fullerenes ( $C_{180}$ ,  $C_{240}$ ,  $C_{540}$ ) the expected increase in  $\chi_{RC}$  is obtained.<sup>204</sup> For still larger

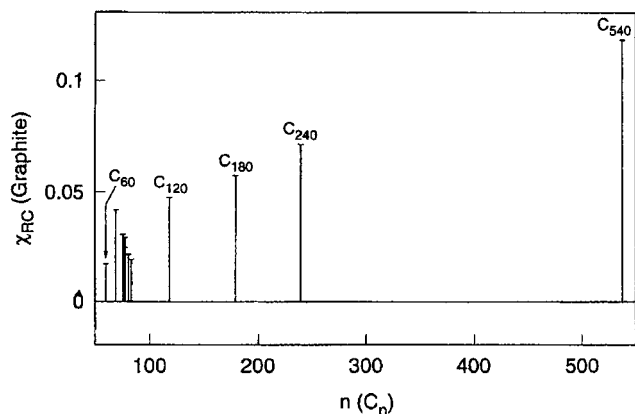


**Figure 14.**  $\pi$ -Electron ring-current magnetic susceptibilities ( $\chi_{RC}$  given as fraction of that of graphite) as a function of fullerene size  $n$ , calculated with the London method.<sup>204</sup> Note the small convergence toward the graphite value and the irregular behavior of the higher fullerenes  $70 < n \leq 84$ . (Reprinted with permission from ref 204. Copyright 1994 American Physical Society.)

fullerenes, the value of the magnetic susceptibility (on a per carbon basis) should eventually approach that of graphite, albeit, apparently, very slowly (see Figure 14). The irregular behavior of the fullerenes in the size regime  $n$  up to  $\approx 100$  has been attributed to “quantum size effects”,<sup>204</sup> that is, to the particular electronic structure of each fullerene and isomer, which should, of course, be intimately related to the aromatic character.

As mentioned above,  $^{13}\text{C}$  chemical shifts are not a good probe for ring-current effects in fullerenes. It has been suggested to group  $\delta(^{13}\text{C})$  values of fullerenes according to the carbon sites into pyracyclene, corannulene, and pyrene types,<sup>205</sup> for which a trend toward higher shifts with increasing degree of pyramidalization (as assessed by the  $\pi$ -orbital axis vector) can be noted. In  $\text{C}_{70}$ , for instance, the equatorial carbon atoms are the least pyramidalized and the most shielded ones in the NMR spectrum. The London  $\pi$ -electron results have led to the suggestion that in fact part of this shielding (on the order of 4–5 ppm) may arise from ring-current effects.<sup>201b</sup> A number of caveats regarding the underlying theoretical model, however, make it unclear to what extent this suggestion is substantiated beyond speculation.

#### A. “Exohedral” Probes

To probe for the secondary magnetic field induced by the ring currents, it would be desirable to bring hydrogen nuclei close to the  $\pi$  system of fullerenes. One way to achieve this is through addition of suitable substituents to the fullerene cage.<sup>206</sup> Such a transformation, however, inevitably alters the  $\pi$  system, for instance by effective removal of two electrons upon addition across a double bond. Fullerene derivatives of that type will be considered in section V.2.B. Yet there is one family of derivatives in which the  $\pi$  system of the parent fullerene is preserved to a large extent, namely, the fulleroids. Formal addition of a carbene fragment  $:\text{CRR}'$  to  $\text{C}_{60}$  can occur in two ways, across a [6,6]-bond (that is, at two abutting hexagons) or across a [5,6]-bond. The [6,6]-products are usually cyclopropane (or methanofullerene) derivatives,<sup>207</sup> whereas all of the [5,6]-

adducts have so far been characterized as fulleroids (methanoannulenes),<sup>139,208–210</sup> Evidence for the small perturbation of the fullerene  $\pi$  system in the fulleroids is given, for instance, by the high similarity of the UV spectra to that of the parent fullerene,<sup>139,209</sup> and by similar endohedral chemical shifts (see section V.1.B).

The  $^1\text{H}$  chemical shifts of the parent  $\text{C}_{61}\text{H}_2$  isomers **18** and **19** are particularly instructive (Figure 15): In the methanofullerene **18**, a noticeable deshielding of the methylene protons is observed,<sup>209b</sup> ca. 3 ppm with respect to homoacenaphthene **20**. The latter has been shown, unlike the parent 1,6-methano[10]-annulene, to adopt the closed, norcaradiene-like structure.<sup>211</sup> A similar deshielding of the  $^1\text{H}$  resonance is found in dibenzohomopyracyclene **21**, a closer structural model for **18**.<sup>212</sup> This deshielding may to a large extent be due to a paratropic ring current along the pyracyclene perimeter with its 12  $\pi$  electrons.<sup>213,214</sup>

The fulleroid **19** is characterized by a large difference between the chemical shifts of the two inequivalent methylene protons, with  $\Delta\delta$  as large as 3.5 ppm.<sup>209</sup> In the initial communication it has been noted<sup>209a</sup> that the same shift difference has been obtained for another hydrocarbon, **22**, which is supposedly free of ring currents, suggesting that other factors could also be responsible for the  $^1\text{H}$  shifts of **19**. However, the cyclooctadiene moiety in **22** adopts a boat conformation which brings the two methylene groups in close proximity to each other.<sup>215</sup> Since this structural feature is absent in the fulleroids, it is reasonable to assume that much of the observed  $\Delta\delta$  in the latter is indeed due to different (or “segregated”)<sup>216</sup> ring currents in the two adjacent carbocycles. In fact, the above-mentioned predictions of dia- and paratropicity of six- and five-membered rings, respectively, have been used in the assignments of the  $^1\text{H}$  resonances in **19** and, by analogy, in the other derivatives discussed below. Thus, the high-frequency resonance is attributed to the proton located above the pentagon, in bearing with the expected paratropicity, whereas the low-frequency signal is attributed to the proton above the hexagon, reflecting the diatropic character of the latter.

The same characteristic patterns in  $^1\text{H}$  chemical shifts are found in fulleroid derivatives such as **23–28** or **29–33**,<sup>210,217</sup> where either a proton or a methyl group is placed above a fullerene ring (Figure 15). In the case of the methyl groups, the effects appear to be somewhat attenuated (for instance,  $\Delta\delta$  between **30** and **31** is only 1.9 ppm), certainly due to the averaging of the three methyl protons, only one of which will be located in close proximity to the ring at a given time.

The same type of methanofullerene and fulleroid derivatives as for  $\text{C}_{60}$  can be observed for  $\text{C}_{70}$ . For derivatives of the latter, several isomers are possible, some of which have been observed and characterized,<sup>217</sup> namely, the cyclopropane derivatives **34** and **35** and the fulleroids **36** and **37** (Figure 16).<sup>218</sup> The  $\delta(^1\text{H})$  values of the “polar adduct” **36** are very similar to those of the corresponding  $\text{C}_{60}$  derivative, **19** (Figure 15). The same is true for the low-frequency

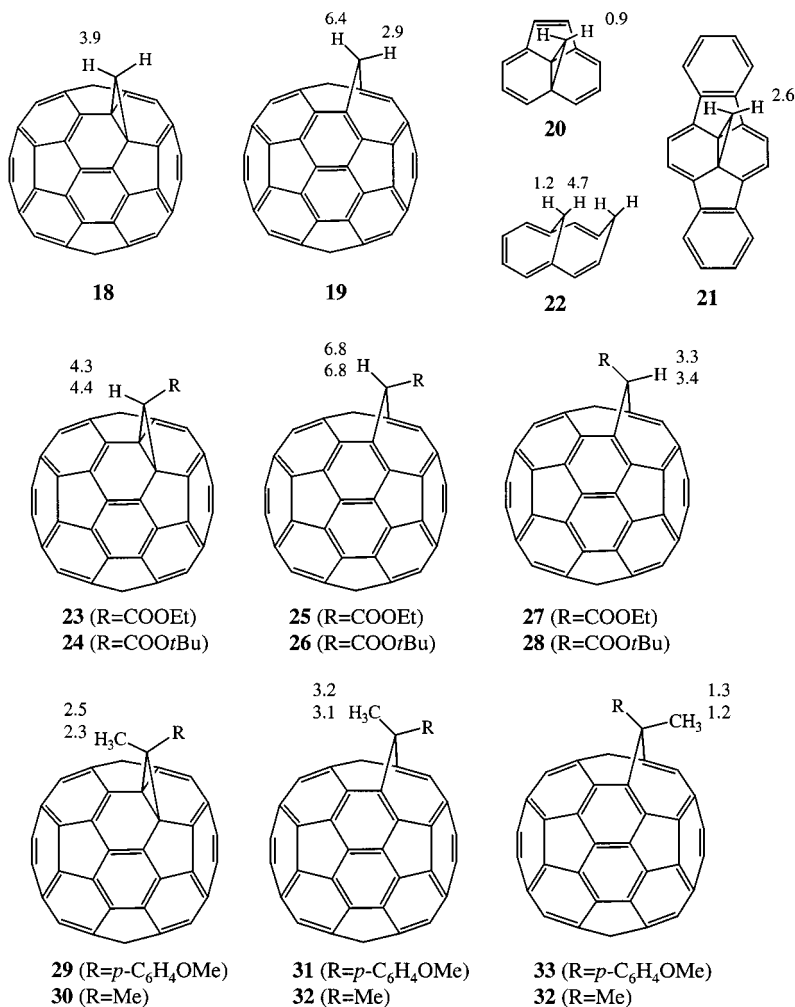


**Figure 15.** Methanofullerene and fulleroid isomers of  $C_{60}$  adducts, together with the  $^1H$  chemical shifts (no assignment was reported for **32**).

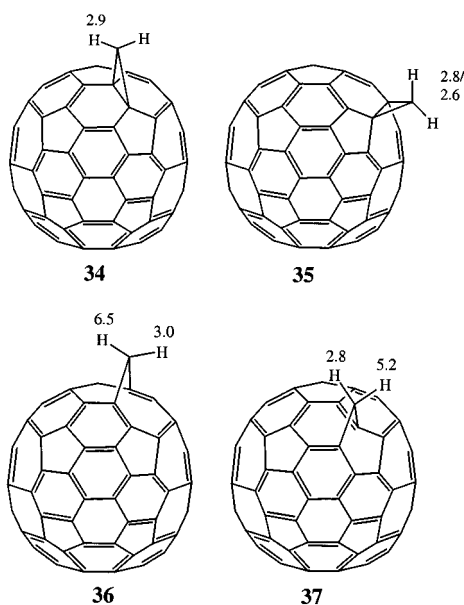


**Figure 16.** Methanofullerene and fulleroid isomers of  $C_{70}$  adducts, together with the  $^1H$  chemical shifts.

resonance of the less abundant isomer **37**, whereas the high-frequency proton shift is less pronounced in this isomer,  $\delta = 5.2$ , compared to that in **19** (6.4 ppm) or **36** (6.5 ppm). Since one

methylene hydrogen atom in each **36** and **37** is located above the same six-membered ring, the close similarity of the two low-frequency proton shifts in these isomers provides additional evidence for the assignment of the  $^1H$  resonances.

These findings suggest that the ring-current flows in  $C_{60}$  and in the polar region of  $C_{70}$  are qualitatively similar and that the diatropic and paratropic current strengths in the hexagons and pentagons, respectively, are of comparable magnitude. In contrast, the paratropicity of the five-membered rings near the equatorial belt of  $C_{70}$  is indicated to be considerably reduced. These observations are fully consistent with the predictions based on the theoretical London results<sup>201b</sup> (see also section V.1.C).

Compared to  $C_{60}$  and  $C_{70}$ , the chemistry of the higher fullerenes is still in its infancy and is essentially restricted to reduction and addition reactions of the most abundant isomers of  $C_{76}$ ,  $C_{78}$ , and  $C_{84}$ .<sup>15,16</sup> Cyclopropanation has emerged as a versatile means of derivatization, but no fulleroid-type derivatives have been reported so far. Even if these could be isolated eventually, assignment of the plethora of possible regioisomers will be extremely difficult. Thus, exohedral NMR probes will, at least in the near future, be of limited use for the study of ring currents in the higher fullerenes.



### B. "Endohedral" Probes

In the preceding section, exohedrally placed NMR nuclei were employed as probes for ring currents in specific five- or six-membered rings. Of course, as anticipated from the very beginning of the modern fullerene history,<sup>1</sup> such ring currents also affect the magnetic field inside the fullerene. An NMR-active nucleus placed endohedrally at or near the center would sense the combined effect of all ring currents present, be they confined in particular rings or extended over larger areas. For magnetically isotropic molecules with  $\pi$  electrons on a sphere with radius  $r$ , there is a simple relation between the ring-current magnetic susceptibility  $\chi_{RC}$  and the ring-current contribution  $\delta_{RC}$  to the chemical shift of a nucleus at the center<sup>198</sup>

$$\delta_{RC} = 2\chi_{RC}/r^3 \quad (6)$$

On the basis of the very small net  $\chi_{RC}$  obtained in the London calculations for  $C_{60}$ , a very small value for  $\delta_{RC}$  has been predicted, ca. 0.5 ppm,<sup>198</sup> and a more pronounced shielding in the center of  $C_{70}$ .<sup>201a</sup> The development of techniques to produce macroscopic amounts of fullerenes doped endohedrally with  $^3\text{He}$ , an excellent NMR nucleus, eventually enabled M. Saunders and associates to test this prediction. For  $\text{He}@C_{60}$  and  $\text{He}@C_{70}$ ,  $\delta(^3\text{He})$  values of  $-6.3$  and  $-28.8$  ppm, respectively, were measured relative to free  $\text{He}$ .<sup>219</sup> The predicted  $\delta_{RC}$  and experimental  $\delta(^3\text{He})$  in the case of  $C_{60}$  did not agree in a quantitative sense, but qualitatively, the large difference in the  $^3\text{He}$  chemical shifts between  $C_{60}$  and  $C_{70}$  was confirmed. This difference also reflects the susceptibility exaltation of the latter over the former.

Subsequently, theoretical calculations of the endohedral chemical shifts of fullerenes were performed at increasing levels of sophistication.<sup>201,203,220–222</sup> Several technical issues need to be addressed when the computational results are compared to experiment: First, when employing the semiempirical London method, which considers the  $\pi$  electrons only, the anisotropy effects due to the  $\sigma$  bonds should also be accounted for. Such effects may not be fully negligible, as ab initio Hartree–Fock computations for the fully hydrogenated  $\text{He}@C_{60}\text{H}_{60}$  and  $\text{He}@C_{70}\text{H}_{70}$  have afforded a noticeably shielded endohedral helium, with  $\delta(^3\text{He})$  around  $-5$  ppm.<sup>203</sup> Since these saturated compounds cannot sustain  $\pi$ -electron ring currents, part of the endohedral shielding observed in the fullerenes, for  $\text{He}@C_{60}$  in fact most of it, may arise from the  $\sigma$ -framework. Of course, in the ab initio and density-functional methods, the response from all electrons is obtained.

Second, is there any interaction between the helium and the fullerene host which would manifest itself in the chemical shifts and to what extent are the latter affected by the mobility of the endohedral noble gas? Mixing between the orbitals of the  $C_{60}$  cage and those of endohedral guests have long been found to be negligible.<sup>223</sup> In the ab initio Hartree–Fock calculations, virtually the same result is obtained for  $\delta(^3\text{He})$  of  $\text{He}@C_{60,70}$  and for the chemical shift at the center of the pristine cages.<sup>221b</sup> It is only for the

heavier noble gases such as Kr and Xe that qualitatively different chemical shifts are predicted.<sup>224</sup>  $\text{Kr}@C_{60}$  has recently been isolated, and from the spectroscopic properties (unfortunately Kr NMR is not feasible), a "small but detectable interaction between the endohedral krypton atom and the  $\pi$ -electron system of the  $C_{60}$  cage"<sup>225</sup> has been inferred. As for the mobility of endohedral helium, the magnetic field inside the fullerenes is computed to be very homogeneous in quite a large area around the center. This was apparent from the early London results, as well as from the later ab initio Hartree–Fock computations, either by performing them for endohedral compounds with He atoms displaced from the center by as much as  $1 \text{ \AA}$ <sup>203</sup> or by sampling over several points within this region in the pristine fullerenes<sup>221b</sup> (and still further away from the center, see below). Effects of He mobility estimated this way have been invariably small, on the order of 0.1–0.2 ppm. Experimental support for the homogeneity of the magnetic field inside the fullerenes has been furnished by the  $\delta(^3\text{He})$  value assigned to  $\text{He}_2@C_{70}$ , which differs by a mere 0.01 ppm from that of  $\text{He}@C_{70}$ .<sup>226</sup> All these data suggest that endohedral chemical shifts, either obtained experimentally by  $^3\text{He}$  NMR of the  $^3\text{He}$ -labeled fullerenes or theoretically for some point at or near the center of the pristine fullerene, are true probes for ring-current effects in the latter and can thus be used as an aromaticity criterion. In a way,  $^3\text{He}$  NMR of endohedral helium–fullerene compounds can be viewed as applied NICS spectroscopy!

Finally, to what extent do the theoretical values depend on geometries and, in case of ab initio methods, on computational details such as basis sets? In the first London-type calculations for  $C_{60}$  it has been noted that the  $\pi$ -electron magnetic susceptibility, and by consequence also the endohedral chemical shift, is quite sensitive to the relative bond strengths of the two bond types (or rather to the ratio of the corresponding resonance integrals).<sup>198</sup> The same has been found later in the ab initio Hartree–Fock computations, which indicated a pronounced dependence of the endohedral chemical shift on the geometry employed, in particular on the extent of bond alternation in  $C_{60}$ .<sup>203</sup> In contrast, results obtained for  $C_{70}$  are less sensitive to the geometry (see entries 1–5 in Table 5)<sup>227</sup> but require larger basis sets (compare for instance entries 3 and 6). Going beyond the Hartree–Fock approximation to a DFT level reduces the endohedral shielding in  $C_{70}$  to a small extent and that in  $C_{60}$  to a large extent (compare entries 7 and 9 or 8 and 10). All in all it appears that the results for  $C_{60}$  are much more sensitive to the computational setup than those of  $C_{70}$  (and also than those of other neutral derivatives, see section V.2.B). By analogy to the data for  $C_{70}$ , computations for the higher fullerenes are not very critical with respect to geometries or method (HF vs DFT) but should employ a basis set of at least DZP quality.

As mentioned above, London calculations for selected isomers of  $C_{76}$ ,  $C_{78}$ ,  $C_{82}$ , and  $C_{84}$  have indicated that their ring-current magnetic susceptibilities should be bracketed by those of  $C_{60}$  and  $C_{70}$  and that the same should be expected for the corresponding en-

**Table 5. Dependence of Computed Endohedral Chemical Shifts of C<sub>60</sub> and C<sub>70</sub> on the Level of Theory**

entry no.	GIAO variant <sup>a</sup>	basis set <sup>b</sup>	geometry	endohedral chemical shift <sup>c</sup>	
				C <sub>60</sub>	C <sub>70</sub>
1	HF	DZ	MNDO	-11.7	-23.0
2	HF	DZ	SCF/3-21G	-12.9	-24.0
3	HF	DZ	BP86/3-21G	-11.0	-25.2
4	HF	DZ	MP2/TZP <sup>d</sup>	-8.7	-27.0 <sup>e</sup>
5	HF	DZP	equalized <sup>f</sup>	-2.0 <sup>e</sup>	
6	HF	DZP	BP86/3-21G	-11.1	-28.4
7	HF	DZP	BP86/TZP	-10.3	-29.2
8	HF	DZP	MP2/TZP <sup>e</sup>	-8.5	-31.1 <sup>e</sup>
9	DFT	DZP	BP86/TZP	0.2	-28.7
10	DFT	DZP	MP2/TZP <sup>d</sup>	1.5	-30.8 <sup>e</sup>
11	DFT	DZP	equalized <sup>f</sup>	6.7 <sup>e</sup>	
exp. He@C <sub>60</sub> , C <sub>70</sub> <sup>g</sup>				-6.3	-28.8

<sup>a</sup> GIAO = gauge-including atomic orbitals; HF = Hartree–Fock; DFT = Becke (1988) + Perdew/Wang (1991) combination of density functionals; tzp basis on helium for the endohedral He compounds. <sup>b</sup>  $\delta(^3\text{He})$  for the endohedral He compounds. <sup>c</sup> From refs 203, 221b, and 222. <sup>d</sup> For C<sub>70</sub>: RI-MP2 (Weigend, F. Unpublished results. For the RI-MP2 method, see: Weigend, F.; Häser, M. *Theor. Chem. Acc.* **1997**, *97*, 331–340). <sup>e</sup> Bühl, M. Unpublished results. <sup>f</sup> Employing equal CC bond lengths of 1.448 Å. <sup>g</sup> Reference 219.

dohedral chemical shifts.<sup>204</sup> Likewise, ab initio Hartree–Fock calculations have found the endohedral shielding inside C<sub>76</sub> between those of C<sub>60</sub> and C<sub>70</sub>.<sup>220b</sup> These predictions were borne out by <sup>3</sup>He NMR spectroscopy of <sup>3</sup>He-labeled and partially separated mixtures of the higher fullerenes.<sup>228</sup> In fact, the <sup>3</sup>He NMR spectra, in particular those of the fraction containing C<sub>84</sub>, showed many more signals than expected from other experimental data on the isomeric composition available at that time. These findings underscored the analytical potential of the <sup>3</sup>He labeling and NMR technique.<sup>229</sup> Later, additional isomers of C<sub>84</sub> were isolated<sup>45,230</sup> and some of the <sup>3</sup>He signals were recognized, in analogy to He<sub>2</sub>@C<sub>70</sub>,<sup>226</sup> as those of doubly labeled isomers.<sup>231</sup> The <sup>3</sup>He NMR spectra are now interpreted in terms of 1, 3, 7, and 1 different isomers for C<sub>76</sub>, C<sub>78</sub>, C<sub>84</sub>, and C<sub>86</sub>, respectively. Assignments are difficult where several isomers are present, except perhaps for the major one. Since most of the signals of these isomers cover a chemical-shift range comparable to or smaller than the variations of the ab initio results with the level of theory (Table 5), the theoretical data are of limited use for the assignments. An exception may be one particular isomer of C<sub>84</sub>, D<sub>2d</sub>(4),<sup>232</sup> the endohedral chemical shift of which has been computed far outside the range covered by the other isomers<sup>221b</sup> and close to a resonance that has initially been found in the C<sub>84</sub> fraction<sup>228</sup> (see second to the last entry in Table 6).

It had been speculated that the five signals ascribed to C<sub>78</sub> could be due to the five possible isolated-pentagon isomers.<sup>221b</sup> Since two of these resonances were recently identified as doubly labeled species,<sup>231</sup> this speculation is refuted. For the three isomers suspected to be present, the accord between theoretical and experimental endohedral shifts would be improved if the recent (unsubstantiated) assignment of the C<sub>2v</sub>' and D<sub>3</sub> isomers<sup>233</sup> would be reversed.

Similar endohedral shifts around -19 ppm are computed for the symmetrical isomers of the larger C<sub>120</sub> and C<sub>180</sub> fullerenes, whereas much larger shieldings are found in smaller fullerene structures down to C<sub>32</sub>.<sup>221a,234</sup> Both trends reflect the radial dependence of  $\delta_{\text{endo}}$  (eq 6), from which, together with the

**Table 6. Endohedral Chemical Shifts of the Higher Fullerenes**

fullerene	isomer <sup>a</sup>	calcd <sup>b</sup>	expt <sup>c</sup>	(He <sub>2</sub> @C <sub>n</sub> )	assignment
C <sub>76</sub>	D <sub>2</sub>	-20.4	-18.70	(-18.56)	
C <sub>78</sub>	D <sub>3</sub>	-15.0	-11.91	(-11.82)	C <sub>2v</sub> '
	D <sub>3h</sub> '	-17.8			
	D <sub>3h</sub>	-18.5			
	C <sub>2v</sub> '	-18.7			
	C <sub>2v</sub> '	-19.1	-16.89	(-16.77)	C <sub>2v</sub> <sup>d</sup>
C <sub>84</sub>			-17.57		D <sub>3</sub>
			-7.50	(-7.54)	
			-8.40	(-8.37)	
	D <sub>3d</sub> (19)	-9.4			
	D <sub>2d</sub> (23)	-11.9			
	D <sub>2</sub> (22)	-12.1	-8.96		D <sub>2</sub> <sup>d</sup>
			-9.61	(-9.65)	
			-10.01		
			-11.11		
	D <sub>6h</sub> (24)	-14.8			
		-14.15			
C <sub>86</sub>	D <sub>2d</sub> (4)	-25.0	-24.35		
			-10.58		

<sup>a</sup> Labeling as in refs 232 and 233. <sup>b</sup> GIAO–HF/DZP level for BP86/3-21G geometries, from ref 221b. <sup>c</sup>  $\delta(^3\text{He})$  from refs 228 and 231 (in parentheses, values for doubly labeled species). <sup>d</sup> Major isomer.

monotonic increase of  $\chi_{\text{RC}}$  for larger  $n$  (Figure 14), it has already been inferred that endohedral chemical shifts will be of “less use in the regime of the giant fullerenes”.<sup>204</sup>

Even though the isomeric composition of the higher fullerenes (in particular, of the <sup>3</sup>He-labeled mixtures) may well reflect kinetic rather than thermodynamic stabilities, the most abundant isomers of C<sub>84</sub> and C<sub>78</sub> are also the most stable ones, according to ab initio calculations. Such calculations also predict that the energy per carbon atom decreases monotonically as the fullerenes become larger and that no correlation between this stabilization and  $\delta_{\text{endo}}$  is apparent (Figure 17, top). A very rough, common trend is found when the  $\delta_{\text{endo}}$  values are scaled to account for the radial dependence in eq 6 (that is, when the trend in  $\chi_{\text{RC}}$  is sought and assuming that the radius of a spherical fullerene C<sub>n</sub> is proportional to  $n^{3/2}$ ).<sup>204</sup> However, in the regime of the higher fullerenes, 60 <  $n$  < 100, large oscillations are apparent in the

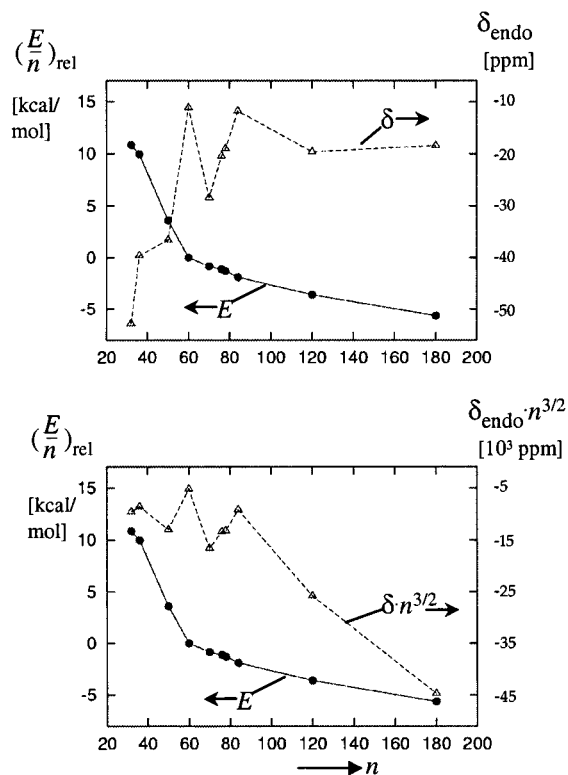


**Figure 17.** Plot of the relative energy  $E$  per carbon atom in fullerenes  $C_n$  (relative to  $C_{60}$ ) versus the endohedral chemical shift  $\delta_{\text{endo}}$  (top) and versus  $\delta_{\text{endo}}$  scaled for fullerene size (bottom), see text. Data are computed at the ab initio Hartree–Fock/DZP level.<sup>214,234</sup>

scaled  $\delta$  values (which actually reflect the trend in  $\chi_{\text{RC}}$ , Figure 14). Thus, there is no relation between relative stabilities of fullerenes and their aromatic character, as assessed by the endohedral shieldings. This is also the case for relative stabilities of fullerene isomers, i.e., on a smaller energetic scale, as can be seen, for instance, from the  $^3\text{He}$  NMR spectrum of the isomeric  $C_{84}$  mixture: the most abundant isomer (which is almost certainly also the most stable one) does not have the highest endohedral shielding (Table 6). The energetic ordering of fullerene isomers is emerging as a compromise between steric and electronic effects.<sup>233</sup> Structures that are the least strained are not necessarily those that allow for the most efficient  $\pi$ -electron delocalization. As an efficient probe for the latter, endohedral chemical shifts will continue to play a pivotal role in fullerene chemistry.

Finally, it is interesting to note that the different magnetic fields inside the fullerenes cannot only be probed by NMR, but can also be detected by EPR spectroscopy of endohedrally trapped radicals. It has been shown that atomic nitrogen can be implanted into the  $C_{60}$  cage and that, according to ENDOR and EPR spectroscopy, the endohedral N atom rests at the center with its atomic  $^4S_{3/2}$  ground-state configuration, preserving spherical symmetry.<sup>235</sup> The same is true for  $\text{N}@C_{70}$ , the  $g$  value of which was found to be smaller by 19 ppm than that recorded for  $\text{N}@C_{60}$ .<sup>236</sup> This difference has been interpreted in analogy to the chemical shift as arising from the different magnetic field strengths sensed by the N atom in the two fullerenes. In fact, the value of 19 ppm is surprisingly

close to the corresponding difference in  $\delta(^3\text{He})$  between  $\text{He}@C_{60}$  and  $\text{He}@C_{70}$ , ca. 22 ppm. The electrons of the N atom are probably occupying a larger space than that covered by the  $^3\text{He}$  nucleus (the van der Waals radius of nitrogen is 1.55 Å, whereas it has been estimated that the He atom in  $C_{60}$  senses the magnetic field within 0.5 Å from the center<sup>219</sup>). Thus, the similarity of the  $g$ -factor and chemical-shift differences provides further evidence for the homogeneity of the magnetic field inside the fullerenes.<sup>237</sup> Further parallels between the two properties are found in  $C_{60}$  derivatives (see section V.2).

### C. "Theoretical" Probes

Section V.1.A focused on exohedrally attached NMR nuclei, usually protons, as probes for local ("segregated") ring currents in fullerenes. Besides the direct calculations of current densities, the computed NICS values, i.e., the chemical shifts in the centers of the rings, have been established as useful indicators for such local dia- and paratropic ring currents.<sup>196</sup> As with other calculated properties, the NICS values depend somewhat on the particular theoretical models employed. Qualitative trends are very robust, however, especially when the NICS values of the compound under scrutiny are compared to that of some standard, typically benzene, computed at the same level (representative values between  $-9.7$  and  $-11.5$  ppm<sup>196a,234</sup>). For the pentagons and hexagons of  $C_{60}$ , NICS values of 5.4 and  $-6.8$  ppm, respectively (HF/3-21G),<sup>196a</sup> or 8.9 and  $-5.3$ , respectively (HF/DZP),<sup>234</sup> have been computed. Qualitatively, the relative dia- and paratropisms of the two ring types discussed above are nicely reflected in these numbers.

For several neutral and anionic fullerenes, the NICS values have been computed at the ab initio HF/DZP level.<sup>234</sup> The results for selected neutral isomers are presented pictorially in Figure 18. From the color code it appears that the basic finding for  $C_{60}$ , diatropic hexagons and paratropic pentagons, prevails in most of the larger fullerenes but that the extent of the relative dia- and paratropism (i.e., the NICS values themselves) is not transferable between fullerenes nor, as evidenced by the data for  $C_{84}$ , between isomers thereof. For the large symmetric fullerenes  $C_{120}$  and  $C_{180}$ , corannulene- and coronene-like patterns can be discerned, but no uniform patterns emerge in the size regime between  $C_{70}$  and  $C_{84}$ .

For  $C_{70}$ , noticeably different NICS values are computed for the two types of five-membered rings in the polar and the equatorial region,  $+2$  and  $-2$  ppm, respectively.<sup>234</sup> Qualitatively, this result is consistent with the  $^1\text{H}$  chemical shifts of the fullerenes **36** and **37** (see section V.1.A and Figure 16). The experimental data for the latter,<sup>217</sup> however, seems to imply a paratropic ring current in the equatorial pentagons, albeit reduced with respect to that in the polar ones, whereas a very small diatropicity is obtained computationally (Figure 18).

An attempt has been made to relate the NICS values of the individual rings of a fullerene to its endohedral chemical shift.<sup>234</sup> If one assumes that the

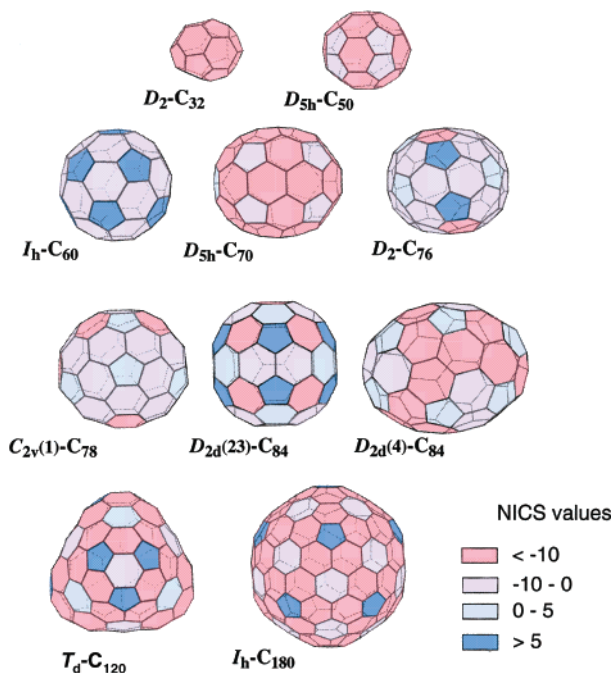


**Figure 18.** Patterns in computed NICS values (nucleus-independent chemical shifts, HF/DZP level) for neutral fullerenes. Diatropic and paratropic rings are depicted in red and blue, respectively (from the data given in ref 234).

chemical shift in the center of a ring originates exclusively from a circular current loop around that ring, one can calculate the induced magnetic field  $B_{\text{ind}}$  and thus the chemical shift from classical electrodynamics. On a line through the center and perpendicular to the loop,  $B_{\text{ind}}$  should be proportional to

$$B_{\text{ind}} \propto a^2 / (a^2 + z^2)^{3/2} \quad (7)$$

where  $a$  is the radius of the loop and  $z$  the distance from the center. From the NICS value of a given ring, together with the appropriate geometrical parameters, one can thus arrive at an estimated increment to the chemical shift at the center of the fullerene. In fact, a reasonable correlation is obtained between the sum of these increments and the actual computed  $\delta_{\text{endo}}$  value, affording further evidence that the observed endohedral shifts are indeed a direct consequence of ring currents in the fullerene cage.<sup>234</sup> The slope of 0.7 in this correlation suggests that in fact the principal part of  $\delta_{\text{endo}}$  can be interpreted in terms of ring currents localized in the individual pentagons and hexagons (those in the latter being particularly important because of the larger radius  $a$ ). Theoretical NICS values are thus a useful probe for local aromatic and antiaromatic character in fullerenes, which add up to the total, “ambiguous” one.

## 2. Application of Magnetic Criteria to Fullerene Derivatives

As discussed in section IV, fullerenes are deprived of the archetypical reactions of aromatic compounds, electrophilic or nucleophilic substitution, due to the lack of substituents. Rather, the reactivity of  $C_{60}$  and  $C_{70}$  has been compared to that of electron-deficient olefins (see refs 4–11 and 20–26 for reviews on

fullerene reactivity). In the frequently observed reduction and adduct-formation reactions, electrons are effectively added to or removed from the  $\pi$  system, respectively. The following two sections are a summary of the concomitant changes in the NMR properties. Section V.2.C will deal with similar effects brought about by replacement of carbon atoms in the fullerenes with heteroatoms.

### A. Anions

The chemistry of fullerene anions, or fullerides, has recently been reviewed.<sup>238</sup> In solution, reaction of  $C_{60}$  and  $C_{70}$  with excess lithium affords diamagnetic species, presumably the hexaanions.<sup>239</sup> By electrochemical reduction, both fullerenes can reversibly accept up to six electrons.<sup>240</sup> Most of the resulting anions are paramagnetic, and the magnetic response properties are dominated by the effect of the unpaired electrons, rather than by ring currents. Of these anions, the hexaanion  $C_{60}^{6-}$  is the only closed-shell species.<sup>241</sup> London calculations have predicted only diatropic ring currents, a large diamagnetic susceptibility, and a huge endohedral shielding for  $C_{60}^{6-}$ , indicative of a highly aromatic compound.<sup>198,201</sup> In contrast, it has been predicted that a large part of the diatropicity of  $C_{70}$  will be lost upon formation of the hexaanion.<sup>201</sup> The same trends were apparent from subsequent ab initio Hartree–Fock computations of the endohedral shielding, which afforded values between  $-58$  and  $-64$  ppm for  $C_{60}^{6-}$ <sup>203,234</sup> and  $-11$  ppm for  $C_{70}^{6-}$ .<sup>234</sup> The qualitative trends, i.e., the respective gain and loss of aromaticity upon reduction, were then confirmed experimentally by  $^3\text{He}$  NMR spectroscopy of the lithiated,  $^3\text{He}$ -labeled species:  $\delta(^3\text{He})$  values of  $-48.7$  and  $+8.3$  ppm were reported for  $\text{He}@C_{60}^{6-}$  and  $\text{He}@C_{70}^{6-}$ , respectively.<sup>242</sup> Very similar shieldings and deshieldings with respect to the neutral complexes are noted in the  $g$ -shifts of  $\text{N}@C_{60}^{6-}$  and  $\text{N}@C_{70}^{6-}$ .<sup>243</sup> The less satisfactory accord between theory and experiment is not due to the effects of ion pairing neglected in the calculations for the pristine anions, as virtually the same results are obtained for  $C_{60}^{6-}$  and  $\text{Li}_6C_{60}$ .<sup>244</sup> Rather, the Hartree–Fock approximation appears to be less suited for the fullerides and agreement with experiment is improved at a density-functional level, with computed endohedral shifts of  $-47.4$ <sup>222</sup> and  $+17.6$  ppm<sup>214</sup> for  $C_{60}^{6-}$  and  $C_{70}^{6-}$ , respectively.

The enormous endohedral shielding in  $C_{60}^{6-}$  can be traced back to strong diatropic ring currents, both in the pentagons and hexagons, as evident from London and NICS calculations.<sup>201,234</sup> In going from  $C_{70}$  to  $C_{70}^{6-}$ , the diatropicity of the five- and six-membered rings are significantly increased and decreased, respectively,<sup>201,234</sup> and the latter decrease is responsible for the endohedral deshielding. These changes in the local ring currents have recently been confirmed experimentally by the exohedral  $^1\text{H}$  probes in the reduced fulleroids: In contrast to **19**, **36**, and **37**, each of which has one strongly deshielded resonance assigned to the proton above a five-membered ring, the reduced analoga **38**,<sup>245</sup> **39**, and **40**<sup>246</sup> have only shielded methylene protons (Figure 19).

Qualitatively similar diatropicities are computed for both types of pentagons in  $C_{70}^{6-}$ , as assessed by

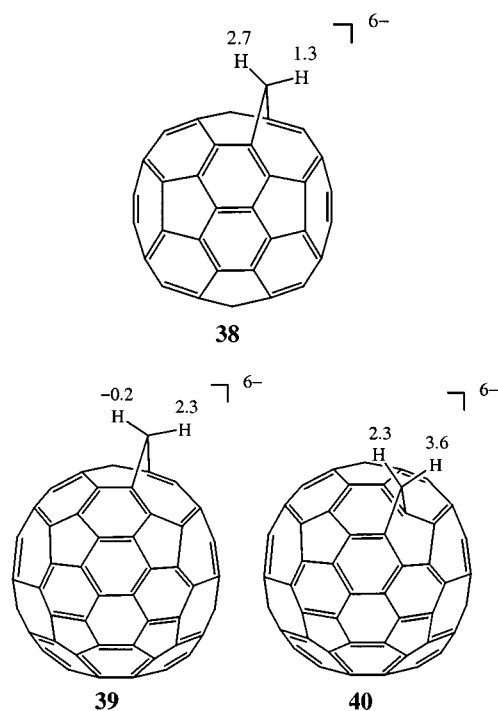


**Figure 19.** Hexaanions of the  $C_{60}$  and  $C_{70}$  fullerenes together with the  $^1H$  chemical shifts (no assignment was reported for **38**).

the London ring-current strengths and the ab initio NICS values.<sup>201,234</sup> In the experiment, a somewhat stronger shielding is found above the polar five-membered rings, compared to those close to the equator (cf. **39** and **40** in Figure 19), which has been taken as evidence for a higher charge concentration at the poles.<sup>246</sup> Interestingly, from the exohedral NMR probes in **39** and **40**, no manifestation of paratropic ring currents is apparent, which would be expected from the endohedral deshielding. The dianion of **21**, for example, is a [6,6]-open form, with notably deshielded methylene protons,  $\delta(^1H) = 4.6$ .<sup>212</sup>

Ring-current effects may also be responsible for the deshielding of the  $^{13}C$  resonance of  $C_{60}^{6-}$  relative to that of neutral  $C_{60}$  ( $\Delta\delta = 14.0$ ).<sup>239</sup> Usually, an increased negative charge at an aromatic carbon atom is paralleled by a higher shielding of its  $\delta(^{13}C)$  value.<sup>247</sup> Qualitatively, a strong diatropic current localized in a particular ring should indeed reduce the shieldings of nuclei attached to that ring. London calculations for  $C_{60}^{6-}$  have been consistent with such an interpretation,<sup>201b</sup> but the above-mentioned caveats regarding the underlying theoretical model preclude quantitative estimates.

Ring-current effects may also come to the fore in the  $^{13}C$  NMR spectrum of  $C_{70}^{6-}$ : Upon reduction of  $C_{70}$ , some signals appear to be shifted to higher frequency and some to lower frequency, with a small average deshielding of 0.9 ppm per carbon atom.<sup>239</sup> DFT results for pristine  $C_{70}^{6-}$  are in good accord with the experimental  $^{13}C$  data but suggest a completely different assignment of the signals, compared to that in neutral  $C_{70}$  (Table 7). Note, in particular, the pronounced shielding of the polar carbon atoms (a) upon reduction and the notable deshielding of most other nuclei.

**Table 7.**  $^{13}C$  Chemical Shifts of  $C_{60}$ ,  $C_{70}$ , and Their Hexaanions

fullerene carbon <sup>a</sup>	neutral		hexaanion	
	calcd <sup>b</sup>	expt <sup>c</sup>	calcd	expt <sup>d</sup>
$C_{60}$	(142.7)	142.7	158.6	156.7
$C_{70}$				
a	152.6	150.1	132.6	133.7
b	148.1	146.8	161.0	158.3
c	149.5	147.5	155.3	152.3
d	147.5	144.8	142.7	137.9
e	131.4	130.3	153.0	149.6

<sup>a</sup> Labeling a–e in  $C_{70}$  from pole to equator. <sup>b</sup> DFT values from ref 214, using neutral  $C_{60}$  as primary reference (cf. the procedure in ref 244). <sup>c</sup> From Taylor, R.; Hare, J. P.; Abdulsala, A. K.; Kroto, H. W. *J. Chem. Soc., Chem. Commun.* **1990**, 1423–1424. <sup>d</sup> From ref 239; no assignment reported for reduced  $C_{70}$ .

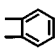
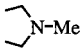
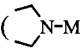
All in all, the available experimental and theoretical data suggest that the degree of aromaticity in  $C_{60}$  and  $C_{70}$  is substantially increased and decreased, respectively, upon formation of the hexaanions. According to London calculations,<sup>201</sup> further reduction of  $C_{60}^{6-}$  to the closed-shell dodecaanion should destroy the exalted diamagnetism of the former. Recent ab initio and DFT results for  $I_h$ -symmetric  $Li_{12}C_{60}$  came to the same conclusion, since an endohedral chemical shift of +11.4 ppm (DFT level) has been computed.<sup>244</sup>  $Li_{12}C_{60}$  with its  $C_{60}^{12-}$  core has been predicted<sup>248</sup> and observed<sup>249</sup> as a stable entity in the gas phase. A diamagnetic solid with the same composition<sup>250a</sup> probably contains the hexaanion as building block, as judged from the  $^{13}C$  chemical shift: In the solid-state NMR a deshielding (relative to  $C_{60}$ ) similar to that of  $C_{60}^{6-}$  is measured,<sup>250b</sup> whereas an analogous shielding is computed for  $\delta(^{13}C)$  of  $Li_{12}C_{60}$ .<sup>244</sup> Consistent with this interpretation, energetic estimates suggest that in the bulk,  $Li_{12}C_{60}$  should be unstable with respect to disproportionation into  $Li_6C_{60}$  and Li metal.<sup>244</sup>

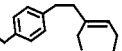
London calculations for the higher fullerenes predict similarly large dependencies of magnetic and NMR properties on the degree of reduction<sup>204</sup> as encountered for  $C_{60}$  and  $C_{70}$ . For the tetra- and hexaanion of  $C_{84}$ , endohedral chemical shifts of –26.3 and –32.7 ppm, respectively, have been predicted at the HF level,<sup>234</sup> suggesting that the  $^3He$  labeling and NMR technique could be a sensitive analytical tool to study the extent of aromatization of the higher fullerenes as function of the oxidation state. More data are probably needed for a consistent interpretation and for an assessment of magic numbers of electrons as discussed in section VI.

### B. Adducts

Attachment of substituents to the cage has been a blossoming branch from the onset of fullerene chemistry.<sup>4–11,20–26</sup> The concomitant removal of electrons from the  $\pi$  system (by localizing them in  $\sigma$  bonds) is bound to affect any resonance mechanism that might be operative. For multiple adducts of  $C_{60}$ , the aromatic character is indicated, by Hückel-type calculations of the topological resonance energy,<sup>251</sup> to depend notably on the addition pattern, and the same is to be expected for the magnetic and NMR proper-

**Table 8.**  $^3\text{He}$  Chemical Shifts of  $\text{C}_{60}$  Adducts

Adduct		$\delta(^3\text{He})$ (assignment) <sup>b</sup>	ref
type	addend(s) <sup>a</sup>		
mono	$\text{>CH}_2$ ( <b>18</b> )	-8.1	255
	$\text{>C(R}^1)_2$	-8.1	229
		-9.1	229
	$\text{C}_{60}$ <sup>c</sup>	-8.8	256
		-9.4	229
	1,2-(H) <sub>2</sub>	-9.7	229
bis	$(\text{>C(R}^1)_2)_2$	-8.7 (a,f), -9.2 (a,h), -9.7 (a,g), -9.9 (a,e) -10.2 (a,c), -10.5 (a,d), -11.0 (a,i)	257
		-10.1 (a,f), -10.9 (a,h), -12.3 (a,d), -12.4 (a,g)	257
	(H) <sub>4</sub> <sup>d</sup>	-10.3, -10.8, -11.3, -11.6, -12.7, -12.8, -12.9	257
	$\text{>C(R}^1)\text{-X}^1$	-11.4 (a,e)	258
	tris	$(\text{>C(R}^1)_2)_3$	-12.0 (a,e,j)
	$\text{>C(X}^1)_2$	-10.3 (a,e,k)	258
tetrakis	$(\text{>C(X}^1)_2)(\text{>C(R}^2)_2)$	-12.3 (a,e,j,k)	258
pentakis	$(\text{>C(X}^1)_2)(\text{>C(R}^2)_2)_2$	-11.8 (a,e,j,k,m), -12.0 (a,e,j,k,l)	258
hexakis	$(\text{>C(X}^1)_2)\text{-}$ $(\text{>C(R}^2)_2)_2(\text{>C(R}^1)_2)$	-11.9 (a,e,j,k,l,m)	258
other	1,4-(Ph) <sub>2</sub>	-10.5	259
	(Ph) <sub>4</sub> <sup>d</sup>	-14.4	259
	Cl <sub>6</sub> ( <b>41</b> )	-12.3	259
	Ph <sub>5</sub> Cl ( <b>42a</b> )	-15.1	259
	(4-F-C <sub>6</sub> H <sub>4</sub> ) <sub>5</sub> Cl ( <b>42b</b> )	-15.0	259
	(4-F-C <sub>6</sub> H <sub>4</sub> ) <sub>5</sub> <sup>+</sup> ( <b>43</b> )	-12.6	259

<sup>a</sup>R<sup>1</sup>=CO<sub>2</sub>Et, R<sup>2</sup>=CO<sub>2</sub>CH<sub>2</sub>CO<sub>2</sub>Et, X<sup>1</sup>=CO<sub>2</sub>- <sup>b</sup> Addition across the bonds

labeled in Figure 20a. <sup>c</sup>[2+2] dimer. <sup>d</sup>Assignment or structure uncertain.

ties. Exohedral NMR probes of the type discussed in section V.1.A are difficult to apply, as the addition chemistry of fullerenes is still in its infancy.<sup>252</sup> NMR nuclei of the addends themselves have been employed as probes for ring-current effects,<sup>216,253,254</sup> but these nuclei are by necessity close to partly saturated ring systems, and local anisotropy effects of the latter may actually be dominant. Endohedral probes are thus preferable, and a sizable amount of  $^3\text{He}$  NMR data has already been accumulated for endohedral He compounds of fullerene derivatives.<sup>229,255–260</sup> As with the fullerene isomers, each fullerene derivative has so far been characterized by a distinct  $^3\text{He}$  chemical shift (which is measurable with high precision), a further testimony to the analytical potential of this technique.<sup>229</sup>

As mentioned above, the entire fullerene  $\pi$  system is largely preserved in the fullerenes. Consequently,

the  $\delta(^3\text{He})$  values recorded for **19** ( $\delta = -6.6$ ) and **36/37** ( $\delta = -27.5/-27.8$ ) are very similar to those of the parent fullerenes.<sup>255</sup> More pronounced effects are encountered for methanofullerenes and other adducts. 1,2-Addition across one [6,6]-double bond of He@C<sub>60</sub> invariably results in an increased endohedral shielding, with  $\delta(^3\text{He})$  between  $-8.1$  and  $-9.7$  ppm (Table 8;  $\Delta\delta$  with respect to He@C<sub>60</sub> between  $-1.8$  and  $-3.4$  ppm). When carbocycles are formed during addition, the magnitude of this low-frequency shift increases with ring size. For methanofullerenes such as **18**, the shielding exaltation with respect to the parent fullerene is about one-half of that observed in unstrained or noncyclic adducts. This trend has been interpreted in terms of a homoconjugative phenomenon wherein the contributions of the cyclopropane-type orbitals are similar to those of double bonds but smaller in magnitude.<sup>255</sup>

The increased endohedral shielding in the adducts is ascribed to the disruption of the paratropic current flows in the two pentagons that are sharing the substituents. This conjecture has received support from NICS calculations for the parent dihydride  $C_{60}H_2$ , which in addition have revealed that the paratropicity of the next-nearest pentagons is also reduced and that the diatropicity of all six-membered rings (except those abutting at the site of addition) is slightly but significantly enhanced.<sup>234</sup>

Double addition can give rise to several isomers (a total of eight when occurring pairwise across [6,6]-bonds in  $C_{60}$ ). In some cases, the  $^3He$  chemical shifts could be assigned to specific isomers, either by separation, purification, and comparison with other spectroscopic data<sup>257</sup> or by using special tethered addends which strongly favor particular geometric arrangements.<sup>258</sup> In all cases, the endohedral shielding of the bisadducts is increased relative to that of the corresponding monoadduct (Table 8). When further addends are placed at [6,6]-bonds pointing toward the vertices of an octahedron (*a, e, j, k, l, m* in Figure 20), the endohedral shielding levels off at ca.  $-12$  ppm (see entries tris to hexakis in Table 8). A similar value,  $-11.1$  ppm, is computed at the HF level for the corresponding  $C_{60}H_{12}$  parent.<sup>214</sup> The  $\pi$  system in these hexaadducts consists of eight interconnected benzene moieties occupying the corners of a cube<sup>70</sup> (cf. **2** in Figure 11).

Depending on the reaction conditions, addition can also occur in a 1,4-fashion rather than 1,2. A few examples with this pattern are included in Table 8 (last six entries). Again, the endohedral shielding increases with the number of addends, except for the hexachloro compound **41** which has a conspicuously higher endohedral chemical shift compared to the arylated derivatives **42**. Quite interesting is the deshielding (by 2.4 ppm) in going from **42b** to the cation **43**,<sup>259</sup> a transformation which leaves the number of  $\pi$  electrons in the fullerene moiety unaltered. The reduced diamagnetism in going to the cation can be rationalized by formation of a substructure with appreciable cyclopentadiene-cation character and partial loss of aromatic character in the adjacent hexagons.<sup>259</sup>

The degree of hydrogenation of fullerenes depends on the reaction conditions. With more drastic methods such as Birch reduction,  $C_{60}H_{36}$  is obtained as the major product, together with smaller amounts of  $C_{60}H_{18}$ . The former is the first derivative of  $C_{60}$  to be produced,<sup>126</sup> but its structure is not yet unambiguously proven, as the acquisition of well-resolved  $^1H$  NMR spectra is hampered by stability problems.  $^3He$  NMR of the labeled reaction mixture has revealed the presence of two isomers with very similar endohedral chemical shifts,  $-7.7$  and  $-7.8$  ppm.<sup>260a</sup> Comparison with ab initio data predicted previously for a number of  $C_{60}H_{36}$  isomers<sup>261</sup> allowed the initially proposed,<sup>126</sup> fully nonconjugated  $T_h$ -symmetric structure to be excluded, but no further definite assignment was possible. The composition of  $C_{60}H_{36}$  samples may also depend on the method of preparation, and the presence of  $D_{3d}$ - and  $S_6$ -symmetric isomers has been supported by IR and Raman spectroscopy.<sup>180</sup> A

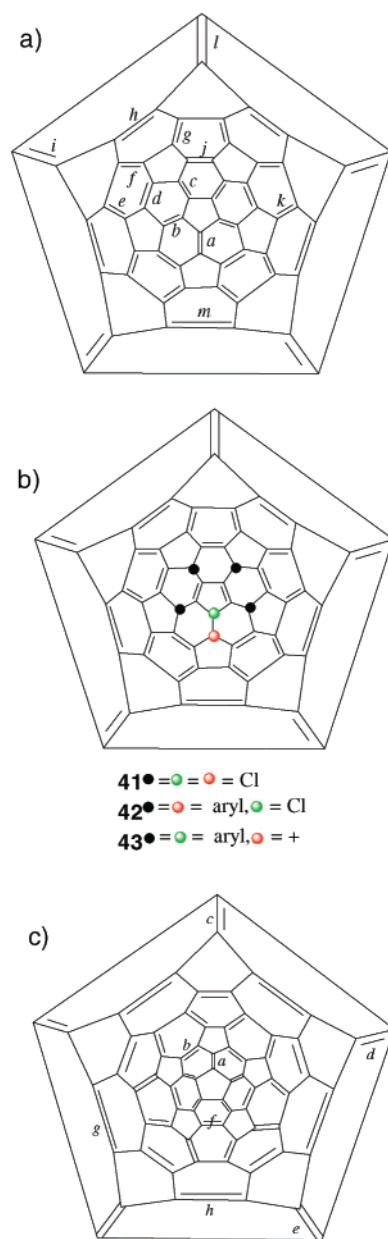


**Figure 20.** Schlegel plots of (a)  $C_{60}$ , (b)  $C_{60}$  adducts, and (c)  $C_{70}$  including bond labels for the multiple adducts in Tables 8 and 9.

tentative assignment of the Birch-reduction products could later be made by analogy with the corresponding fluoro compounds.<sup>184b</sup> Fluorination gives the same regiochemistry as hydrogenation (for instance the same  $C_{3v}$  symmetry crown structure is found for both  $C_{60}H_{18}$  and  $C_{60}F_{18}$ ,<sup>181</sup> see Figure 21 for the Schlegel plot and Chart 6 for a perspective drawing), and the two  $C_{60}F_{36}$  structures could be identified by 2D  $^{19}F$  NMR spectroscopy as the *T* form **46** and one particular  $C_3$ -symmetric isomer **48** (Figure 21). Interestingly, the latter is not among the most stable isomers nor does it contain the structural motif of  $C_{60}F_{18}$ , from which it can also be generated.<sup>184b</sup>

An enhanced endohedral shielding is apparent for the fluorinated species as compared to their hydrogenated counterparts, which is to some extent probably due to anisotropy effects of the CF vs the CH  $\sigma$  bonds: The endohedral shielding in fully saturated  $C_{60}F_{60}$  is computed to be ca. 3 ppm larger than that

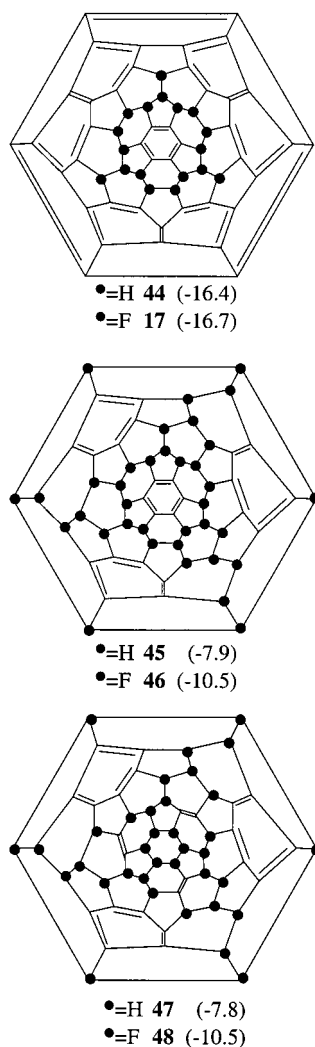


**Figure 21.** Schlegel plots of  $C_{60}X_{18}$  (top) and the  $T$  (middle) and  $C_3$  isomers (bottom) of  $C_{60}X_{36}$  ( $X = H, F$ ). In parentheses, endohedral chemical shifts (assignment for hydrogenated species according to that of the fluorinated ones).

in  $C_{60}H_{60}$  (ab initio HF level).<sup>214</sup> The endohedral shielding in  $C_{60}H_{36}$  isomers is governed by ring-current and anisotropy effects of the benzene and ethylene moieties, respectively, and a simple increment system was suggested on the basis of ab initio HF data.<sup>261</sup>

All in all, the  $^3\text{He}$  NMR data indicate that addition of substituents to  $C_{60}$  increases its aromaticity. The most aromatic derivatives to date are  $C_{60}X_{18}$  **44** and **17**, their aromatic character exceeding that of adducts in which the annelated  $\pi$  system is broken down into separate or conjugated benzene and olefin units.

In contrast, by the  $^3\text{He}$  NMR criteria it is concluded that addends serve to diminish the aromaticity of  $C_{70}$ .<sup>262,255,258</sup> Addition predominantly occurs across two types of bonds (labeled *a* and *b* in Figure 20 and denoted  $\alpha$  and  $\beta$  in ref 258),<sup>263</sup> with distinctly different effects on the endohedral shielding: While addition across bond *a* affords a high-frequency shift with respect to  $C_{70}$  ( $\delta = -28.8$ ) between 0.7 and 1.3 ppm (see entries for **34** and **49**, respectively, in Table 9), addition across bond *b* has a larger effect,  $\Delta\delta = 3.2$  (**35**). The observation of a decrease in the endo-

**Table 9.**  $^3\text{He}$  Chemical Shifts of  $C_{70}$  Adducts

Adduct		$\delta(^3\text{He})$ (assignment) <sup>b</sup>	reference
type	addend(s) <sup>a</sup>		
mono	$\sum\text{CH}_2$	-28.1 ( <i>a</i> , <b>34</b> ), -25.6 ( <i>b</i> , <b>35</b> )	255
	$\sum\text{C}(\text{R}^1)_2$	-27.7 ( <i>a</i> ) (-27.6) <sup>d</sup>	226
	$\sum\text{C}(\text{R}^2)_2$	-27.5 ( <i>a</i> , <b>49</b> )	258
	$\sum\text{N-Me}$ <sup>c</sup>	-27.9, -23.8	262
bis	$(\sum\text{C}(\text{R}^2)_2)_2$	-26.1 ( <i>a,e</i> ), -26.3 ( <i>a,c</i> ), -26.4 ( <i>a,d</i> )	258
tris	$(\sum\text{C}(\text{R}^2)_2)_3$	-23.6 ( <i>a,c,f</i> )	258
tetrakis	$(\sum\text{C}(\text{R}^1)_2)(\sum\text{C}(\text{R}^2)_2)_3$	-20.7 ( <i>a,d,f,g</i> )	258
	$(\sum\text{C}(\text{R}^2)_2)_4$	-21.1 ( <i>a,c,f,h</i> )	258

<sup>a</sup>  $\text{R}^1 = \text{CO}_2\text{Et}$ ,  $\text{R}^2 = \text{CO}_2\text{CH}_2\text{CO}_2\text{Et}$ . <sup>b</sup> Addition across the bonds labeled in Figure 20c. <sup>c</sup> Assignment or structure uncertain. <sup>d</sup> Doubly He labeled compound.

hedral shielding has been attributed<sup>258</sup> to a disruption of the large diatropic ring currents around the polar corannulene perimeter, which have been predicted by the London calculations.<sup>201</sup>

Qualitatively, the same changes in the endohedral chemical shifts upon monoadduct formation of  $\text{He}@C_{60}$  and  $\text{He}@C_{70}$ , namely, shielding and deshielding, respectively, are found in the  $g$ -factors of the corresponding endohedral N compounds.<sup>236b</sup>

When further addends are introduced in **49**, a successive deshielding of  $\delta(^3\text{He})$  is observed. The effects are additive to a large extent, with incremental values that depend little on the degree of functionalization but mainly on the type of bond,  $\alpha$  or  $\beta$ , being saturated.<sup>258</sup> Polyaddition to  $C_{70}$  is being actively investigated,<sup>264</sup> and several endohedral He compounds of higher adducts besides those summarized in Table 8 have recently been prepared and analyzed.<sup>258b,c</sup> Many interesting results of future application of this technique can be anticipated. For instance, if  $C_{70}H_{36}$  or  $C_{70}H_{40}$  should have only isolated double bonds, as predicted by semiempirical MNDO calculations,<sup>265</sup> the expected nonaromaticity should manifest itself in very small endohedral chemical shifts.

Despite considerable progress in the addition chemistry of the higher fullerenes,<sup>15,16</sup> we are not aware of any  $^3\text{He}$  labeling and NMR studies of, for instance, derivatives of  $C_{76}$ ,  $C_{78}$ , or  $C_{84}$ . According to a preliminary calculation at the RHF level,<sup>214</sup> a small increase in the endohedral shielding by 1.8 ppm is predicted upon bisadduct formation of  $C_{76}$  ( $C_{76}H_4$  derived by addition across the polar [6,6]-bonds connecting the dark blue pentagons in Figure 18). More work is needed to elucidate the relation between addition pattern and aromaticity in derivatives of  $C_{70}$  and the higher fullerenes.

$C_{36}H_x$  and  $C_{36}OH_x$  ( $x = 4, 6$ ) have been identified mass-spectroscopically,<sup>266</sup> following the proposed synthesis of the  $C_{36}$  fullerene.<sup>267</sup> Neither the structure of the latter nor those of its possible derivatives are known. For several symmetric  $C_{36}H_x$  isomers ( $x = 6, 12, 36$ ), large variations have been computed for the endohedral chemical shifts (between ca.  $-3$  and  $-44$



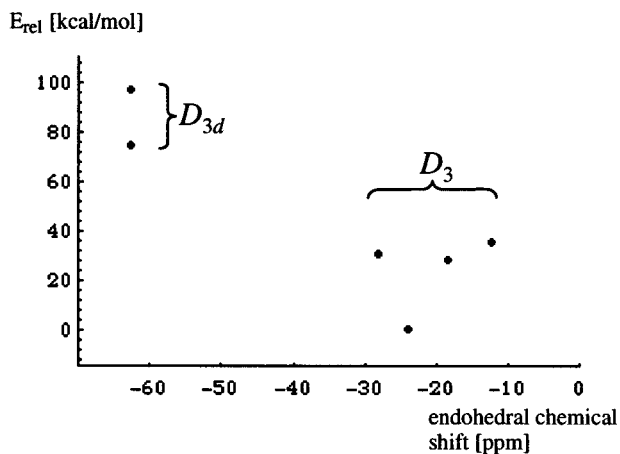


**Figure 22.** “Noncorrelation” of the relative stabilities of the  $D_{3d}$  and  $D_3$ -symmetric  $C_{54}N_6$  isomers with their aromatic character, as assessed from endohedral  $\delta(^3\text{He})$  values (RHF/DZP level, data taken from ref 273).

ppm) depending on number and positions of the substituents.<sup>268</sup>

### C. Heterofullerenes

Replacement of one or more carbon atoms in the cage with heteroatoms can lead to species with a perturbed  $\pi$  system and new electronic properties. The correspondingly doped fullerenes are usually characterized by mass spectrometry, as pure compounds are rarely available in macroscopic amounts. The chemistry of azafullerenes is especially well developed, and a number of derivatives with nitrogen atoms incorporated in the  $C_{60}$  or  $C_{70}$  framework have been isolated and characterized.<sup>269</sup> Examples of stable diamagnetic species comprise  $C_{59}NH$  (**50**), the  $(C_{59}N)_2$  dimer with its weak CC bond, and the corresponding  $(C_{69}N)_2$ .<sup>270</sup> Alas, the magnetic and NMR properties pertinent to the aromatic character of these molecules have yet to be determined, but a few theoretical predictions are available.

At the Hartree–Fock level and employing the BLYP geometry, the endohedral shielding of the parent hydroazafullerene **50** is computed to be higher than that of  $C_{60}$  by ca. 2 ppm,<sup>214,271</sup> similar to the finding for the isoelectronic 1,2- $C_{60}H_2$  (Table 8). Apparently the lone pair at nitrogen is not involved in significant cyclic conjugation, even though some delocalization onto the next-nearest-neighboring  $sp^2$  carbon atoms is indicated from the canonical Kohn–Sham orbitals<sup>270b</sup> and from the  $^{13}C$  chemical shifts.<sup>272</sup>

For selected isomers of  $C_{54}N_6$ , isoelectronic with the highly aromatic hexaanion of  $C_{60}$ , huge endohedral shieldings approaching that of the latter have been computed.<sup>273</sup> Other isomers with lower symmetry, however, are predicted to be more stable but less aromatic (Figure 22). For two particular N-doped  $C_{36}$  fullerenes, i.e.,  $C_{30}N_6$  and  $C_{24}N_{12}$ , reduced endohedral shieldings with respect to neutral  $C_{36}$  have been predicted, whereas for one  $C_{24}B_{12}$  isomer, a large endohedral shielding has been computed, ca.  $-45$  ppm.<sup>268</sup> Preliminary calculations for  $C_{60-2n}(BN)_n$ , formally isoelectronic with  $C_{60}$  itself, indicate a slightly increased endohedral shielding ( $\Delta\delta \sim -2$  ppm).<sup>274</sup>

## 3. Summary

In conclusion, there is ample evidence both from experiment and theoretical calculations that fullerenes and their derivatives can sustain ring currents, just like their planar cousins, polycyclic aromatic hydrocarbons, as a consequence of the cyclic delocalization of  $\pi$  electrons. To the extent that such ring-current effects are taken as a measure of aromaticity in planar molecules, the same criterion can be applied to the three-dimensional fullerenes. Because of the large number of annelated rings and the particular connectivity in each fullerene, topologically complex patterns of ring currents are induced. Reflecting the frequent presence of both dia- and paratropic ring currents, the term “ambiguous aromatic character” has been coined for the fullerenes. The center of each cage “feels” the combined effects of all ring currents and is thus probably the best means to assess the overall degree of aromaticity or antiaromaticity, either computationally, via the endohedral chemical shift at the center, or experimentally, via  $\delta(^3\text{He})$  of the corresponding endohedral helium compound.

It is also apparent, however, that for fullerenes enhanced aromaticity as assessed by magnetic criteria does not necessarily translate into additional stabilization. The considerable strain inherent in the skeletal cages and its variation between isomers or during chemical transformations can easily dominate stability and reactivity.

Changes in endohedral shifts upon adduct formation can often be rationalized qualitatively in terms of quenching of either dia- or paratropic ring currents close to the region of addition. Ring currents all over the molecule tend to be affected, however, and the nontransferability of localized ring-current contributions, as assessed by NICS calculations, make quantitative predictions difficult. Effects on the magnetic properties of ionization or reduction, i.e., removal or addition of electrons to the  $\pi$  system, are even less amenable to an intuitive understanding. Here the electronic structures, that is, the energies and nodal properties of the individual MOs, will have to be analyzed in detail. In the following section, the simple MO shell model outlined in section II (cf. Table 3) is taken as the starting point for a first step toward a conceptual connection between electronic structure and aromaticity in three dimensions.

## VI. Nature of Aromaticity in Fullerenes and Count Rules

### 1. Topological Count Rules—“Magic Numbers”

In an early treatment, magic numbers for icosahedral fullerenes (Goldberg-type fullerenes) were found to be  $60n$  for closed-shell systems and  $60n + 20$  for open-shell system.<sup>33</sup> A geometrical interpretation of this rule is that open-shell fullerenes have atoms on the  $C_3$  axes, while closed-shell fullerenes do not. Closed shells were predicted for  $C_{60}$ ,  $C_{180}$ ,  $C_{240}$ ,  $C_{420}$ ,  $C_{540}$ , etc. A tetrahedral structure was found to be the best candidate for  $C_{120}$ . The open-shell icosahedral fullerenes  $C_{20}$ ,  $C_{80}$ ,  $C_{140}$ , etc., have a 4-fold degenerate HOMO occupied by two electrons and a

**Table 10.** Calculated Endohedral  $^3\text{He}$  Chemical Shifts and Symmetry  $\text{He}@C_{20}$  and  $\text{He}@C_{80}$  Species with Different Filling Degree of the  $\pi$ -Electron System<sup>66</sup>

species	symmetry	$\delta(^3\text{He})^a$	NICS(5) <sup>b</sup>	NICS(6) <sup>c</sup>
$C_{20}^{2+}$ (closed $l = 2$ shell)	$I_h$	-66.2	-25.1	
$C_{20}$	$C_2$	-31.7	-1.1–12.7	
$C_{60}^{+10}$ (closed $l = 4$ shell)	$I_h^a$	-78.9 <sup>b</sup>		
$C_{80}^{8+}$ (closed $l = 5$ shell)	$I_h$	-82.9	-29.1	-30.3
$C_{80}^{6+}$	$D_{5d}$	-70.0	-25.1	-26.6
$C_{80}^{2+}$	$D_{5d}$	-54.5	-17.2	-20.2
$C_{80}$ (triplett)	$D_{5d}$	-8.4	-17.2	-4.2
$C_{80}^{2-}$	$D_{5d}$	+78.6	-3.7	+29.8
$C_{80}^{6-}$	$D_{5d}$	-32.8	-18.9	-13.4

<sup>a</sup> GIAO-SCH/3-21G//HF/6-31G.<sup>18</sup> <sup>b</sup> Nucleus-independent chemical shifts in the center of the five-membered rings. <sup>c</sup> Nucleus-independent chemical shifts in the center of the six-membered rings.

4-fold degenerate LUMO. Conversely, the closed-shell fullerenes exhibit a 5-fold degenerate HOMO and a 3-fold degenerate LUMO. It was expected that the neutral open-shell fullerenes would lift the degeneracy by Jahn–Teller distortion to a structure of lower symmetry. Therefore, the equilibrium geometry of  $C_{20}$ ,  $C_{80}$ ,  $C_{140}$ ,  $C_{260}$ , etc., was suggested to be not icosahedral. Icosahedrally-shaped  $C_{180}$ ,  $C_{240}$ ,  $C_{540}$ , and  $C_{960}$  were found to be more stable than the spherical-shaped conformers with an evenly distributed curvature.<sup>275</sup> Although this count rule is able to predict stable closed-shell fullerenes, it does not consider the aspect of aromaticity.

In another investigation, a correlation between the stability of a fullerene, expressed by the HRE, the CCRE, and the HOMO–LUMO gap, and the cage structure was found.<sup>276</sup> This investigation is related to the topological search for magic numbers of fullerenes,<sup>27–29,34,37,38</sup> fulleride anions,<sup>37</sup> and fullerene cations.<sup>37</sup> In particular, stable cages  $C_n$  were predicted for  $n = 60 + 6m$  with  $m$  being any nonnegative integer other than 1. These fullerenes are characterized by the presence of hexagons that are completely surrounded by other hexagons and were termed as Clar-sextet<sup>277</sup> cages. It was suggested that these fullerenes exhibit an enhanced aromaticity. However,  $C_{72}$  has not been found in isolable quantities and the Clar-sextet cage of  $C_{78}$  is not among the isolated  $C_{78}$  isomers. It was found that probably due to strain effects,<sup>63,278</sup> the Clar-sextet isomer of  $C_{78}$  is very high in energy. As a consequence, it could not be demonstrated experimentally, for instance by  $^3\text{He}$  NMR spectroscopy, whether these Clar-sextet cages exhibit a pronounced diamagnetic shielding in their interior, which would have been an important measure for the magnetic criterion of aromaticity. Also, calculations of the magnetic properties have not been carried out so far.

## 2. Spherical Aromaticity in $I_h$ Symmetrical Fullerenes: The $2(N + 1)^2$ Rule

The aromaticity of annulenes and heteroannulenes can be described with the Hückel rule.<sup>12</sup> Due to their closed-shell structures, annulenes with  $4N + 2$  electrons are not distorted ( $D_{nh}$  symmetry) and show strong diamagnetic ring currents while singlet  $4N$  annulenes are often distorted and have paratropic character. However, the Hückel rule cannot be applied in polycyclic systems, where, for example,

benzenoid rings are joined by four- or five-membered rings. Thus, neither biphenylene nor fluoranthene are antiaromatic, although they represent  $12\pi$  and  $16\pi$  systems, respectively. In fact, they are both typical aromatics, for example, as far as the reactivity criterion<sup>30</sup> (electrophilic substitution reactions) and the diamagnetic shielding of their six-membered rings is concerned.<sup>13</sup> It was emphasized<sup>279</sup> that the nature of the smallest circuit in a planar polycyclic aromatic rather than the molecular perimeter governs its overall classification and behavior. Spherical fullerenes represent a special group of polycyclic  $\pi$  systems. To explain the nature of aromaticity of fullerenes and to deduce a count rule for their aromatic character, it is important to choose the most suitable and unambiguous criterion. Due to the reasons outlined in sections II–IV, structural, energetic, and reactivity criteria alone are insufficient to properly describe the aromaticity of fullerenes. The magnetic behavior, however, evaluated, for example, by  $^3\text{He}$  NMR spectroscopy or by NICS calculations (section V), seems to be the most independent criterion. Moreover, in a series of cases it correlates well with specific structural aspects.<sup>67</sup> As demonstrated in section V, no correlation between the diamagnetic shielding in the center of the fullerenes and the cluster size or charge of the fullerenes was discovered until recently such a correlation was established for the icosahedral fullerenes  $C_{20}$ ,  $C_{60}$ , and  $C_{80}$ .<sup>67</sup> As pointed out in section II, no distortion of the  $\pi$ -electron system is expected in these fullerenes if their shells are fully filled. Closed-shell situations are realized if the fullerene contains  $2(N + 1)^2$   $\pi$  electrons. This is closely related to the stable noble-gas configuration of atoms or atomic ions. In this case, the electron distribution is spherical and all angular momenta are symmetrically distributed. The correlation of the aromatic character determined by the magnetic properties is shown in Table 10.

The closed-shell systems  $C_{20}^{2+}$  ( $N = 2$ ),  $C_{60}^{10+}$  ( $N = 4$ ), and  $C_{80}^{8+}$  ( $N = 5$ ) exhibit very pronounced  $^3\text{He}$  chemical shifts in the center of the cage. With  $\delta = -81.4$ ,  $C_{60}^{10+}$  has the largest theoretically determined diamagnetic shielding up to now. Both six- and five-membered rings exhibit very large diamagnetic ring currents. Therefore, icosahedral fullerenes that contain  $2(N + 1)^2$   $\pi$  electrons show the maximum degree of spherical aromaticity. Exceptions are possible if levels of the most outer shell are occupied before all “inner” shells are completely filled. This is

the case for  $C_{60}$ <sup>12, 244</sup> In this case, the  $t_{1g}$  levels of the  $l = 6$  shell are filled prior to the  $t_{2u}$  levels of the  $l = 5$  shell. This is in analogy to the filling of the atomic 4s levels prior to the 3d levels. Compared to the cyclic annulenes which follow the  $4N + 2$  rule, the spherical fullerenes show the maximum diatropicity more rarely and there are numerous intermediate situations, including molecules with both aromatic and antiaromatic regions. One key conclusion is that the entire molecule must be taken into account in order to understand the aromatic properties of icosahedral fullerenes. The applicability of this concept to less symmetrical fullerenes must be examined. A broad variety of smaller, less symmetrical fullerenes also obey this rule of spherical aromaticity as demonstrated with NICS calculations. It is clear that in the case of fullerenes with a lower symmetry, local substructures, like the cyclic phenylene belt of  $C_{70}$ , can also determine the magnetic behavior to a large extent.

Now, after a decade of extensive fullerene research, it can be concluded that the early predictions of Kroto<sup>1,3</sup> became true, namely, that the fullerenes can exhibit three-dimensional superaromaticity. Of course, the superior three-dimensional aromaticity does not appear within neutral buckminsterfullerene  $C_{60}$ , whose outer shell is incompletely filled resulting in the establishment of both moderately aromatic and antiaromatic character. The three-dimensional counterpart of Hückel aromaticity in pure form requires a noble-gas configuration of the cluster and can appear, for example, in charged icosahedral fullerenes.

## VII. Conclusion

Are fullerenes aromatic? In this review we have attempted to summarize the current state of research related to this question. The classical criteria for aromaticity of planar, unsaturated compounds, namely, those based on structure, energetics, reactivity, and magnetic properties, are applied to fullerenes and their derivatives. Magnetic and NMR properties are probably the most general indicators for aromaticity, and the wealth of accumulated data clearly demonstrates that extensive cyclic delocalization of  $\pi$  electrons takes place in fullerenes. The observed properties are often the result of the simultaneous presence of locally diatropic and paratropic ring currents.

According to estimated resonance energies, the  $\pi$ -electron delocalization in fullerenes, the origin of their special NMR properties, should indeed provide some energetic stabilization. However, while such an aromatic stabilization can be a major driving force in annulene chemistry, other contributions, in particular strain, can be competitive or even decisive for fullerenes. The same is true for structural and reactivity aspects of fullerenes.

The scope of aromaticity is thus much broader for Hückel-type annulenes than for fullerenes, where it is essentially limited to delocalization evidenced by ring currents. The prediction that according to the computed NMR criteria  $C_{60}^{10+}$  should be the most aromatic fullerene derivative to date does not mean it will be easily, or ever, synthesized. Yet the classifica-

tion of a fullerene or one of its derivatives as "highly aromatic" will be useful because one can expect outstanding NMR properties which can lead to its identification and characterization.

Qualitative relations between spherical aromaticity and electronic structure are only beginning to emerge: When the  $\pi$  MOs on the surface of a sphere are grouped into shells according to their nodal properties, a simple model predicts that maximum aromaticity is reached when the individual shells are completely filled. The shell model appears to be an attractive starting point for an eventual, generalized description of three-dimensional aromaticity. To answer the initial question, yes, fullerenes can be aromatic, but compared to the cyclic annulenes, which follow the  $4N + 2$  rule, the maximum diatropicity occurs more rarely and there are numerous intermediate situations, including molecules with both aromatic and antiaromatic regions.

## VIII. Acknowledgment

M.B. thanks Professor W. Thiel for continuous support and the Fonds der chemischen Industrie and the Deutsche Forschungsgemeinschaft for a Liebig and Heisenberg fellowship, respectively. A.H. thanks the Deutsche Forschungsgemeinschaft, the Stiftung Volkswagenwerk, and the Fond der Chemischen Industrie for financial support. Thanks are also due to Professor K.-P. Dinse, Dr. P. Jakes, Professor M. Rabinovitz, and Professor A. Weidinger for making material available prior to publication.

## IX. References

- (1) Kroto, H. W.; Heath, J. R.; O'Brien, S. C.; Curl, R. F.; Smalley, R. E. *Nature* **1985**, *318*, 162–163.
- (2) Krätschmer, W.; Lamb, L. D.; Fostiropoulos, K.; Huffman, D. R. *Nature* **1990**, *347*, 354–358.
- (3) Kroto, H. W. *Pure Appl. Chem.* **1990**, *62*, 407–415.
- (4) *Fullerenes*; Hammond, G. S., Kuck, V. J., Eds.; American Chemical Society: Washington, DC, 1992.
- (5) *Buckminsterfullerenes*; Billups, W. E., Ciufolini, M. A., Eds.; VCH Publishers: New York, 1993.
- (6) *The Fullerenes*; Kroto, H. W., Fischer, J. E., Cox, D. A., Eds.; Pergamon Press: Oxford, 1993.
- (7) *The Fullerenes*; Kroto, H. W., Walton, D. R. M., Eds.; Cambridge University Press: New York, 1993.
- (8) Hirsch, A. *The Chemistry of the Fullerenes*, Thieme, New York, 1994.
- (9) *The Chemistry of Fullerenes*; Taylor, R., Ed.; World Scientific Publishing: Singapore, 1995.
- (10) Dresselhaus, M. S.; Dresselhaus, G.; Eklund, P. C. *Science of Fullerenes and Carbon Nanotubes*, Academic Press: San Diego, 1996.
- (11) (a) Kroto, H. W.; Allaf, A. W.; Balm, S. P. *Chem. Rev.* **1991**, *91*, 1213–1235. (b) Reed, C. A.; Bolskar, R. D. *Chem. Rev.* **2000**, *100*, 1075–1120. (c) Martin, N.; Sanchez, L.; Illescas, B.; Perez, I. *Chem. Rev.* **1998**, *98*, 2527–2547.
- (12) Minkin, V. I.; Glukhovtsev, M. N.; Simkin, B. Y. *Aromaticity and Antiaromaticity*. John Wiley & Sons: New York, 1994.
- (13) Schleyer, P. v. R.; Jiao, H. *Pure Appl. Chem.* **1996**, *68*, 209–218.
- (14) Krygowski, T. M.; Cyranski, M. K.; Czarnocki, Z.; Häfelinger, G.; Katritzky, A. R. *Tetrahedron* **2000**, *56*, 1783–1796.
- (15) Thilgen, C.; Diederich, F. *Top. Curr. Chem.* **1999**, *199*, 135–171.
- (16) Thilgen, C.; Herrmann, A.; Diederich, F. *Angew. Chem.* **1997**, *109*, 2362–2374; *Angew. Chem., Int. Ed. Engl.* **1997**, *36*, 2269–2280.
- (17) Balch, A. L.; Olmstead, M. M. *Chem. Rev.* **1998**, *98*, 2123–2165.
- (18) Haddon, R. C. *Science* **1993**, *261*, 1545–1550.
- (19) Haddon, R. C.; Raghavachari, K. *Tetrahedron*, **1996**, *52*, 5207–5220.
- (20) Hirsch, A. *Synthesis* **1995**, 895–913.

- (21) Diederich, F.; Thilgen, C. *Science* **1996**, *271*, 317–323.
- (22) Diederich, F. *Pure Appl. Chem.* **1997**, *69*, 395–400.
- (23) Hirsch, A. *Top. Curr. Chem.* **1998**, *199*, 1–65.
- (24) Diederich, F.; Kessinger, R. *Acc. Chem. Res.* **1999**, *32*, 537–545.
- (25) Hirsch, A.; Nuber, B. *Acc. Chem. Res.* **1999**, *32*, 795–804.
- (26) Diederich, F.; Gomez-Lopez, M. *Chem. Soc. Rev.* **1999**, *28*, 263–277.
- (27) Diederich, F.; Kessinger, R. In *Templated Organic Synthesis*; Diederich, F., Stang, P. J., Eds.; Wiley-VCH Verlag: Weinheim, 2000; pp 189–218.
- (28) (a) Schmalz, T. G.; Seitz, W. A.; Klein, D. J.; Hite, G. E. *Chem. Phys. Lett.* **1986**, *130*, 203–207. (b) Schmalz, T. G.; Seitz, W. A.; Klein, D. J.; Hite, G. E. *J. Am. Chem. Soc.* **1988**, *110*, 1113–1127.
- (29) Kroto, H. W. *Nature* **1987**, *329*, 529–531.
- (30) Taylor, R. *Tetrahedron Lett.* **1991**, *32*, 3731–3734.
- (31) Taylor, R. *J. Chem. Soc., Perkin Trans. 2* **1992**, 3–4.
- (32) (a) Campbell, E. E. B.; Fowler, P. W.; Mitchell, D.; Zerbetto, F. *Chem. Phys. Lett.* **1996**, *250*, 544–548. (b) Ayuela, A.; Fowler, P. W.; Mitchell, D.; Schmidt, R.; Seifert, G.; Zerbetto, F. *J. Phys. Chem.* **1996**, *100*, 15634–15636. (c) Albertazzi, E.; Domene, C.; Fowler, P. W.; Heine, T.; Seifert, G.; Van Alsenoy, C.; Zerbetto, F. *Phys. Chem. Chem. Phys.* **1999**, *1*, 2913–2918.
- (33) Fowler, P. W. *Chem. Phys. Lett.* **1986**, *131*, 444–450.
- (34) Fowler, P. W.; Steer, J. I. *J. Chem. Soc., Chem. Commun.* **1987**, 1403–1405.
- (35) Schmalz, T. G.; Seitz, W. A.; Klein, D. J.; Hite, G. E. *J. Am. Chem. Soc.* **1988**, *110*, 1113–1127.
- (36) Fowler, P. W.; Batten, R. C. *J. Chem. Soc., Faraday Trans. 1991*, *87*, 3103–3104.
- (37) Fowler, P. W.; Manolopoulos, D. E. *Nature* **1992**, *355*, 428–430.
- (38) Fowler, P. W. *J. Chem. Soc., Perkin Trans. 2* **1992**, 145–146.
- (39) Ettl, R.; Chao, I.; Diederich, F.; Whetten, R. L. *Nature* **1991**, *353*, 149–153.
- (40) Diederich, F.; Whetten, R. L.; Thilgen, C.; Ettl, R.; Chao, I.; Alvarez, M. M. *Science* **1991**, *254*, 1768–1770.
- (41) Taylor, R.; Langley, G. J.; Avent, A. G.; Dennis, T. J. S.; Kroto, H. W.; Walton, D. R. M. *J. Chem. Soc., Perkin Trans. 2* **1993**, 1029–1036.
- (42) Michel, R. H.; Kappes, M. M.; Adelman, P.; Roth, G. *Angew. Chem.* **1994**, *106*, 1742–46; *Angew. Chem., Int. Ed. Engl.* **1994**, *33*, 1651–1654.
- (43) Kikuchi, K.; Nakahara, N.; Wakabayashi, T.; Suzuki, S.; Shiro-maru, H.; Miyake, Y.; Saito, K.; Ikemoto, I.; Kainosho, M.; Achiba, Y. *Nature* **1992**, *357*, 142–145.
- (44) Balch, A. L.; Ginwalla, A. S.; Lee, J. W.; Noll, B. C.; Olmstead, M. M. *J. Am. Chem. Soc.* **1994**, *116*, 2227–2228.
- (45) Dennis, T. J. S.; Kai, T.; Tomiyama, T.; Shinohara, H. *Chem. Commun.* **1998**, 619–620.
- (46) Henrich, F. H.; Michel, R. H.; Fischer, A.; Richard-Schneider, S.; Gilb, S.; Kappes, M. M.; Fuchs, D.; Bürk, M.; Kobayashi, K.; Nagase, S. *Angew. Chem.* **1996**, *108*, 1839–1841; *Angew. Chem., Int. Ed. Engl.* **1996**, *35*, 1732–1734.
- (47) Avent, A. G.; Dubois, D.; Penicaud, A.; Taylor, R. *J. Chem. Soc., Perkin Trans. 2* **1997**, 1907–1910.
- (48) Stevenson, S.; Rice, G.; Glass, T.; Harloh, K.; Cromer, F.; Jordan, M. R.; Craft, J.; Nadju, E.; Bible, R.; Olmstead, M. M.; Maltra, K.; Fisher, A. J.; Balch, A. L.; Dorn, H. C. *Nature* **1999**, *401*, 55–57.
- (49) Ozaki, M.; Takahashi, A. *Chem. Phys. Lett.* **1986**, *127*, 242–244.
- (50) Disch, R. L.; Schulman, J. M. *Chem. Phys. Lett.* **1986**, *125*, 465–466.
- (51) Schulman, J. M.; Disch, R. L.; Miller, M. A.; Peck, R. C. *Chem. Phys. Lett.* **1987**, *141*, 45–48.
- (52) Lüthi, H. P.; Almlöf, J. *Chem. Phys. Lett.* **1987**, *135*, 357–360.
- (53) Dunlap, D. I. *Int. J. Quantum Chem. Symp.* **1988**, *22*, 257.
- (54) Scuseria, G. E. *Chem. Phys. Lett.* **1991**, *176*, 423–427.
- (55) Häser, M.; Almlöf, J.; Scuseria, G. E. *Chem. Phys. Lett.* **1991**, *181*, 497–500.
- (56) Yannoni, C. S.; Bernier, P. P.; Bethune, D. S.; Meijer, G.; Salem, J. R. *J. Am. Chem. Soc.* **1991**, *113*, 3190–3192.
- (57) David, W. I. F.; Ibberson, R. M.; Matthewman, J. C.; Prassides, K.; Dennis, T. J. S.; Hare, J. P.; Kroto, H. W.; Taylor, R.; Walton, D. R. M. *Nature* **1991**, *353*, 147–149.
- (58) Hedberg, K.; Hedberg, L.; Bethune, D. S.; Brown, C. A.; Dorn, H. C.; Johnson, R. D.; de Vries, M. *Science* **1991**, *254*, 410–412.
- (59) Liu, S.; Lu, Y. J.; Kappes, M. M.; Ibers, J. A. *Science* **1991**, *254*, 408–410.
- (60) Scuseria, G. E. *Chem. Phys. Lett.* **1991**, *180*, 451–456.
- (61) Balch, A. L.; Catalano, V. J.; Lee, J. W.; Olmstead, M. M.; Parkin, S. R. *J. Am. Chem. Soc.* **1991**, *113*, 8953–8955.
- (62) Bürgi, H. B.; Venugopalan, P.; Schwarzenbach, D.; Diederich, F.; Thilgen, C. *Helv. Chim. Acta* **1993**, *76*, 2155–2159.
- (63) Bakowies, D.; Gelessus, A.; Thiel, W. *Chem. Phys. Lett.* **1992**, *197*, 324–329.
- (64) Taylor, R. *J. Chem. Soc., Perkin Trans. 2* **1993**, 813–824.
- (65) Stollhoff, G. *Phys. Rev. B* **1991**, *44*, 10998–11000.
- (66) Stollhoff, G.; Scherrer, H. *Mater. Sci. Forum* **1995**, *191*, 81–90.
- (67) Chen, Z.; Jiao, H.; Hirsch, A. *Angew. Chem., Int. Ed.* **2000**, *39*, 3915–3917.
- (68) Haddon, R. C.; Brus, L. E.; Raghavachari, K. *Chem. Phys. Lett.* **1986**, *125*, 459–464.
- (69) Cioslowski, J.; Patchkovskii, S.; Thiel, W. *Chem. Phys. Lett.* **1996**, *248*, 116–120.
- (70) Lamparth, I.; Maichle-Mössmer, C.; Hirsch, A. *Angew. Chem.* **1995**, *107*, 1755–1757; *Angew. Chem., Int. Ed. Engl.* **1995**, *34*, 1607–1609.
- (71) Fowler, P. W.; Woolrich, J. *Chem. Phys. Lett.* **1986**, *127*, 78–83.
- (72) Pascual, J. I.; Gomez-Herrero, J.; Rogero, C.; Baro, A. M.; Sanchez-Portal, D.; Artacho, E.; Ordejon, P.; Soler, J. M. *Chem. Phys. Lett.* **2000**, *321*, 78–82.
- (73) Claxton, T. A.; Shirsat, R. N.; Gadre, S. R. *J. Chem. Soc., Chem. Commun.* **1994**, 731–732.
- (74) (a) Andreoni, W.; Gygi, F.; Parrinello, M. *Phys. Rev. Lett.* **1992**, *68*, 823–826. (b) Yamaguchi, K.; Hayashi, S.; Okumura, M.; Nakano, M.; Mori, W. *Chem. Phys. Lett.* **1994**, *226*, 372–380.
- (75) Rosseinsky, M. J. *J. Mater. Chem.* **1995**, *5*, 1497–1513.
- (76) (a) Fowler, P. W.; Collins, D. J.; Austin, S. J. *J. Chem. Soc., Perkin Trans. 2* **1993**, 275–277. (b) Austin, S. J.; Fowler, P. W.; Hansen, P.; Manolopoulos, D. E.; Zheng, M. *Chem. Phys. Lett.* **1994**, *228*, 478–484.
- (77) Klein, D. J.; Liu, X. *Int. J. Quantum Chem.: Quantum Chem. Symp.* **1994**, *28*, 501.
- (78) Fries, K. *Justus Liebigs Ann. Chem.* **1927**, *545*, 121.
- (79) Fantì, M.; Orlandi, G.; Zerbetto, F.; *J. Phys. Chem. A* **1997**, *101*, 3015–3020.
- (80) Meier, M. S.; Wang, G.-W.; Haddon, R. C.; Brock, C. P.; Lloyd, M. A.; Selegue, J. P. *J. Am. Chem. Soc.* **1998**, *120*, 2337–2342.
- (81) Krygowski, T. M.; Ciesielski, A. *J. Chem. Inf. Comput. Sci.* **1995**, *35*, 1001–1003.
- (82) Haymet, A. D. J. *Chem. Phys. Lett.* **1985**, *122*, 421–424.
- (83) Haymet, A. D. J. *J. Am. Chem. Soc.* **1986**, *108*, 319–321.
- (84) Hess, B. A.; Schaad, L. J. *J. Org. Chem.* **1986**, *51*, 3902–3903.
- (85) Aihara, J.; Hosoya, H. *Bull. Chem. Soc. Jpn.* **1988**, *61*, 2657–2659.
- (86) Aihara, J.; Hosoya, H. *Bull. Chem. Soc. Jpn.* **1993**, *66*, 1955–1958.
- (87) Aihara, J. *J. Mol. Struct.* **1994**, *311*, 1–8.
- (88) Aihara, J.; Takata, S. *J. Chem. Soc., Perkin Trans. 2* **1994**, 65–69.
- (89) Randić, M.; Nicolic, S.; Trinajstić, N. *Croat. Chim. Acta* **1987**, *60*, 595.
- (90) Plavsic, D.; Nikolic, S.; Trinajstić, N. *J. Mol. Struct.* **1992**, *277*, 213–237.
- (91) Trinajstić, N.; Randić, M.; Klein, D. J.; Babić, D.; Mihalic, Z. *Croat. Chim. Acta* **1995**, *68*, 241–267.
- (92) Haddon, R. C. *J. Am. Chem. Soc.* **1986**, *108*, 2837–2842.
- (93) Haddon, R. C.; Brus, L. E.; Raghavachari, K. *Chem. Phys. Lett.* **1986**, *125*, 459–464.
- (94) Haddon, R. C.; Brus, L. E.; Raghavachari, K. *Chem. Phys. Lett.* **1986**, *131*, 165–169.
- (95) Haddon, R. C. *J. Am. Chem. Soc.* **1987**, *109*, 1676–1685.
- (96) Haddon, R. C. *Acc. Chem. Res.* **1988**, *21*, 243–249.
- (97) Haddon, R. C. *J. Am. Chem. Soc.* **1990**, *112*, 3385–3389.
- (98) Beckhaus, H.-D.; Rüchardt, C.; Kao, M.; Diederich, F.; Foote, C. S. *Angew. Chem.* **1992**, *104*, 69–70.
- (99) Schulman, J. M.; Disch, R. L. *J. Chem. Soc., Chem. Commun.* **1991**, 411–412.
- (100) (a) Klein, D. J.; Seitz, W. A.; Schmalz, T. G. *Nature* **1986**, *323*, 703–704. (b) Cioslowski, J. *Chem. Phys. Lett.* **1993**, *216*, 389–393. (c) Jiang, Y.; Zhang, H. *Pure Appl. Chem.* **1990**, *62*, 451.
- (101) Kroto, H. W. *Nature* **1987**, *329*, 529–531.
- (102) Bakowies, D.; Thiel, W. *J. Am. Chem. Soc.* **1991**, *113*, 3704–3714.
- (103) Matsuzawa, N.; Dixon, D. A.; Fukunaga, T. *J. Phys. Chem.* **1992**, *96*, 7594–7604.
- (104) Henderson, C. C.; Röhlfing, C. M.; Cahill, P. A. *Chem. Phys. Lett.* **1993**, *213*, 383–388.
- (105) Karfunkel, H. R.; Hirsch, A. *Angew. Chem.* **1992**, *104*, 1529–1531; *Angew. Chem., Int. Ed. Engl.* **1992**, *31*, 1468–1470.
- (106) Klein, D. J.; Schmalz, T. G.; Hite, G. E.; Seitz, W. A. *J. Am. Chem. Soc.* **1986**, *108*, 1301–1302.
- (107) Fukui, K. *Science* **1982**, *218*, 747.
- (108) Zhang, B. L.; Wang, C. Z.; Ho, K. M. *Chem. Phys. Lett.* **1992**, *193*, 225.
- (109) Pearson, R. G. *J. Am. Chem. Soc.* **1988**, *110*, 7684–7690.
- (110) Parr, R. G.; Pearson, R. G. *J. Am. Chem. Soc.* **1983**, *105*, 7512–7516.
- (111) Zhou, Z.; Parr, R. G.; Garst, J. F. *Tetrahedron Lett.* **1988**, *29*, 4843–4846.
- (112) Pearson, R. G. *J. Chem. Educ.* **1987**, *64*, 561–567.
- (113) Zhou, Z.; Parr, R. G. *J. Am. Chem. Soc.* **1989**, *111*, 7371.
- (114) Fukui, K.; Yonezawa, T.; Nagata, C. *Bull. Chem. Soc. Jpn.* **1954**, *27*, 423.
- (115) Fukui, K.; Yonezawa, T.; Nagata, C. *J. Chem. Phys.* **1957**, *26*, 831.

- (116) Streitwieser, Jr., A. *Molecular Orbital Theory for Organic Chemists*; Wiley: New York, 1961.
- (117) Yoshida, M.; Aihara, J. *Phys Chem. Chem. Phys.* **1999**, *1*, 217–230.
- (118) Aihara, J. *J. Phys. Chem.* **1995**, *99*, 12739–12742.
- (119) Tsuda, M.; Ishida, T.; Nogami, T.; Kurono, S.; Ohashi, M. *J. Chem. Soc., Chem. Commun.* **1993**, 1296–1298.
- (120) Schlueter, J. A.; Seaman, J. M.; Taha, S.; Cohen, H.; Lykke, K. R.; Wang, H. H.; Williams, J. M. *J. Chem. Soc., Chem. Commun.* **1993**, 972–974.
- (121) Komatsu, K.; Murata, Y.; Sugita, N.; Takeuchi, K.; Wan, T. S. M. *Tetrahedron Lett.* **1993**, *34*, 8473–8476.
- (122) Lamparth, I.; Maichle-Mössmer, C.; Hirsch, A. *Angew. Chem.* **1995**, *107*, 1755–1757; *Angew. Chem., Int. Ed. Engl.* **1995**, *34*, 1607–1609.
- (123) Krätzler, B.; Müller, T.; Maynollo, J.; Gruber, K.; Kratky, C.; Ochsenbein, P.; Schwarzenbach, D.; Bürgi, H.-B. *Angew. Chem.* **1996**, *108*, 1294–1296.
- (124) Rotello, V. M.; Howard, J. B.; Yadev, T.; Conn, M. M.; Viani, E.; Giovane, L. M.; Lafleur, A. L. *Tetrahedron Lett.* **1993**, *34*, 1561–1562.
- (125) Lamparth, I.; Herzog, A.; Hirsch, A. *Tetrahedron* **1996**, *52*, 5065–5075.
- (126) Haufler, R. E.; Conceicao, J.; Chibante, L. P. F.; Chai, Y.; Byrne, N. E.; Flanagan, S.; Haley, M. M.; O'Brian, S. C.; Pan, C.; Xiao, Z.; Billups, W. E.; Ciufolini, M. A.; Hauge, R. H.; Margrave, J. L.; Wilson, L. J.; Curl, R. F.; Smalley, R. E. *J. Phys. Chem.* **1990**, *94*, 8634–8636.
- (127) (a) Bingel, C. *Chem. Ber.* **1993**, *126*, 1957–1959. (b) Bingel, C.; Schiffer, H. *Liebigs Ann.* **1995**, 1551–1553.
- (128) Kessinger, R.; Crassous, J.; Herrmann, A.; Rüttimann, M.; Echegoyen, L.; Diederich, F. *Angew. Chem.* **1999**, *110*, 2022–2025; *Angew. Chem., Int. Ed. Engl.* **1999**, *37*, 1919–1922.
- (129) Kessinger, R.; Fender, N. S.; Echegoyen, L. E.; Thilgen, C.; Echegoyen, L.; Diederich, F. *Chem. Eur. J.* **2000**, *6*, 2184–2192.
- (130) Boudon, C.; Gisselbrecht, J.-P.; Gross, M.; Herrmann, A.; Rüttimann, M.; Crassous, J.; Cardullo, F.; Echegoyen, L.; Diederich, F. *J. Am. Chem. Soc.* **1998**, *120*, 7860–7868.
- (131) Crassous, J.; Rivera, J.; Fender, N. S.; Shu, L.; Echegoyen, L.; Thilgen, C.; Herrmann, A.; Diederich, F. *Angew. Chem.* **1999**, *111*, 1716–1721; *Angew. Chem., Int. Ed. Engl.* **1999**, *38*, 1613–1617.
- (132) An, Y.-Z.; Ellis, G. A.; Viado, A. L.; Rubin, Y. *J. Org. Chem.* **1995**, *60*, 6353–6361.
- (133) (a) Cardullo, F.; Isaacs, L.; Diederich, F.; Gisselbrecht, J.-P.; Boudon, C.; Gross, M. *Chem. Commun.* **1996**, 797–799. (b) Cardullo, F.; Seiler, P.; Isaacs, L.; Nierengarten, J.-F.; Haldimann, R. F.; Diederich, F.; Mordasini-Denti, T.; Thiel, W.; Boudon, C.; Gisselbrecht, J.-P.; Gross, M. *Helv. Chim. Acta* **1997**, *80*, 343–371.
- (134) Da Ros, T.; Prato, M.; Novello, F.; Maggini, M.; De Amici, M.; De Micheli, C. *Chem. Commun.* **1997**, 59–60.
- (135) Hirsch, A.; Lamparth, I.; Karfunkel, H. R. *Angew. Chem.* **1994**, *106*, 453–455; *Angew. Chem., Int. Ed. Engl.* **1994**, *33*, 437–438.
- (136) Hirsch, A.; Lamparth, I.; Schick, G. *Liebigs Ann.* **1996**, 1725–1734.
- (137) Hirsch, A.; Lamparth, I.; Grösser, T.; Karfunkel, H. R. *J. Am. Chem. Soc.* **1994**, *116*, 9385–9386.
- (138) Kessinger, R.; Gómez-López, M.; Boudon, C.; Gisselbrecht, J.-P.; Gross, M.; Echegoyen, L.; Diederich, F. *J. Am. Chem. Soc.* **1998**, *120*, 8545–8546.
- (139) Prato, M.; Lucchini, V.; Maggini, M.; Stimpfl, E.; Scorrano, G.; Eiermann, M.; Suzuki, T.; Wudl, F. *J. Am. Chem. Soc.* **1993**, *115*, 8479–8480.
- (140) Prato, M.; Li, Q. C.; Wudl, F.; Lucchini, V. *J. Am. Chem. Soc.* **1993**, *115*, 1148–1150.
- (141) Banks, M. R.; Cadogan, J. I. G.; Gosney, I.; Hodgson, P. K. G.; Langridge-Smith, P. R. R.; Ranking, D. W. H. *J. Chem. Soc., Chem. Commun.* **1994**, 1365–1366.
- (142) Banks, M. R.; Cadogan, J. I. G.; Gosney, I.; Hodgson, P. K. G.; Langridge-Smith, P. R. R.; Millar, J. R. A.; Taylor, A. T. *Tetrahedron Lett.* **1994**, *35*, 9067–9070.
- (143) Ishida, T.; Tanaka, K.; Nogami, R. *Chem. Lett.* **1994**, 561–562.
- (144) Hawker, C. J.; Wooley, K. L.; Fréchet, J. M. J. *J. Chem. Soc., Chem. Commun.* **1994**, 925–926.
- (145) Yan, M.; Cai, S. X.; Keana, J. F. W. *J. Org. Chem.* **1994**, *59*, 5951–5954.
- (146) Averdung, J.; Luftmann, H.; Mattay, J.; Claus, K. U.; Abraham, W. *Tetrahedron Lett.* **1995**, *36*, 2957–2958.
- (147) Banks, M. R.; Cadogan, J. I. G.; Gosney, I.; Hodgson, P. K. G.; Langridge-Smith, P. R. R.; Millar, J. R. A.; Parkinson, J. A.; Rankin, D. W. H.; Taylor, A. T. *J. Chem. Soc., Chem. Commun.* **1995**, 887–888.
- (148) Banks, M. R.; Cadogan, J. I. G.; Gosney, I.; Hodgson, P. K. G.; Langridge-Smith, P. R. R.; Millar, J. R. A.; Taylor, A. T. *J. Chem. Soc., Chem. Commun.* **1995**, 885–886.
- (149) Schick, G.; Grösser, T.; Hirsch, A. *J. Chem. Soc., Chem. Commun.* **1995**, 2289–2290.
- (150) Schick, G.; Hirsch, A.; Mauser, H.; Clark, T. *Chem. Eur. J.* **1996**, *2*, 935–943.
- (151) Grösser, T.; Prato, M.; Luchini, V.; Hirsch, A.; Wudl, F. *Angew. Chem.* **1995**, *107*, 1462–1464; *Angew. Chem., Int. Ed. Engl.* **1995**, *34*, 1343–1345.
- (152) Schick, G.; Hirsch, A. *Tetrahedron* **1998**, *54*, 4283–4296.
- (153) Haldimann, R. F.; Klärner, F.-G.; Diederich, F. *J. Chem. Soc., Chem. Commun.* **1997**, 237–238.
- (154) Shen, C. K.-F.; Yu, H.-H.; Juo, C.-G.; Chien, K.-M.; Her, G.-R.; Luh, T.-Y. *Chem. Eur. J.* **1997**, *3*, 744–748.
- (155) Djojo, F.; Herzog, A.; Lamparth, I.; Hampel, F.; Hirsch, A. *Chem. Eur. J.* **1996**, *2*, 1537–1547.
- (156) Hirsch, A.; Soi, A.; Karfunkel, H. R. *Angew. Chem.* **1992**, *104*, 808–810; *Angew. Chem., Int. Ed. Engl.* **1992**, *31*, 766–768.
- (157) Hirsch, A.; Grösser, T.; Skieba, A.; Soi, A. *Chem. Ber.* **1993**, *126*, 1061–1067.
- (158) Morton, J. R.; Preston, K. F.; Krusic, P. J.; Hill, S. A. Wasserman, E. *J. Phys. Chem.* **1992**, *96*, 3576–3578.
- (159) Fagan, P. J.; Calabrese, J. C.; Malone, B. *J. Am. Chem. Soc.* **1991**, *113*, 9408–9409.
- (160) Hirsch, A.; Vostrowsky, O. *Eur. J. Org. Chem.* **2000**, in press.
- (161) Camps, X.; Hirsch, A. *J. Chem. Soc., Perkin Trans. 2* **1997**, 1595–1596.
- (162) Hetzer, M.; Bayerl, S.; Camps, X.; Vostrowsky, O.; Hirsch, A.; Bayerl, T. M. *Adv. Mater.* **1997**, *9*, 913–917.
- (163) Hetzer, M.; Gutberlet, T.; Brown, M. F.; Camps, X.; Vostrowsky, O.; Schönberger, H.; Hirsch, A.; Bayerl, T. M. *J. Phys. Chem. A* **1999**, *103*, 637–642.
- (164) Hetzer, M.; Clausen-Schaumann, H.; Bayerl, S.; Bayerl, T. M.; Camps, X.; Vostrowsky, O.; Hirsch, A. *Angew. Chem.* **1999**, *111*, 2103–2106; *Angew. Chem., Int. Ed. Engl.* **1999**, *38*, 1962–1965.
- (165) Camps, X.; Schönberger, H.; Hirsch, A. *Chem. Eur. J.* **1997**, *3*, 561–567.
- (166) Camps, X.; Dietel, E.; Hirsch, A.; Pyo, S.; Echegoyen, L.; Hackbarth, S.; Röder, B. *Chem. Eur. J.* **1999**, *5*, 2362–2373.
- (167) Krätzler, B.; Maynollo, J. *Angew. Chem.* **1995**, *107*, 69–71; *Angew. Chem., Int. Ed. Engl.* **1995**, *34*, 87–89.
- (168) Schick, G.; Levitus, M.; Kvetko, L.; Johnson, B. A.; Lamparth, I.; Lunkwitz, R.; Ma, B.; Khan, S. I.; Garcia-Garibay, M. A.; Rubin, Y. *J. Am. Chem. Soc.* **1999**, *121*, 3246–3247.
- (169) Krusic, P. J.; Wassermann, E.; Parkinson, B. A.; Malone, B.; Holler, E. R. Jr.; Keizer, P. N.; Morton, J. R.; Preston, K. F. *J. Am. Chem. Soc.* **1991**, *113*, 6274–6275.
- (170) Krusic, P. J.; Wassermann, E.; Keizer, P. N.; Morton, J. M.; Preston, K. F. *Science* **1991**, *254*, 1183–1185.
- (171) Schick, G.; Kampe, K.-D.; Hirsch, A. *J. Chem. Soc., Chem. Commun.* **1995**, 2023–2024.
- (172) Birkett, P. R.; Avent, A. G.; Darwisch, A. D.; Kroto, H. W.; Taylor, R.; Walton D. R. M. *J. Chem. Soc., Chem. Commun.* **1993**, 1230–1232.
- (173) Birkett, P. R.; Hitchcock, P. B.; Kroto, H. W.; Taylor, R.; Walton D. R. M. *Nature* **1992**, *357*, 479–481.
- (174) Sawamura, M.; Iikura, H.; Nakamura, E. *J. Am. Chem. Soc.* **1996**, *118*, 12850–12851.
- (175) Murata, Y.; Shiro, M.; Komatsu, K. *J. Am. Chem. Soc.* **1997**, *119*, 8117–8118.
- (176) Sawamura, M.; Iikura, H.; Hirai, A.; Nakamura, E. *J. Am. Chem. Soc.* **1998**, *120*, 8285–8286.
- (177) Reuther, U.; Hirsch, A. *J. Chem. Soc., Chem. Commun.* **1998**, 1401–1402.
- (178) (a) Darwisch, A. D.; Avent, A. G.; Taylor, R.; Walton, D. R. M. *J. Chem. Soc., Perkin Trans. 2* **1996**, 2051–2054. (b) Avent, A. G.; Darwisch, A. D.; Heimbach, D. K.; Kroto, H. W.; Meidine, M. F.; Parsons, J. P.; Remars, C.; Roers, R.; Ohashi, O.; Taylor, R.; Walton, D. R. M. *J. Chem. Soc., Perkin Trans. 2* **1994**, 15–22.
- (179) Taylor, R. *Philos. Trans. R. Soc. London, A* **1993**, *343*, 87–101.
- (180) Bini, R.; Ebenhoch, J.; Fanti, M.; Fowler, P. W.; Leach, S.; Orlandi, G.; Rüchardt, Ch.; Sandall, J. P. B.; Zerbetto, F. *Chem. Phys.* **1998**, *232*, 75–94.
- (181) Neretin, I. S.; Lyssenko, K. A.; Antipin, M. Y.; Slovokhotov, Y. L.; Boltalina, O. V.; Troshin, P. A.; Lukonin, A. Y.; Sidorov, L. N.; Taylor, R. *Angew. Chem., Int. Ed. Engl.* **2000**, *39*, 3273–3276.
- (182) Boltalina, O. V.; Lukonin, A. Y.; Avent, A. G.; Street, J. M.; Taylor, R.; *J. Chem. Soc., Perkin Trans. 2* **2000**, 683–686.
- (183) (a) Gakh, A. A.; Tuinman, A. A.; Adcock, J. L.; Sachleben, R. A.; Compton, R. N. *J. Am. Chem. Soc.* **1994**, *116*, 819–820. (b) Boltalina, O. V.; Sidorov, L. N.; Bagryantsev, V. F.; Seredenko, V. A.; Zapolskii, A. S.; Taylor, R. *J. Chem. Soc., Perkin Trans. 2* **1996**, 2275–2278.
- (184) (a) Boltalina, O. V.; Street, J. M.; Taylor, R. *J. Chem. Soc., Perkin Trans. 2* **1998**, 649–654. (b) Boltalina, O. V.; Bühl, M.; Khong, A.; Saunders, M.; Street, J. M.; Taylor, R. *J. Chem. Soc., Perkin Trans. 2* **1999**, 1475–1479.
- (185) Circular current loops are a normal response of an atom or a molecule to an external magnetic field. These loops are usually centered around individual nuclei and are responsible for the particular magnetic shielding of each nucleus in an NMR

- experiment. Ring currents are a special case since they enclose more than one atomic center.
- (186) See, for instance, section 2.4 in ref 12.
- (187) See also related articles in this issue: (a) Aihira, A. manuscript in preparation. (b) Mallion, R. B.; Gomes, J. A. N. F. *Chem. Rev.* **2001**, *101*, 1349. (c) Mitchell, R. H. *Chem. Rev.* **2001**, *101*, 1301.
- (188) (a) Dauben, H. J.; Wilson, J. D.; Laity, J. L. *J. Am. Chem. Soc.* **1969**, *91*, 1991–1998. (b) Dauben, H. J.; Wilson, J. D.; Laity, J. L. In *Nonbenzenoid Aromatics*; Snyder J. P., Ed.; Academic Press: New York, 1971; Vol. 2, pp 167–206.
- (189) Haigh, C. W.; Mallion, R. B. *Prog. NMR Spectrosc.* **1980**, *13*, 303–344.
- (190) Paquette, L. A.; Bauer, W.; Sivik, M. R.; Bühl, M.; Feigel, M.; Schleyer, P. v. R. *J. Am. Chem. Soc.* **1990**, *112*, 8776–8790.
- (191) Fleischer, U.; Kutzelnigg, W.; Lazzeretti, P.; Mühlenkamp, V. *J. Am. Chem. Soc.* **1994**, *116*, 5298–5306.
- (192) Kutzelnigg, W.; van Wüllen, C.; Fleischer, U.; Franke, R.; von Mourik, T. In *Nuclear Magnetic Shieldings and Molecular Structure*; Tossell, J. A., Ed.; NATO ASI Series C 386; Kluwer Academic Publishers: Dordrecht, 1993; pp 141–161.
- (193) (a) Steiner, E.; Fowler, P. W. *Int. J. Quantum Chem.* **1996**, *60*, 609–616. (b) Fowler, P. W.; Zanasi, R.; Cadioli, B.; Steiner, E. *Chem. Phys. Lett.* **1996**, *251*, 132–140. (c) Černušák, I.; Fowler, P. W.; Steiner, E. *Mol. Phys.* **1997**, *91*, 401–412.
- (194) Bilde, M.; Hansen, Aa. E. *Mol. Phys.* **1997**, *92*, 237–250.
- (195) Ligabue, A.; Pincelli, U.; Lazzeretti, P.; Zanasi, R. *J. Am. Chem. Soc.* **1999**, *121*, 5513–5518.
- (196) (a) Schleyer, P. v. R.; Maerker, C.; Dransfeld, A.; Jiao, H.; Hommes, N. J. v. E., *J. Am. Chem. Soc.* **1996**, *118*, 6317–6318. For extensions to points above the ring plane see, e.g., (b) Schleyer, P. v. R.; Jiao, H.; Hommes, N. J. v. E.; Malkin, V. G.; Malkina, O. L. *J. Am. Chem. Soc.* **1997**, *119*, 12669–12670. (c) Jusélius, J.; Sundholm, D. *Phys. Chem. Chem. Phys.* **1999**, *2*, 3429–3435.
- (197) Lazzeretti, P. *Prog. Nucl. Magn. Reson. Spectrosc.* **2000**, *36*, 1–88.
- (198) Elser, V.; Haddon, R. C. *Nature* **1987**, *325*, 792–794.
- (199) Haddon, R. C.; Schneemeyer, L. F.; Waszczak, J. V.; Glarum, S. H.; Tycko, R.; Dabbagh, R.; Kortan, A. R.; Muller, A. J.; Mujsc, A. M.; Rosseinsky, M. J.; Zahurak, S. M.; Makhija, A. V.; Thiel, F. A.; Raghavachari, K.; Cockayne, E.; Elser, V. *Nature* **1991**, *350*, 46–47.
- (200) Similar values have been reported in an independent, simultaneous study: Ruoff, R. S.; Beach, D.; Cuomo, J.; McGuire, T.; Whetten, R. L.; Diederich, F. *J. Phys. Chem.* **1991**, *95*, 3457–3459.
- (201) (a) Pasquarello, A.; Schlüter, M.; Haddon, R. C. *Science* **1992**, *257*, 1660–1661. (b) Pasquarello, A.; Schlüter, M.; Haddon, R. C. *Phys. Rev. A* **1993**, *47*, 1783–1789.
- (202) Zanasi, R.; Fowler, P. W. *Chem. Phys. Lett.* **1995**, *238*, 270–280.
- (203) Bühl, M.; Thiel, W.; Jiao, H.; Schleyer, P. v. R.; Saunders, M.; Anet, F. A. L. *J. Am. Chem. Soc.* **1994**, *116*, 6005–6006.
- (204) Haddon, R. C.; Pasquarello, A. *Phys. Rev. B* **1994**, *50*, 16459–16463.
- (205) (a) Heine, T.; Fowler, P. W.; Seifert, G.; Zerbetto, F. *J. Phys. Chem. A* **1999**, *103*, 8738–8746. (b) Heine, T.; Bühl, M.; Fowler, P. W.; Seifert, G. *Chem. Phys. Lett.* **2000**, *316*, 373–380.
- (206) Wudl, F.; Sukuki, T.; Prato, M. *Synth. Met.* **1993**, *59*, 297–305.
- (207) Diederich, F.; Isaacs, L.; Philp, D. *Chem. Soc. Rev.* **1994**, *23*, 243–255.
- (208) Wudl, F. *Acc. Chem. Res.* **1992**, *25*, 157–161.
- (209) (a) Suzuki, T.; Li, Q.; Khemani, K. C.; Wudl, F. *J. Am. Chem. Soc.* **1992**, *114*, 7301–7302. (b) Smith, A. B., III; Strongin, R. M.; Brard, L.; Furst, G. T.; Romanow, W. J.; Owens, K. G.; King, R. C. *J. Am. Chem. Soc.* **1993**, *115*, 5829–5830.
- (210) Isaacs, L.; Wehrsig, A.; Diederich, F. *Helv. Chim. Acta* **1993**, *76*, 1231–1250.
- (211) Arnz, R.; Carneiro, J. W. de M.; Klug, W.; Schmickler, H.; Vogel, E.; Breuckmann, R.; Klärner, F.-G. *Angew. Chem., Int. Ed. Engl.* **1991**, *30*, 683–685.
- (212) Gerson, F.; Merstetter, P.; Barbosa, F.; Vogel, E.; König, C.; Lex, J.; Müllen, K.; Wagner, M. *Chem. Eur. J.* **1999**, *5*, 2757–2761.
- (213) This interpretation is supported by model calculations<sup>214</sup> for the [6,6] closed isomer of homopyracyclene, which afford large positive NICS values in the five- and six-membered rings and an even larger deshielding of the methylene hydrogens (computed  $\delta \approx 7$ , DFT level).
- (214) Bühl, M. Unpublished calculations. Chemical shifts were computed at the GIAO-HF or GIAO-DFT/DZP level (the latter using the BPW91 combination of density functionals) employing BP86/3-21G geometries; for details, see refs 222 and 234.
- (215) The closest intramolecular H...H contact between the methylene groups is 1.82 Å in **22** (DFT optimization)<sup>214</sup> and 2.1 Å in the 3,5-diformyl derivative (X-ray; Bianchi, R.; Pilati, T.; Simonetta, M. *Acta Crystallogr.* **1980**, *36b*, 3144–3146). In fact, the computed methylene <sup>1</sup>H resonances of the cycloheptatriene moiety in **22** differ by 3.9 ppm in the boat conformer but only by 1.6 ppm in the less stable chair isomer with remote methylene groups.
- (216) Prato, M.; Suzuki, T.; Wudl, F.; Lucchini, V.; Maggini, M. *J. Am. Chem. Soc.* **1993**, *115*, 7876–7877.
- (217) Smith, A. B., III; Strongin, R. M.; Brard, L.; Furst, G. T.; Romanow, W. J.; Owens, K. G.; Goldschmidt, R. J.; King, R. C. *J. Am. Chem. Soc.* **1995**, *117*, 5492–5502.
- (218) Another C<sub>70</sub>-based fulleroid has recently been characterized, namely, the CCl<sub>2</sub> adduct across the C7–C8 bond: Kiely, A. F.; Haddon, R. C.; Meier, M. S.; Selegue, J. P.; Brock, C. P.; Patrick, B. O.; Wang, G.-W.; Chen, Y. *J. Am. Chem. Soc.* **1999**, *121*, 7971–7972.
- (219) Saunders, M.; Jiménez-Vázquez, H. A.; Cross, R. J.; Mroczkowski, S.; Freedberg, D. I.; Anet, F. A. L. *Nature* **1994**, *367*, 256–258.
- (220) (a) Cioslowski, J. *J. Am. Chem. Soc.* **1994**, *116*, 3619–3620. (b) Cioslowski, J. *Chem. Phys. Lett.* **1994**, *227*, 361–364.
- (221) (a) Bühl, M.; Thiel, W. *Chem. Phys. Lett.* **1995**, *233*, 585–589. (b) Bühl, M.; van Wüllen, C. *Chem. Phys. Lett.* **1995**, *247*, 63–68.
- (222) Bühl, M.; Kaupp, M.; Malkin, V. G.; Malkina, O. L. *J. Comput. Chem.* **1999**, *20*, 91–105.
- (223) See for instance Cioslowski, J.; Fleischmann, E. D. *J. Chem. Phys.* **1991**, *94*, 3730–3734.
- (224) Bühl, M.; Patchkovskii, S.; Thiel, W. *Chem. Phys. Lett.* **1997**, *275*, 14–18.
- (225) Yamamoto, K.; Saunders, M.; Khong, A.; Cross, R. J.; Grayson, M.; Gross, M. L.; Benedetto, A. F.; Weisman, R. B. *J. Am. Chem. Soc.* **1999**, *121*, 1591–1596.
- (226) Khong, A.; Jiménez-Vázquez, H. A.; Saunders, M.; Cross, R. J.; Laskin, J.; Peres, T.; Lifshitz, C.; Strongin, R.; Smith, A. B., III *J. Am. Chem. Soc.* **1998**, *120*, 6380–6383.
- (227) Large geometric distortions, however, can affect the computed endohedral shifts more strongly, see: Hedberg, K.; Hedberg, L.; Bühl, M.; Bethune, D. S.; Brown, C. A.; Johnson, R. D. *J. Am. Chem. Soc.* **1997**, *119*, 5314–5320.
- (228) Saunders, M.; Jiménez-Vázquez, H. A.; Cross, R. J.; Billups, W. E.; Gesenberg, C.; Gonzalez, A.; Luo, W.; Haddon, R. C.; Diederich, F.; Herrmann, A. *J. Am. Chem. Soc.* **1995**, *117*, 9305–9308.
- (229) Saunders, M.; Cross, R. J.; Jiménez-Vázquez, H. A.; Shimshi, R.; Khong, A. *Science* **1996**, *271*, 1693–1697.
- (230) (a) Tagmatarchis, N.; Avent, A. G.; Prassides, K.; Dennis, T. J. S.; Shinohara, H. *J. Chem. Soc., Chem. Commun.* **1999**, 1023–1024. (b) Dennis, T. J. S.; Kai, T.; Tomiyama, T.; Shinohara, H. J.; Yoshida, T.; Kobayashi, Y.; Ishiwatari, H.; Miyake, Y.; Kikuchi, K.; Achiba, Y. *J. Phys. Chem. A* **1999**, *103*, 8747–8752.
- (231) Wang, G.-W.; Saunders, M.; Khong, A.; Cross, J. R. *J. Am. Chem. Soc.* **2000**, *122*, 3216–3217.
- (232) Labeling as in Fowler, P. W.; Manolopoulos, D. E. *An Atlas of Fullerenes*; Oxford University Press: Oxford, 1995.
- (233) Labeling as in Raghavachari, K.; Rohlfing, C. M. *Chem. Phys. Lett.* **1993**, *208*, 436–440.
- (234) Bühl, M. *Chem. Eur. J.* **1998**, *4*, 734–739.
- (235) (a) Almeida Murphy, T.; Pawlik, T.; Weidinger, A.; Höhne, M.; Alcalá, R.; Spaeth, J.-M. *Phys. Rev. Lett.* **1996**, *77*, 1075. (b) Knapp, C.; Dinse, K.-P.; Pietzak, B.; Waiblinger, M.; Weidinger, A. *Chem. Phys. Lett.* **1997**, *272*, 433–437.
- (236) (a) Lips, K.; Waiblinger, M.; Pietzak, B.; Weidinger, A. *Phys. Stat. Sol. A* **2000**, *177*, 81–91. (b) Pietzak, B. Diploma thesis, Technical University of Berlin, 1998.
- (237) According to calculations at the Hartree-Fock level,<sup>214</sup> the average chemical shifts for 32 points on a sphere with radius 1.55 Å around the center are very similar (within 0.1 ppm) to the endohedral chemical shift at the center itself, both for C<sub>60</sub> and C<sub>70</sub>.
- (238) Reed, C. A.; Bolskar, R. D. *Chem. Rev.* **2000**, *100*, 1075–1120.
- (239) Bausch, J. W.; Prakash, G. K. S.; Olah, G. A. *J. Am. Chem. Soc.* **1991**, *113*, 3205–3206.
- (240) Xie, Q.; Pérez-Cordero, E.; Echegoyen, L. *J. Am. Chem. Soc.* **1992**, *114*, 3978–3980.
- (241) C<sub>60</sub><sup>2-</sup> has probably a singlet ground state slightly below the triplet state, which is thermally populated at room temperature: (a) Bhyrappa, P.; Paul, P.; Stinchcombe, J.; Boyd, P. D. W.; Reed, C. A. *J. Am. Chem. Soc.* **1993**, *115*, 11004–11005. (b) Green, W. H., Jr.; Gorun, S. M.; Fitzgerald, G.; Fowler, P.; Ceulemans, A.; Titeca, B. C. *J. Phys. Chem.* **1996**, *100*, 14892–14898.
- (242) Shabtai, E.; Weitz, A.; Haddon, R. C.; Hoffman, R. E.; Rabinovitz, M.; Khong, A.; Cross, R. J.; Saunders, M.; Cheng, P. C.; Scott, L. T. *J. Am. Chem. Soc.* **1998**, *120*, 6389–6393.
- (243) Jakes, P.; Dinse, K.-P. To be published.
- (244) Bühl, M. *Z. Anorg. Allg. Chem.* **2000**, *626*, 332–337.
- (245) Sternfeld, T.; Wudl, F.; Hummel, K.; Weitz, A.; Haddon, R. C.; Rabinovitz, M. *J. Chem. Soc., Chem. Commun.* **1999**, 2411–2412.
- (246) Sternfeld, T.; Hoffmann, R. E.; Thilgen, C.; Diederich, F.; Rabinovitz, M. *J. Am. Chem. Soc.* **2000**, *122*, 9038–9039.

- (247) Spiesscke, H.; Schneider, W. *Tetrahedron Lett.* **1961**, *14*, 468–472.
- (248) Kohanoff, J.; Andreoni, W.; Parrinello, M. *Chem. Phys. Lett.* **1992**, *198*, 472–477.
- (249) Zimmermann, U.; Malinowski, N.; Burkhard, A.; Martin, T. P. *Carbon* **1995**, *33*, 995–1006.
- (250) (a) Cristofolini, L.; Riccò, M.; De Renzi, R. *Phys. Rev. B* **1999**, *59*, 8343–8346. (b) Cristofolini, L. Private communication to M.B.
- (251) Aihira, J.; Takata, S. *J. Chem. Soc., Perkin Trans. 2* **1994**, 65–69.
- (252) See, for instance: Weedon, B. R.; Haddon, R. C.; Spielmann, H. P.; Meier, M. S. *J. Am. Chem. Soc.* **1999**, *121*, 335–340.
- (253) Meier, M. S.; Poplawska, M.; Compton, A. L.; Shaw, J. P.; Selegue, J. P.; Guarr, T. F. *J. Am. Chem. Soc.* **1994**, *116*, 7044–7048.
- (254) Cardullo, F.; Seiler, P.; Isaacs, L.; Nierengarten, J.-F.; Haldimann, R. F.; Diederich, F.; Mordasini-Denti, T.; Thiel, W. *Helv. Chim. Acta* **1997**, *80*, 343–371.
- (255)  $C_{60}$  and  $C_{70}$  epoxides, methanofullerenes, and fulleroids: Smith, A. B., III; Strongin, R. M.; Brard, L.; Romanow, W. J.; Saunders, M.; Jiménez-Vázquez, H. A.; Cross, J. R. *J. Am. Chem. Soc.* **1994**, *116*, 10831–10832.
- (256)  $C_{120}$ : Komatsu, K.; Wang, G.-W.; Murata, Y.; Tanaka, T.; Fujiwara, Yamamoto, K.; Saunders, M. *J. Org. Chem.* **1998**, *63*, 9358–9366.
- (257)  $C_{60}H_4$ , bisadducts: (a) Cross, J. R.; Jiménez-Vázquez, H. A.; Lu, Q.; Saunders, M.; Schuster, D. I.; Wilson, S. R.; Zhao, H. *J. Am. Chem. Soc.* **1996**, *118*, 11454–11459. (b) Billups, W. E.; Luo, W.; Gonzalez, A.; Arguello, D.; Alemany, L.; Marriott, T.; Saunders, M.; Jiménez-Vázquez, H. A.; Khong, A. *Tetrahedron Lett.* **1997**, *38*, 171–174.
- (258) Multiple  $C_{60}$  and  $C_{70}$  adducts: (a) Rüttimann, M.; Haldimann, R. F.; Isaacs, L.; Diederich, F.; Khong, A.; Jiménez-Vázquez, H. A.; Cross, J. R.; Saunders, M. *Chem. Eur. J.* **1997**, *3*, 1071–1076. (b) Wang, G. W.; Weedon, B. R.; Meier, M. S.; Saunders, M.; Cross, R. J. *Org. Lett.* **2000**, *2*, 2241–2243. (c) Wang, G. W.; Saunders, M.; Cross, R. J. *J. Am. Chem. Soc.* **2001**, *123*, 256–259.
- (259)  $C_{60}R_5^+$ : Birkett, P. R.; Bühl, M.; Khong, A.; Saunders, M.; Taylor, R. *J. Chem. Soc., Perkin Trans. 2* **1999**, 2037–2039.
- (260)  $C_{60}X_{18,36}$ : (a) Billups, W. E.; Gonzalez, A.; Gesenber, C.; Luo, W.; Marriott, T.; Alemany, L.; Saunders, M.; Jiménez-Vázquez, H. A.; Khong, A. *Tetrahedron Lett.* **1997**, *38*, 175–178. (b) References 183b.
- (261) Bühl, M.; Thiel, W.; Schneider, U. *J. Am. Chem. Soc.* **1995**, *117*, 4623–4627.
- (262) Saunders, M.; Jiménez-Vázquez, H. A.; Bangerter, B. W.; Cross, J. R.; Mroczkowski, S.; Freedberg, D. I.; Anet, F. A. L. *J. Am. Chem. Soc.* **1994**, *116*, 3621–3622.
- (263) Addition may occur also across other bond types, even across a [5,6] ring fusion: Meier, M. S.; Wang, G.-W.; Haddon, R. C.; Brock, C. P.; Lloyd, M. A.; Selegue, J. P. *J. Am. Chem. Soc.* **1998**, *120*, 2337–2342.
- (264) See, for instance: Taylor, R.; Abdul-Sada, A. K.; Boltalina, O. V.; Street, J. M. *J. Chem. Soc., Perkin Trans 2* **2000**, 1013–1021 and references therein.
- (265) Fowler, P. W.; Sandall, J. P. B.; Austin, S. J.; Manolopoulos, D. E.; Lawrenson, P. D. M.; Smallwood, J. M. *Synth. Met.* **1996**, *77*, 97–101.
- (266) (a) Koshio, A.; Inakamuna, M.; Sugai, T.; Shinohara, H. *J. Am. Chem. Soc.* **2000**, *122*, 398–399. (b) Koshio, A.; Inakamuna, M.; Wang, Z. W.; Sugai, T.; Shinohara, H. *J. Phys. Chem. B* **2000**, *104*, 7908–7913.
- (267) Piskoti, C.; Yarger, J.; Zettl, A. *Nature* **1998**, *393*, 771–774.
- (268) Chen, Z.; Jiao, H.; Hirsch, A.; Thiel, W. *Chem. Phys. Lett.* **2000**, *329*, 47–51.
- (269) Reviews: (a) Hirsch, A.; Nuber, B. *Acc. Chem. Res.* **1999**, *32*, 795–804. (b) Hummelen, J. C.; Bellavia-Lund, C.; Wudl, F. *Top. Curr. Chem.* **1999**, *199*, 93–143. (c) Reuther, U.; Hirsch, A. *Carbon* **2000**, *38*, 1539–1549.
- (270) (a) Hummelen, J. C.; Knight, B.; Pavlovich, J.; González, R.; Wudl, F. *Science* **1995**, *269*, 1554–1556. (b) Keshavarz-K., M.; González, R.; Hicks, R. G.; Srdanov, G.; Srdanov, V. I.; Collins, T. G.; Hummelen, J. C.; Bellavia-Lund, C.; Pavlovich, J.; Wudl, F.; Holczer, K. *Nature* **1996**, *383*, 147–150. (c) Nuber, B.; Hirsch, A. *J. Chem. Soc., Chem. Commun.* **1996**, 1421–1422.
- (271) The BLYP geometry is taken from Andreoni, W.; Curioni, A.; Holczer, K.; Prassides, K.; Keshavarz-K., M.; Hummelen, J. C.; Wudl, F. *J. Am. Chem. Soc.* **1996**, *118*, 11335–11336.
- (272) Bühl, M.; Curioni, A.; Andreoni, W. *Chem. Phys. Lett.* **1997**, *274*, 231–234.
- (273) Bühl, M. *Chem. Phys. Lett.* **1995**, *242*, 580–584
- (274) Chen, Z.; Hirsch, A. To be published.
- (275) Bakowies, D.; Bühl, M.; Thiel, W. *J. Am. Chem. Soc.* **1995**, *117*, 10113–10118.
- (276) Liu X.; Klein D. J.; Schmalz, T. G. *Fullerene Sci. Technol.* **1994**, *2*, 405–422.
- (277) Clar, E. *The Aromatic Sextet*; John Wiley & Sons: New York, 1972.
- (278) Colt, J. R.; Scuseria, G. E. *Chem. Phys. Lett.* **1992**, *199*, 505–512.
- (279) Randić, M. *J. Am. Chem. Soc.* **1977**, *99*, 444–450.

CR990332Q

